Dynamics of Magnetic Ordering in Pulsed Magnetic Field

Yoshitomo Karaki

1985

Osaka University
Graduate School of Engineering Science
Department of Material Physics
Toyonaka Osaka

Abstract

The dynamical behavior of some paramagnetic compounds are studied in a pulsed magnetic field.

In the course of a pulsed adiabatic demagnetization, spin system changes from paramagnetic to an ordered state. We expected that a spin system needs a certain time to build up an ordered structure. This characteristic time has never been studied up to now. The characteristic time of spin ordering is determined by a pulsed magnetic field with fast sweep rate in Cs_3CoCl_5. The order of the time is $1 \sim 100\mu$ sec.

Sufficiently rapid reversal of the direction of a magnetic field can produce a magnetization opposed to the new sense of the field at a sufficiently small entropy of Cs_3CoCl_5. The quasi-thermal equilibrium state possessing a negative sense of magnetization is described by a negative spin temperature. The pulsed adiabatic demagnetization with the negative initial magnetization is tried. Spin ordering at negative temperature, however, could not be observed because of still higher initial entropy.

In the pulsed adiabatic magnetization cooling of $HoVO_4$, a field induced spin ordering is observed around level crossing field $H_c \approx 11$T. Two sets of double peak of dM/dt in total 4 peaks are obtained. In the case of simple 3 dimensional antiferromagnet, only two peaks corresponding to the phase boundary are predicted theoretically. It is thought that the anomalous peaks arise from strong hyperfine coupling between Ho^{3+} electronic spin and nuclear spin(I=7/2), which has the magnitude of the same as order with interaction between electron spins.

The most exciting in present work using pulsed magnetic field is that a spin ordering at excited state have been observed in $NaNiAcac_3$benzene. A pulsed magnetic field is used for lifting up the population at the ground state to the excited state and at the same time, for performing the adiabatic magnetization cooling among excited levels. The observed ordered state is quasi-thermal equilibrium and destroyed by a cross-relaxation between ground state and excited state.

CONTENTS

Chap. I General Introduction

Recently the technique for generating high magnetic fields has been extensively developed. Steady magnetic fields higher than 20 T are available owing to the development of superconductive materials. Transient methods are enable us to perform measurements in Megagauss range. For example, Fowler et al. reported the production of ultra-high magnetic fields (1000~1500 T) by explosive flux compression techniques[1]. In non destructive methods maximum field is about 100 T. In general, accuracy of measurement in a pulsed magnetic field is inferior to steady measurement. Therefore, much effort has been done to make a pulse field with long duration as well as high field.

The purpose of the present investigation is to study of dynamical properties of spin systems making use of one character of pulsed magnetic fields; high sweep rate. The typical example in which sweep rate of a magnetic field plays an essential part is magnetization process. Magnetization process consists of three parts. The first is an adiabatic process (quantum mechanical) for which no transition among levels is induced and the change of magnetization is due to the change of states. The second is an adiabatic (isentropic) proceess. There is no heat contact with a lattice but thermal equilibrium in spin system is attained. The third is an isothermal process. The spin system is, now, coupled with lattice and spin temperature is equal to the lattice. Each process can be achieved at certain sweep rate. If sweep rate is much faster than spin-spin relaxation rate, the isolated condition is achived. And when sweep rate is much slower than

spin-lattice relaxation rate, the isothermal condition is achived. Using high sweep rate we can make a lot of populations in excited state and observe the state which can never be produced in isothemal condition.

Generally speaking, a pulsed magnetic field with high sweep rate can make an unusual condition and enables us to observe an unusual spin ordering. In Chap. II, we describe the characterestic time of spin ordering τ_{ord}. A spin system needs a certain time to build up an ordered spin arrangement. We obtain τ_{ord} of Cs_3CoCl_5. In the course of adiabatic demagnetization, spin system cools and spin ordering occurs if entropy S is small enough. The spin ordering depends on sweep rate of the magnetic field. When sweep rate is large enough, spins cannot order. Experiments are carried out with a pulsed magnetic field and a steady magnetic field as well. An initial magnetic field is produced by superconducting solenoid and a pulsed magnetic field is applied antiparallel to cancell the former steady field so as to cross zero field pulsively. When the total magnetic field passes through zero field, the time interval of passing across the local field of the spin system is given by

$$\tau = 2H_{loc}/(dH/dt)$$

A spin ordering occurs only in the interval τ, so spin ordering can not occur if τ is very small. We observe the time derivative of magnetization dM/dt and obtain the critical τ_c when spin ordering doesn't occur. The τ_c is roughly equal to τ_{ord}. τ_{ord} becomes longer toward lower initial temperatures. At initial temperature low enough and sweep rate large enough, negative magnetization appears when the magnetic field passes

through zero field. The negative magnetization corresponds to the state possessing a negative temperature if it can be defined. We describe the pulsed adiabatic demagnetization with negative initial magnetization.

In Chap.III we discuss adiabatic magnetization cooling of $HoVO_4$. Ho^{3+} in $HoVO_4$ is the ground state singlet with large initial splitting which results the level crossing between the ground state singlet and one of excited state at high field H_c. Around H_c, field induced spin ordering occurs as discussed by Tachiki et al.[2] Pulsed magnetic field with quarter period τ_p is applied. If τ_p is much smaller than spin-lattice relaxation rate, a spin system is isolated from a lattice system. Therefore, spin ordering isolated from a lattice system can be observed.

In Chap.IV we discuss the spin ordering among excited spin states of $NaNiAcac_3$benzene. Ni^{2+} of $NaNiAcac_3$benzene has the energy levels given by the following spin Hamiltonian.

$$\mathcal{H} = DS_z^2 + g\beta\vec{H}\cdot\vec{S} \qquad (S=1)$$

Where $D<0$. Ground state doublet $|\pm1\rangle$ splits and $|+1\rangle$ is lifted by a magnetic field parallel to z axis. At H_c $(=D/g\beta)$ excited singlet $|0\rangle$ and $|+1\rangle$ make a cross. Spin population of ground state lifts up to the crossing point by appling a pulsed magnetic field. Sweep rate of pulsed magnetic field must be fast enough compared with cross-relaxation rate with which the spin population redistributes, that is, no trantition allows in the course of the magnetization process. This process is considered to be adiabatic maznetization cooling among excited $|0\rangle$ and $|+1\rangle$

and spin temperature is defined among two states low enough around H_c, spin ordering should occur in the excited state. This spin ordering is the same as that of the spin ordering of ground state singlet. We succeeded to observe spin ordering among excited levels of $NaNiAcac_3$benzene. The excited state spin ordering, however, breaks down in a moment just at H_{c1}. This is due to cross-relaxation among three spin levels which is very fast at H_c. In order to observe the spin ordering at the magnetic field higher than H_c, we make miniature pulse coil which can produce the pulsed magnetic field. We could not detect the phase boundary at higher magnetic field corresponded to H_{c2} which is described by Tachiki et al[2].

References (I)

1. C.M.Fowler, W.B.Garn, R.S.Caird: J. Appl. Phys. 31(1960) 588.

2. M.Tachiki, Y.Yamada: Suppl. Prog. Theor. Phys. 46(1970)291

Chap. II. Pulsed Adiabatic Demagnetization

§ 2.1. Introduction

In this part we describe the experiment to determine the characteristic time of spin ordering. Generally speaking a spin system needs a certain time to build up an ordering spin arrangement. We call such charactaristic time ordering relaxation time τ_{ord}. τ_{ord} depends on many factors such as type of interaction, dimension, spin structure and anisotropy and so on. A.C.susceptibility measurement is useful for studying relaxation phenomena in general but not suitable for the measurement of τ_{ord}. The reason is the following. In this method, the response is measured corresponding to the small excitation on the system. The system is, therefore, in either ordered or disordered state and only the small deviation from the equilibrium state is studied. Experiment on the pulsed adiabatic demagnetization is, however, most direct method of inducing the order-disorder transition. In this type of experiment, the process to be observed is not even quasi-static but non equilibrium. The time constant τ_{ord} for spin ordering is given by detection of the formation through total response of magnetization.

When the magnetic field passes through zero field at low enough initial temperature T_i and large (dH/dt) , magnetization can't follow the reversal of the magnetic field. This, we call as a negative magnetization. If this spin system is settled in a thermal equilibrium state, the spin temperature can be defined and it is negative. In the latter part we will discuss the negative magnetization and spin temperature.

§ 2.2. Experimentals

2.2.1 Sample

Single crystal of Cs_3CoCl_5 is obtaind by slow evaporation of saturated aqueous solution which contains $CoCl_2 2H_2O$ and few excess moles of CsCl.

The crystal structure of Cs_3CoCl_5 was determined by Powell et al.[1] and Figgis et al.[2]. The crystal structure is tetragonal as shown in Fig.1. The dimensions of tetragonal unit cell are 9.219 ± 0.005 A along a and b axis, and 14.554 ± 0.007 A along the c axis at room temperature. The unit cell contains four molecules of Cs_3CoCl_5 and it is divided into two parts. Each part is equivalent except for a rotation of the $CoCl_4$ and mirror-reflection of $ClCs_4$. Since the exchange interactions between Co^{2+} ions are not influenced by the Cs^{+1} ions, we assume all Co^{2+} ions are identical. Therefor the dimension of unit cell can be reduced as $\sqrt{2}/2$ a = 6.519 A and c/2 = 7.277 A. This unit cell is drawn by thick line in Fig.1.

Co^{2+} ions are surrounded tetrahedrally by four chlorine ions. ^4F state of free Co^{2+} ion is split into two triplets T and lowest singlet $^4A_2$. The fourfold spin degeneracy of $^4A_2$ is lifted to two Kramers doublets by the uniaxial distortion of the crytalline field. Therefore the spin Hamiltonian for Co^{2+} ion is given by

$$\mathcal{H} = D[S_z^2 - S(S+1)/3] + g_{\parallel}\beta H_z S_z + g_{\perp}\beta(H_x S_x + H_y S_y) \quad (S=3/2) \quad (1)$$

where $D = -4.31 \pm 0.04$ cm^{-1}, $g_{\parallel} = 2.41$, $g_{\perp} = 2.33$ [3].

The energy levels are given in Fig.2. The energy defference between two doublets is $2|D|/k = 12.4$ K . At liq. He^4 temperature, the energy of the spin system is described only by

$S_z = \pm 3/2$. Therefor we can regard the spin system as the effective spin $S' = 1/2$, $g_{//} = 7.2$ and $g_{\perp} = 0$ below liq. He^4 temperature region.

Huiskamp et al.[4] measured susceptibility and heat capacity of Cs_3CoCl_5 and concluded that Cs_3CoCl_5 is three dimensional Ising antiferromagnetic spin system and Neel temperature T_N is 0.527K. The phase diagram is shown in Fig.3. The asymptotic value of the critical field H_c at absolute zero is approximately 1900 Oe.

Mess et al.[5] obtained spin-lattice relaxation times at various temperatures 1.2 and 4 K and magnetic fields (up to 4kOe) by a.c.susceptibility measurement. The temperature dependence of the spin-lattice relaxation time is given by

$$\tau_{1s} = 0.83T^{-7} \quad \text{sec} \quad (2)$$

There is not so noticeable dependence of the relaxation time on the external magnetic field. They may indicate that spin-lattice relaxation is dominated by Raman process. Cross-relaxation time are also measured by Roest[6]. Results are given in table 1.

Table 1. Observed values of Cross-relaxation time of Cs_3CoCl_5

CR process	H (kOe)	(μsec)
1	15.2	>4
2	18.9	2
3	25.5	0.4
4		
5	38.2	<<0.2

CR processes are shown in Fig.2.

Direct measurement of exchange interaction was performed by Van Staple et al.[7] They observed the ESR spectrum of pairs Co^{2+} ions in Cs_3ZnCl_5 doped with 3% Co^{2+} ions. Cs_3ZnCl_5 is isomorphous with Cs_3CoCl_5. The lattice parameters of Cs_3ZnCl_5 were determined from X-ray diffraction of powder sample a= 9.251$\pm$0.005 A and c= 14.500$\pm$0.007 A . The exchange constant for the nearest neighbor Co^{2+} pairs in parallel to c axis is

$$J_c/k = 0.0154 \quad K$$

For the nearest neighbor Co^{2+} pairs in plane perpendicular to c axis is

$$J/k = -0.0204 \quad K$$

Local field H_{loc} is calculated using J_c,J and dipole interaction is

$$H_{loc} = 1040 \quad Oe$$

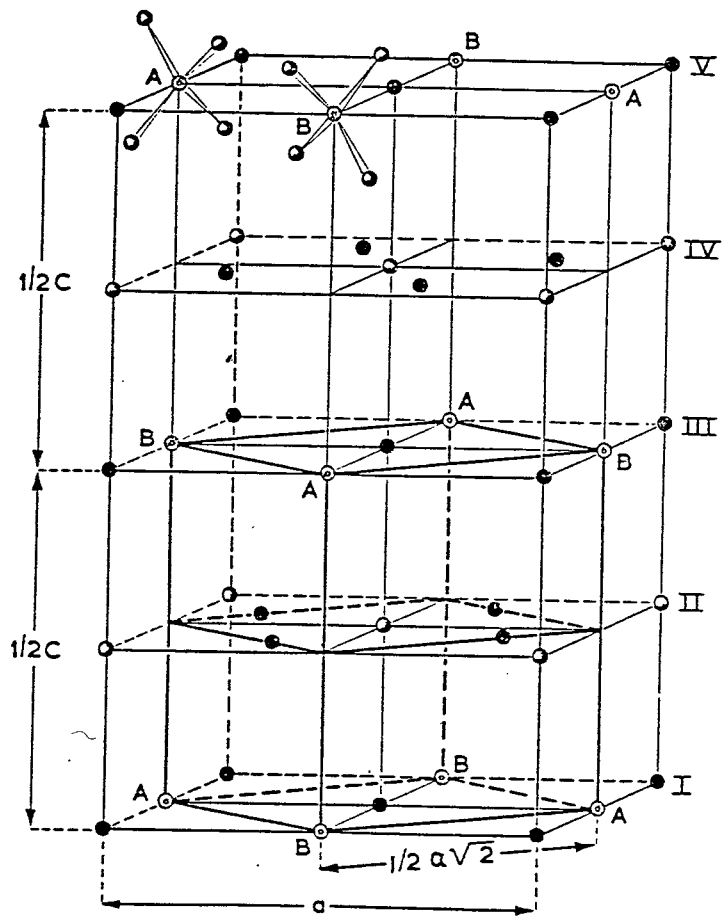

Fig. 1. Crystal structure unit cell of $CoCs_3Cl_5$

● Cs^+ ⊛ Co ◐ Cl

The chlorine tetrahedra at position A and B are rotated around the *c* axis with respect to each other.

Plane II differs from plane IV by a mirror reflection. The parallelepiped indicated by thick lines is the simple Co-Bravais lattice mentioned in the text.

$\frac{1}{2}c = 7.277$ Å $\quad a = 9.219$ Å $\quad \frac{1}{2}a\sqrt{2} = 6.52$ Å

ref. 4)

Fig. 2 Energy level scheme of Cs_3CoCl_5

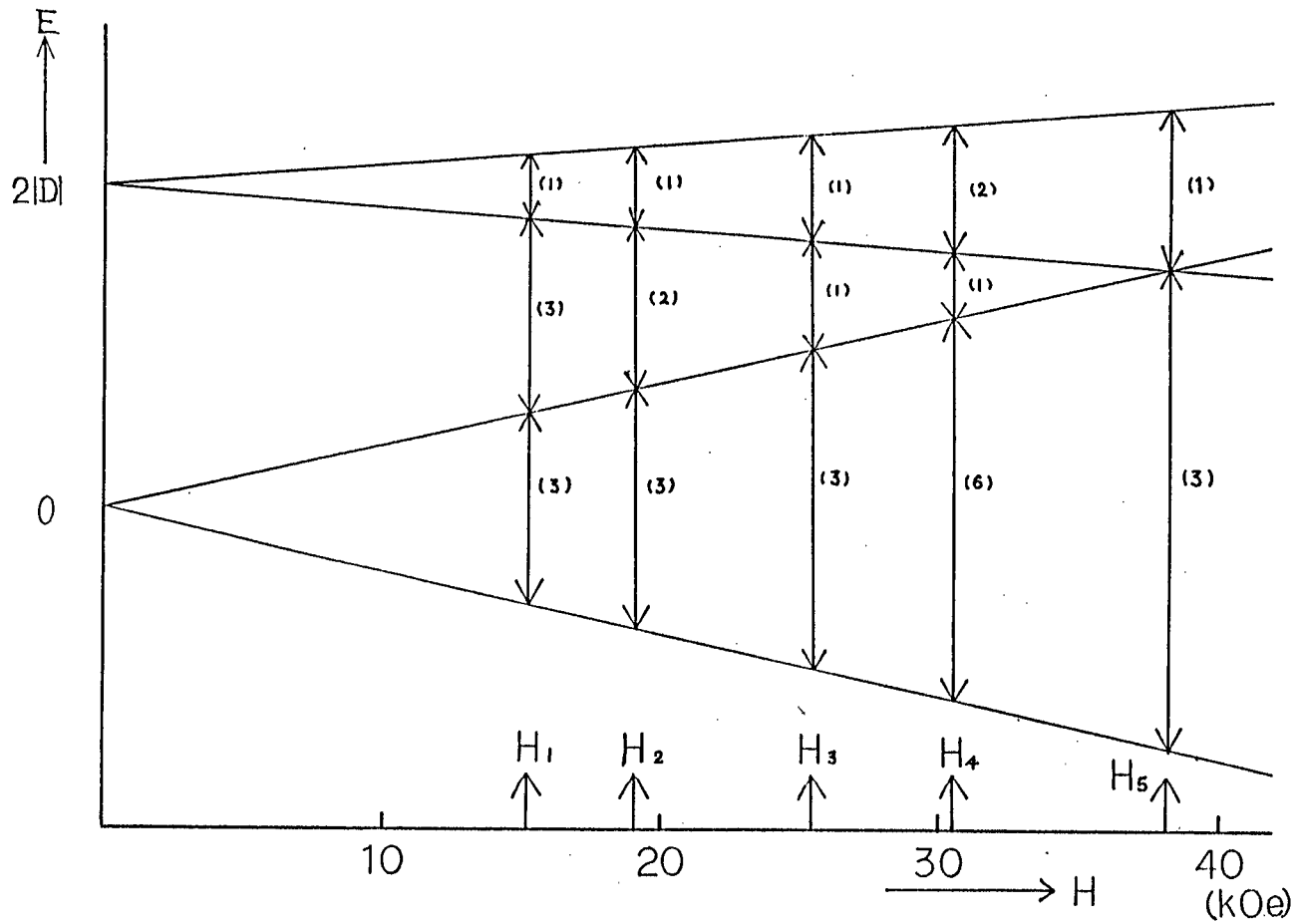

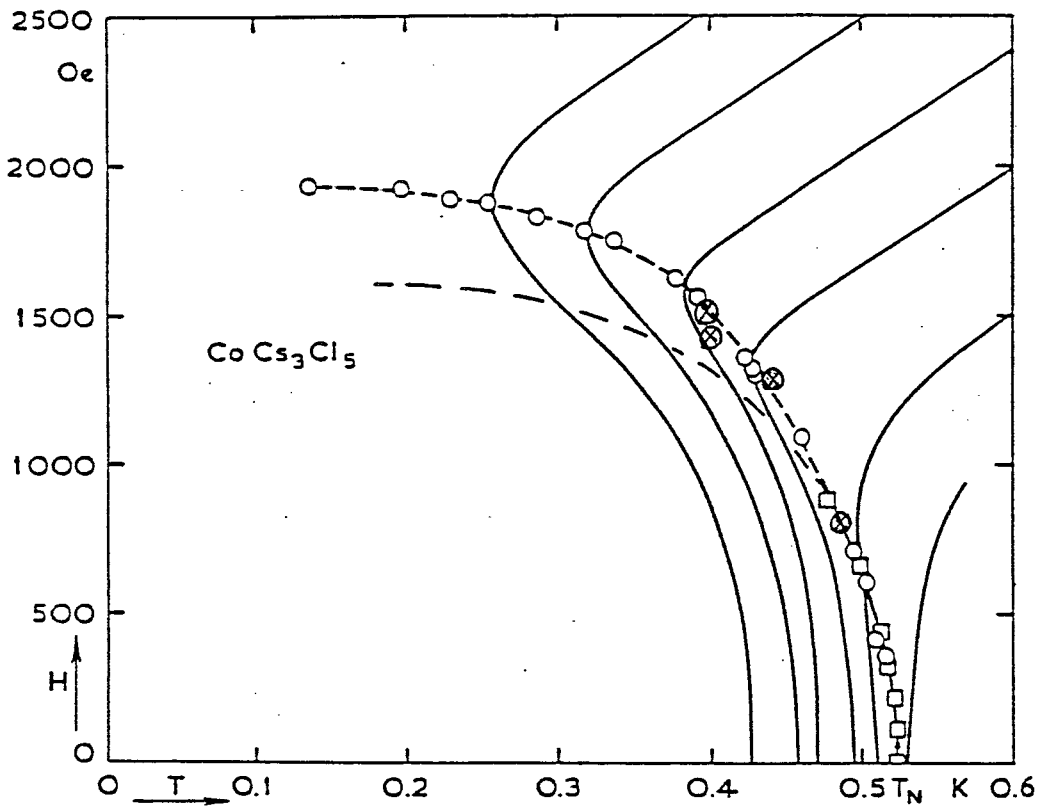

Fig. 3 Phase diagram of $CoCs_3Cl_5$. The drawn line are isentropes , the circles indicate the temperature minima in these isentropes; the locus of these minima is indicated by the upper dashed line (phase boundary); the lower dashed line indicates the locus of inflection points of the isentropes. The square points are obtained from heat capacity measurement.
⊗ are obtained by our χ' measurement described in § 2.3.3.

ref. 4)

2.2.2. Experimental apparatus

Experiment on a pulsed adiabatic demagnetization cooling is performed by combining two types of magnet; one is steady and the other is transient type. Combination of a superconducting solenoid and a pulsed magnetic coil is most suitable for our purpose. When a pulsed magnetic field is applied, an induced voltage appears across the superconducting solenoid by the inductive coupling between two coils. At first, we made a compensated pulse coil. This coil consists of two layers wound coaxially but oppositely each other connected in series. Each turn and cross-sectional area of two coils are determined as the total fulx outside the coil to cancell but the magnetic field inside to remain. Later, non compensated single layer pulsed coil is tried. There is no trouble on the superconducting solenoid and a constant current power supply using the latter system. Therefor, we use mainly the latter type on the experiment.

An apparatus which can produce two pulsed magnetic fields is also made. The pulse magnet consists of two coils which are wound coaxially. By two timing circuits and condenser banks the sequence and hight of pulsed field are controled. The coil system is shown in Fig.4.

The time derivative of the magnetization dM/dt is measured using a conventional pick up coil system. The magnetization is obtained by the integration of dM/dt with a Miller-integrator. The pulsed magnetic field is also obtained using the integration of the voltage across a search coil. Integrators of Miller's type are constructed by high speed operational amplifiers. Signals are stored in a digital memory Biomation 8100 and IWATSU

DM-901, and recorded in a X-Y recorder.

A.C.suscetpibility is measured in a static magnetic field. A He^3-He^4 dilution refrigerator is used for cooling a sample below 1K. The thermometer is a fixed chip resistor of TBL100F20 manufactured by ALPS ELECTRIC CO., LTD. A.C.susceptibility measurement is performed with Hartshorn bridge at a frequency from 20Hz to 2kHz.

Fig. 4 Pulsed coil and superconducting magnet.

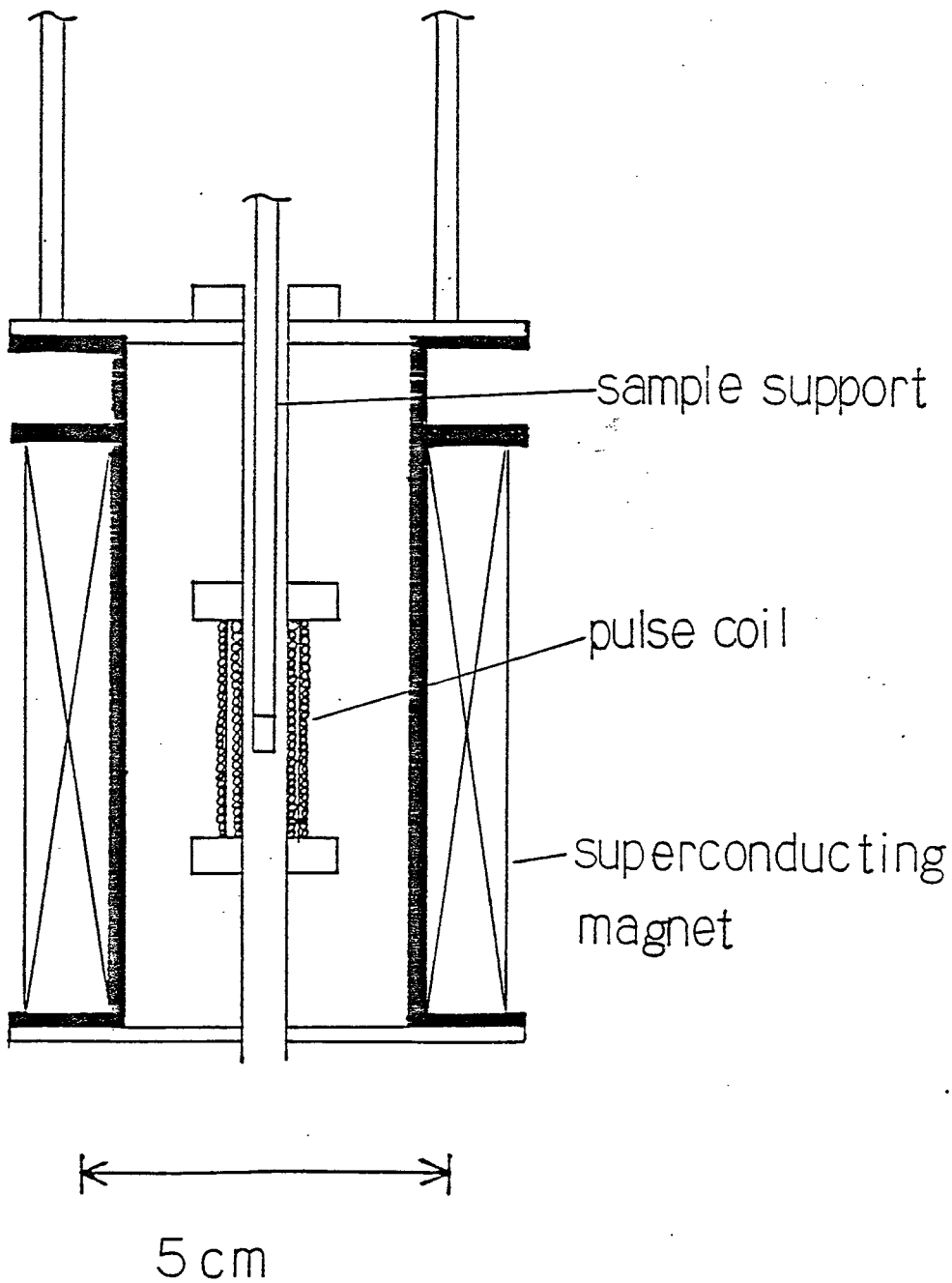

2.2.3. Experimental procedure

The initial state is in a high magnetic field which are produced the by superconducting magnet. All spins are aligned by the magnetic field at low enough initial temperaure. Then, a pulsed magnetic field is applied so as the total magnetic field H_t to cancell. When the total magnetic field H_t decreases down to the order of the local field H_{loc} of the spin system ,the spin starts ordering and settles in the ordered state within the local field.

In this process, spin system could be in ordered state for time interval τ given by

$$\tau = 2H_{loc}/(dH/dt) \qquad (3)$$

where (dH/dt) is the sweep rate of the pulsed magnetic field around $H_t=0$. In our experiment, the sweep rate dependence of the time derivative of the total magnetization dM/dt is observed.

We describe here a comparison of the pulsed adiabatic demagnetization with the usual adiabatic demagnetization method. Usual method of adiabatic demagnetization cooling has been done using steady magnetic fields. In the experiment, cooling substance is isolated thermally from surroundings. The magnetic field is decreased slowly to keep the process in isentropic condition. Then, in the course of demagnetization, the spin tempearture is neary equal to the lattice. Therefor both spin and lattice are cooled at the same time in the process.

In our method, we are using a pulsed magnetic field. If the pulse duration time τ_p is much smaller than spin-lattice relaxation time τ_{ls} , only the spin system cooles itself. The spin system under the pulsed magnetic field is isolated from

lattice. Therefor, we can observe spin ordering described by the temperature of spin itself.

§ 2.3. Experimental results

2.3.1. Ordering relaxation time

Fig.5 shows typical example of experimental results. The double peaks of dM/dt is observed and each of them corresponds to the metamagnetic phase transition. An antiferromagnetic spin ordering exists between peaks. The initial temperature dependence of dM/dt in a decreasing field around zero field is shown in Fig.6 when the initial temperature T_i is changed from 4.2 to 2.21K. Fig.7 shows dM/dt when T_i is below 2.21K. Initial static magnetic field H_i is 10kOe and the sweep rate of pulsed magnetic field dH/dt at zero field is 6.5×10^{7} Oe/sec for all cases. Double peaks become sharp when T_i is decreased. But when T_i is lower than 2.21K, the second peak becomes small. Finally the second peak disappears below at T_i=1.8K.

In Fig.8, dM/dt obtained in the temperature range 4.2 K $>T_i>$2.81 K with $dH/dt=0.53\times10^{9}$ Oe/sec is shown. dM/dt in lower temperature range 2.81 K $>T_i>$1.30 K is shown in Fig.9. Fig.9 shows the second peak vanished below T_i=2.1 K. Thus we obtain many pairs of the critical starting temperature T_i^c and the critical sweep rate $(dH/dt)^c$. When T_i is lower than T_i^c at sweep rate $(dH/dt)^c$, the second peak disappears. In order to estimate τ_{ord}, we suppose that antiferromagnetic spin ordering is not established when the second peak vanishes. τ_{ord} is given roughly by the time passing through local field at the condition the second peak vanishes as below.

$$\tau_{ord} = 2H_{loc}/(dH/dt)^c \qquad (4)$$

In Fig.10 the initial temperature dependence of τ_{ord} at H_i=10kOe is shown. θ given in Fig.10 is the angle between pulsed

magnetic field and steady field. The magnetic field perpendicular to crystal c axis is about 900 Oe at $\theta = 5^{\circ}$ when the magnetic field parallel to c axis is zero.

Fig. 5 dM/dt, magnetic field and M.

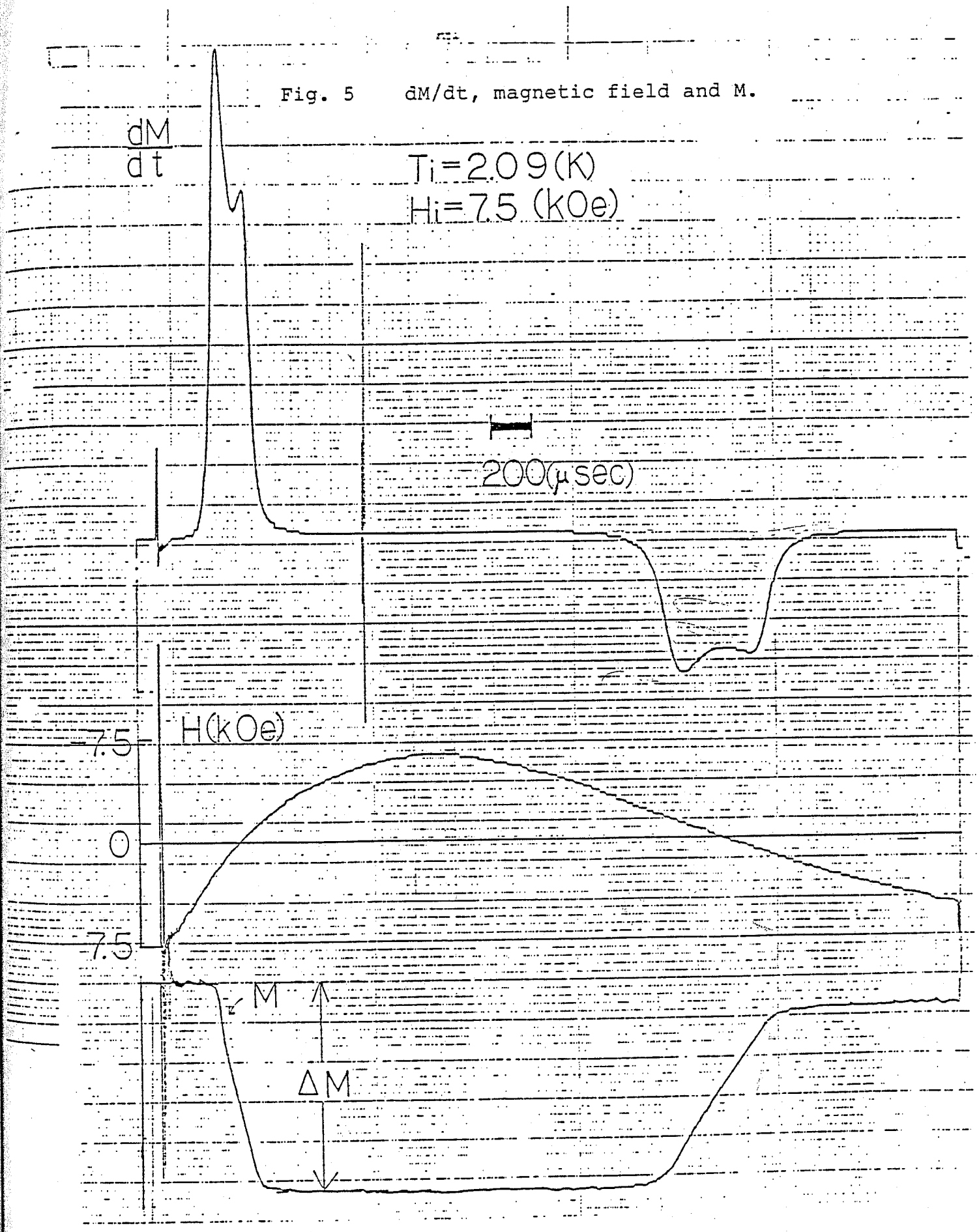

Fig. 6 dM/dt around zero field in Cs_3CoCl_5

4.21K ≧ Ti ≧ 2.21K, Hi = 10KOe and dH/dt = 6.5×10^7Oe/sec

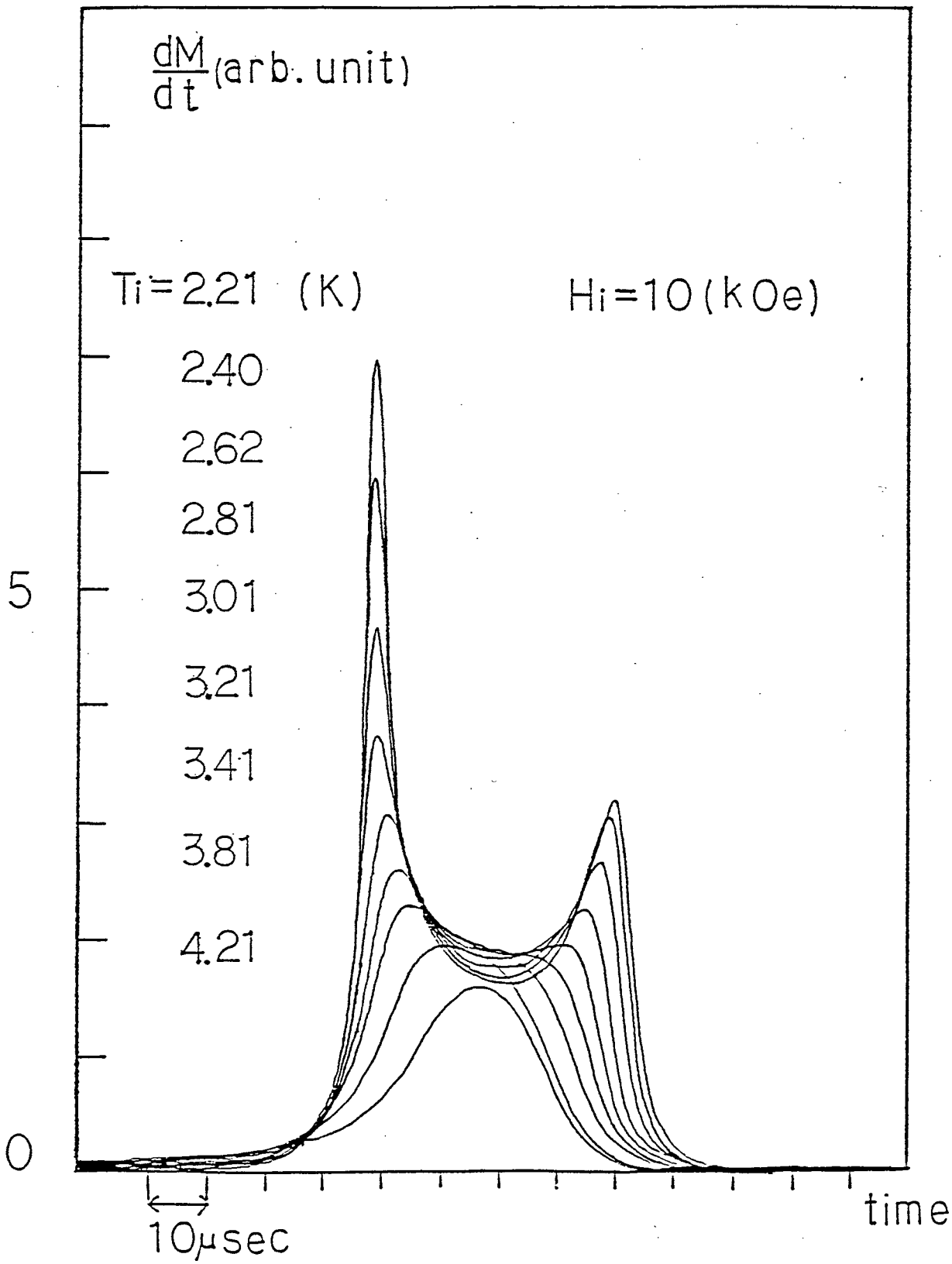

Fig. 7 dM/dt arpund zero field in Cs_3CoCl_5

2.00K ≧ Ti ≧ 1.28K, Hi = 10kOe and dH/dt = 6.5×10^7Oe/sec

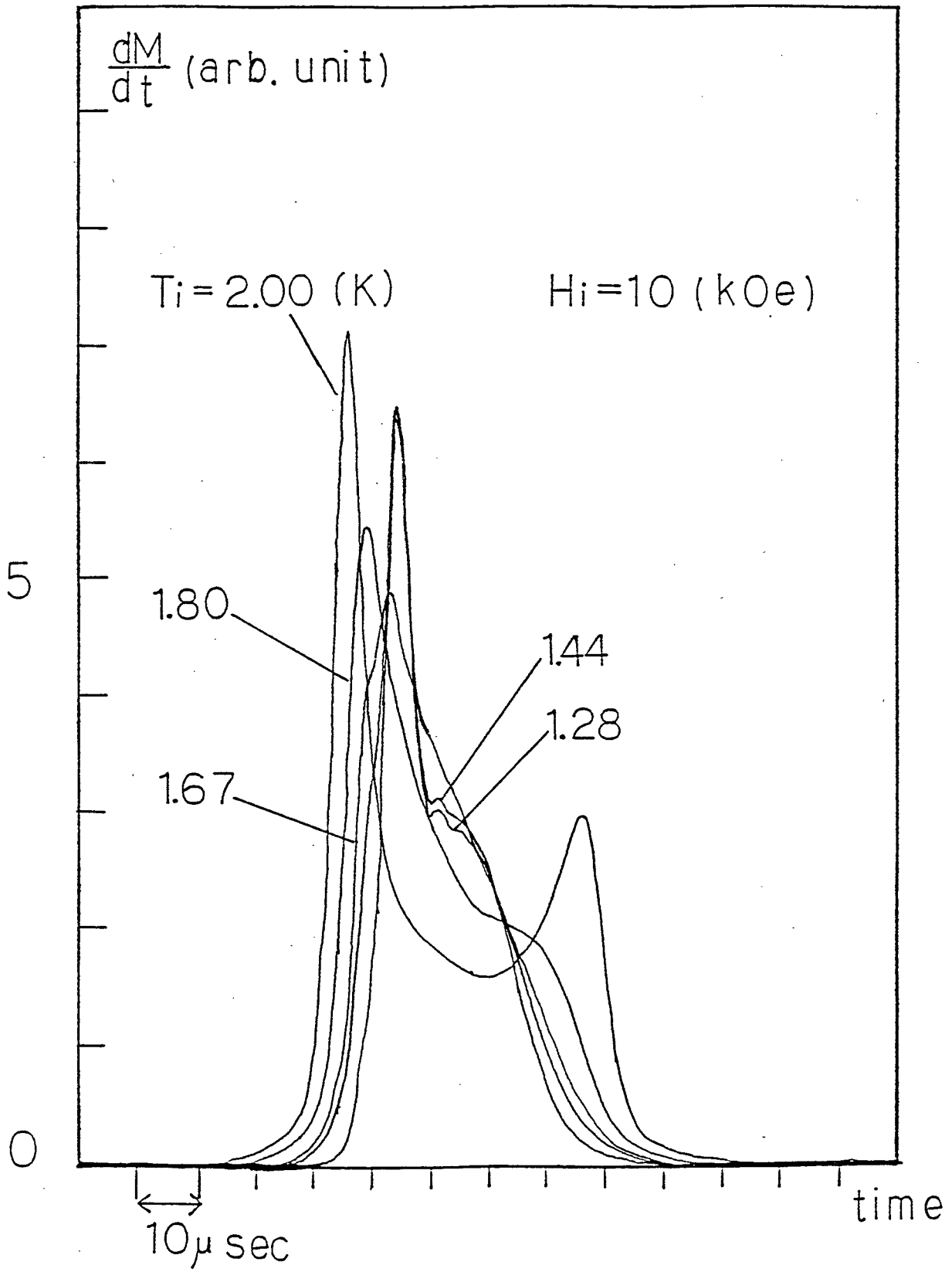

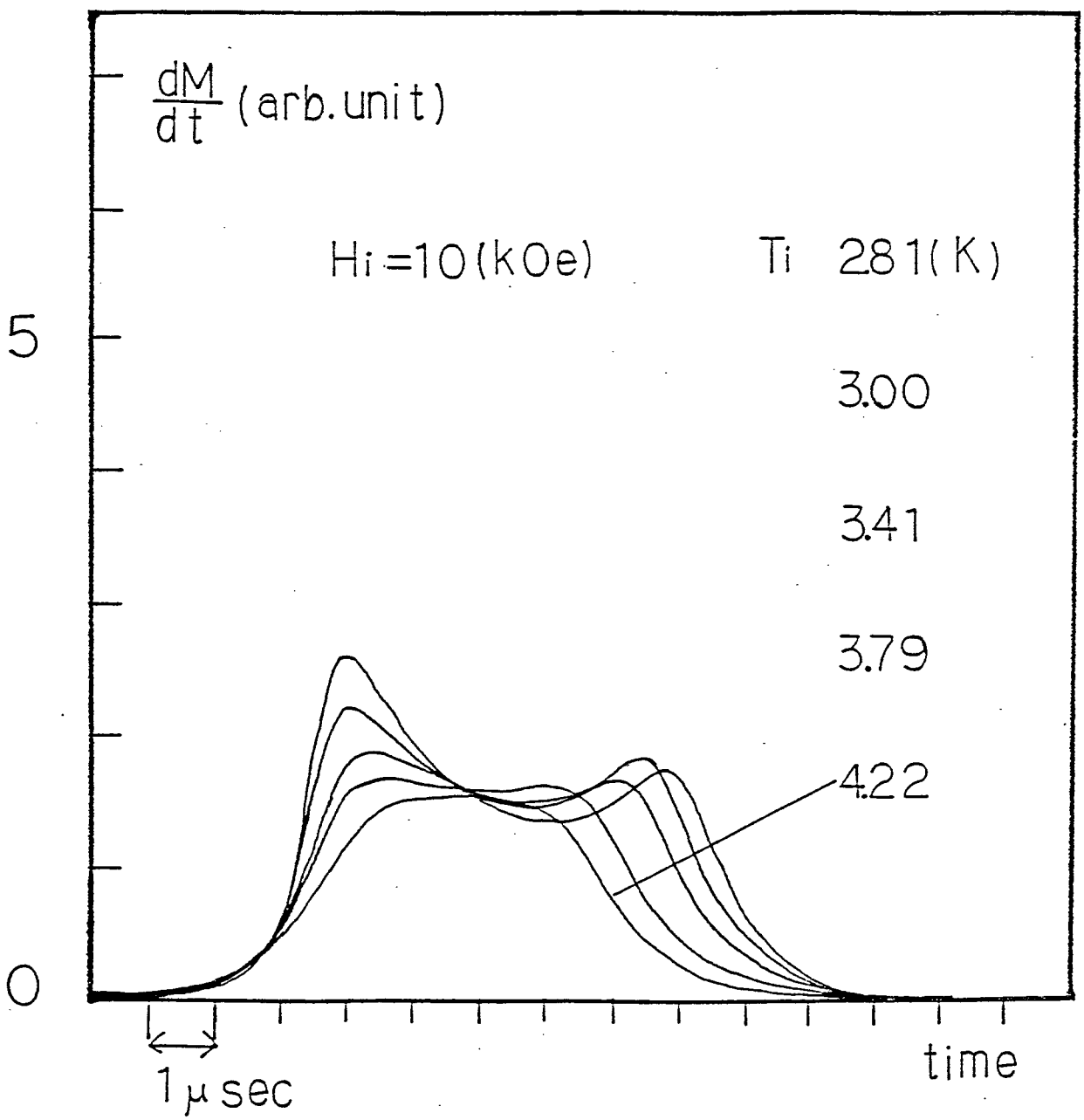

Fig. 8 dM/dt around zero field in Cs_3CoCl_5

4.22K ≧ Ti ≧ 2.81K, Hi = 10kOe and dH/dt = 0.53×10^9Oe/sec

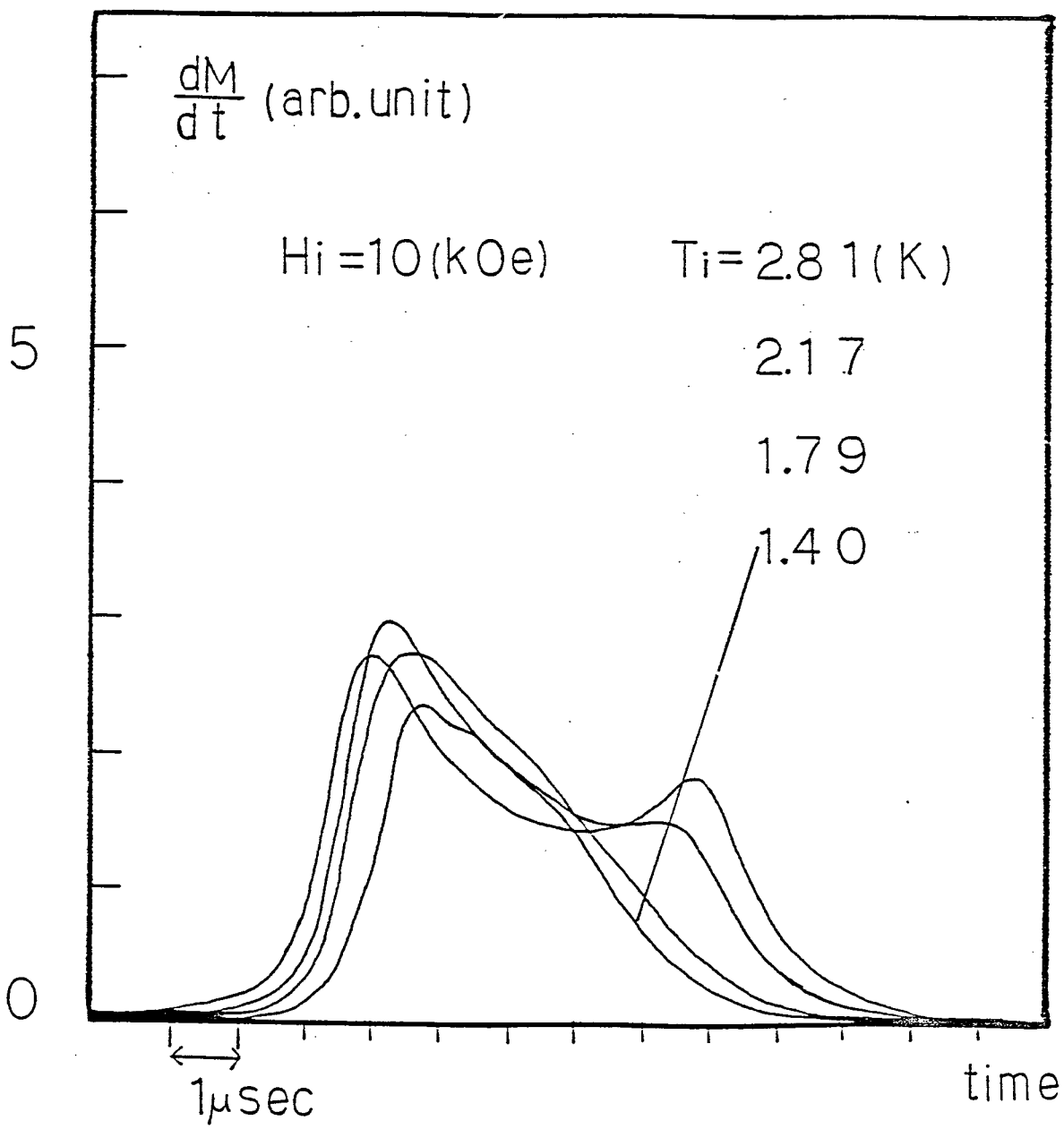

Fig. 9 dM/dt around zero field in Cs_3CoCl_5
2.81K ≧ Ti ≧ 1.40K, Hi = 10kOe and dH/dt = 0.53×10^9Oe/sec

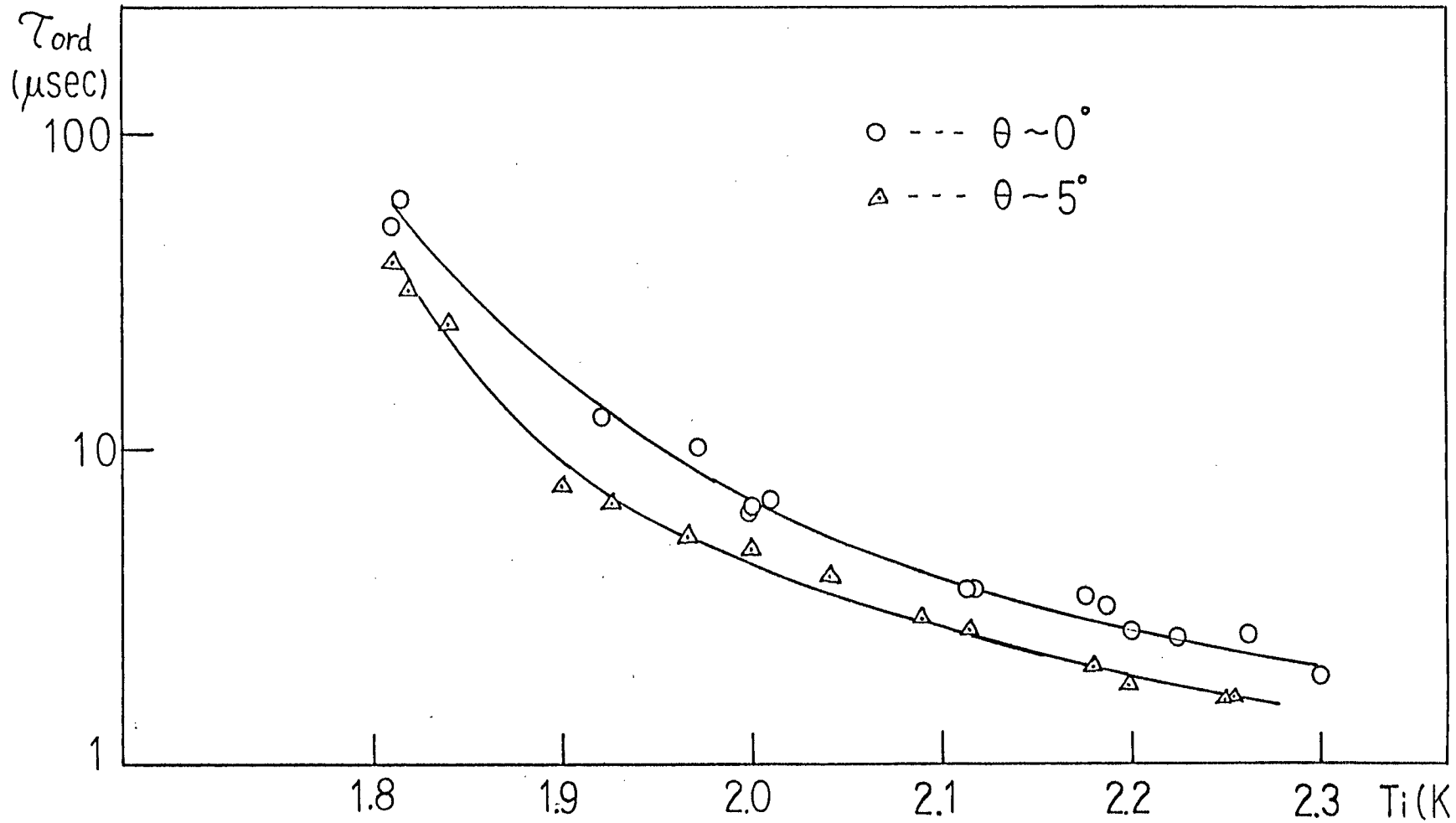

Fig. 10 τ_{ord} vs. Ti θ is given in the text.

2.3.2. Negative magnetization

As discussed in the last section, when starting T_i is low enough and the sweep rate of the magnetic field (dH/dt) is large enough, the spin ordering can not be established. In this section we will describe the change of the magnetization M when T_i is lower and (dH/dt) is larger. The sweep rate dependence of dM/dt at T_i=1.32K, H_i=15kOe is shown in Fig. 11. At this initial temperature the double peaks do not appear under the lowest sweep rate in our experiment. The distinctive feature of dM/dt appeares when sweep rate of magnetic field is large. The sence of dM/dt in a increasing magnetic field (corresponding to the second peak) changes from negative to positive (see Fig.11(c),(d)). This reversal of the sign of dM/dt suggests the establishment of the negative magnetization as described following. In order to discuss quantitatively, we measure the magnetization M by integration of dM/dt. Typical result of the magnetization M, dM/dt and H at T_i=2.09k ,H_i=7.5kOe is shown in Fig.5. We define M as shown in Fig.5. ΔM is the change of magnetization from starting value $M_i(T_i,H_i)$ to the value M when a magnetic field is reversed. If population of each level is constant in the course of demagnetization, ΔM is twice as large as starting value $M_i(T_i,H_i)$. The sweep rate and T_i dependence of ΔM is given in Figs.12,13,14. In the limiting case of slow sweep rate, ΔM is twice as large as the equilibrium $M_i(T_i,H_i)$. At T_i=3.50K and H_i=10kOe, however, M becomes small when (H/dt) is small as shown in Fig.12. The reason for this is given below. At T_i=3.50K, the population of upper doublet $S_z=\pm 1/2$ is about 2.8%. The magnetization can be changed by cross-relaxation among

four levels when sweep rate is small. Thus the $M_i(T_i,M_i)$ is not obtained in limiting case of the slow sweep rate in Fig.12. M is, however, almost constant when $(dH/dt) > 0.5\ 10^9$ Oe/sec. In this case total M can follow the reversal of the magnetic field and the constant value of M shown as dotted line in Fig.12 indicates twice as large as the equilibrium M_i at T_i=3.50K and H_i=10kOe. At T_i=2.07K and H_i=10kOe, M increases when (dH/dt) becomes small as shown in Fig.13. We obtain the 2Mi by an extraporation for (dH/dt) =0. Thus we determine the saturation M_s by comparing theoretical values of M_i at various T_i's. From this value we can determine M_i at T_i=1.18 K and H_i=10kOe. $M=M_i(T_i=1.18K,H_i)$ is shown as dotted line in Fig.14. Under this line the direction of M is same with that of starting magnetic field, while the direction of the magnetic field is, now, reversed. Cosequently, M is opposed to the new direction of the field. At T_i=1.18K and H_i=10kOe, we can obtain negative magnetization state when $(dH/dt) > 0.08\ 10^9$ Oe/sec.

There is another method to obtain M_i. At a certain sweep rate, the dM/dt signal in increasing magnetic field disappears . Under the sweep rate, M in decreasing field is just equal to $M_i(T_i,H_i)$ or M at $H_t<0$ is equal to zero if second reversal of the magnetic field is adiabatic. The observed saturation magnetization M_s is about 7% larger than the value which is obtained by the first method. We adopt the latter value because the latter method is more direct measurement.

By further investigation, we tried experiments on the sequence of two pulsed magnetic fields. Results are shown in

Fig.15. The arrows indicate the sense of the magnetic field. When it points up, the sense of the magnetic field is the same as the direction of starting steady magnetic field produced by the superconducting magnet. The reversal of the magnetic field repeats four times while two pulsed fields are applied. At the first reversal of the magnetic field a negative magnetization is produced as is shown in Fig.14. Before the second reversal of the magnetic field the magnetization is positive and the magnetic field is negative, so the magnetization is negative, in other word, spin temperature is negative if it can be defined. We call negative magnetization when the sense of the magnetization is same with the sense of the magnetization keeping negative spin temperatuer. Before the seconed reversal of the magnetic field, the magnetization is decreased down to 27% of the saturation magnetization. This corresponds to the magnetization at T=-8.7K, H=10kOe and S/R=0.28 for ground doublet. The socond reversal is not considered to perfect adiabatic, for the magnetization after the revasel is about 14% of saturation value. Except for small decay of magnetization which may be due to cross-relaxation, the changes of the magnetization seem almost reversible at the third and fourth reversal. The establishment of negative spin temperature is not concluded from present work only, however.

In Fig.16, the time interval of two pulsed magnetic fields is 420 sec. The recovery of magnetization from negative to positive appears. This recovery is due to cross-relaxation among four levels ($S_z=\pm 3/2, \pm 1/2$). In this process, the population of upper doublet is increasing. At the third reversal the population of upper doublet begines to join the cross-

relaxation among four spin levels around zero field, so at the third and fourth reveral of magnetic field, the change of magnetization is not adiabatic(isentropic).

In order to obtain large negative magnetization, a pulsed adiabatic demagnetization starts at He^3 temperature range (>0.5K). We use only one pulsed magnetic field and sweep rate is not so fast to accomplish thermal equilibrium state around zero field. dM/dt and M are observed at the same time. From the M after the first reversal of the magnetic field, we determined the entropy of the system or H/T. This value corresponds to the initial condition of second reversal of the magnetic field. Result is shown in Fig.17. Temperatures given in Fig.17 are obtained above at H=10kOe.

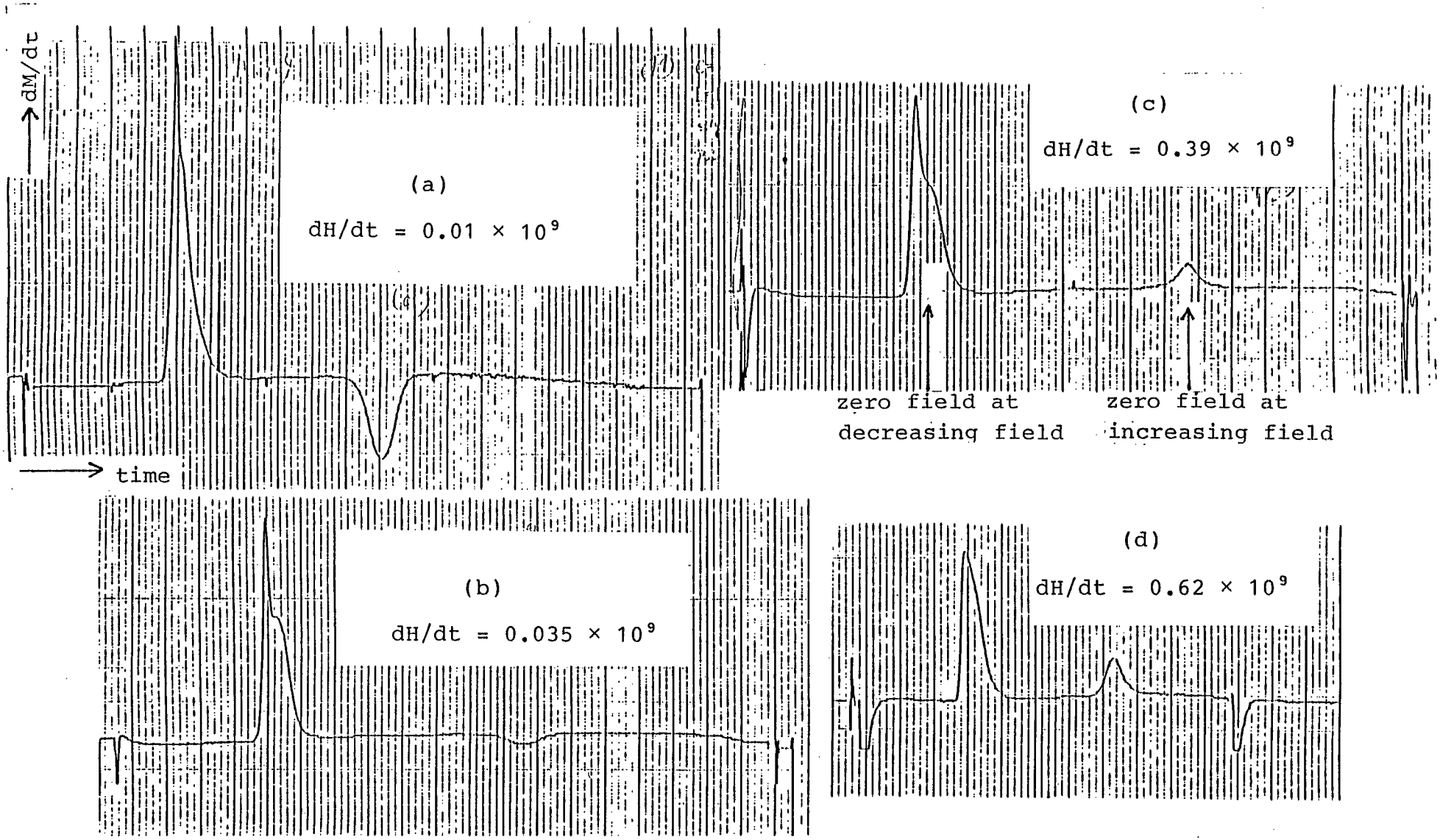

Fig. 11 dM/dt at various sweep rate T = 1.32K and Hi = 15kOe

Fig. 12 ΔM vs. dH/dt

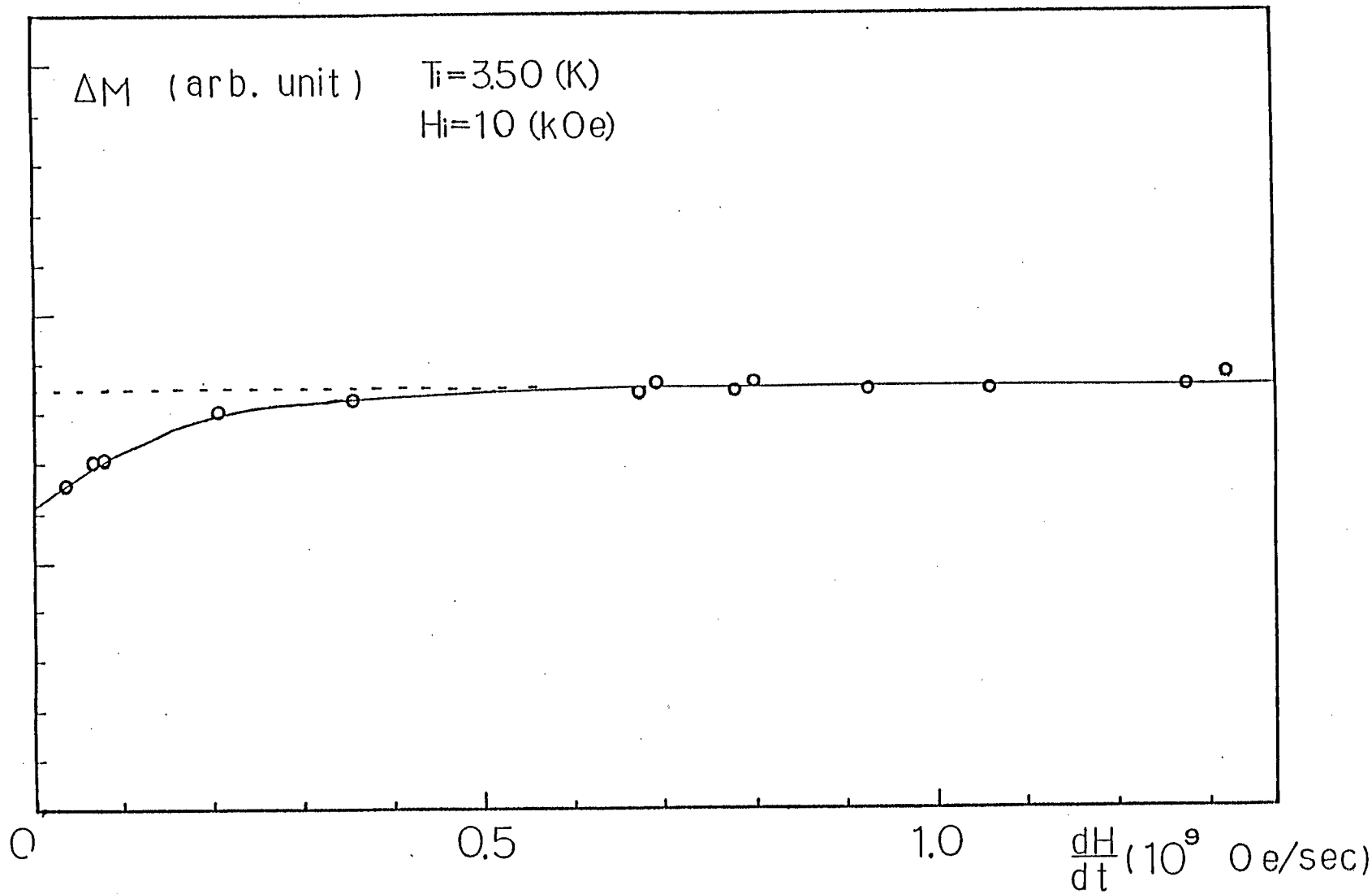

Fig. 13 ΔM vs. dH/dt

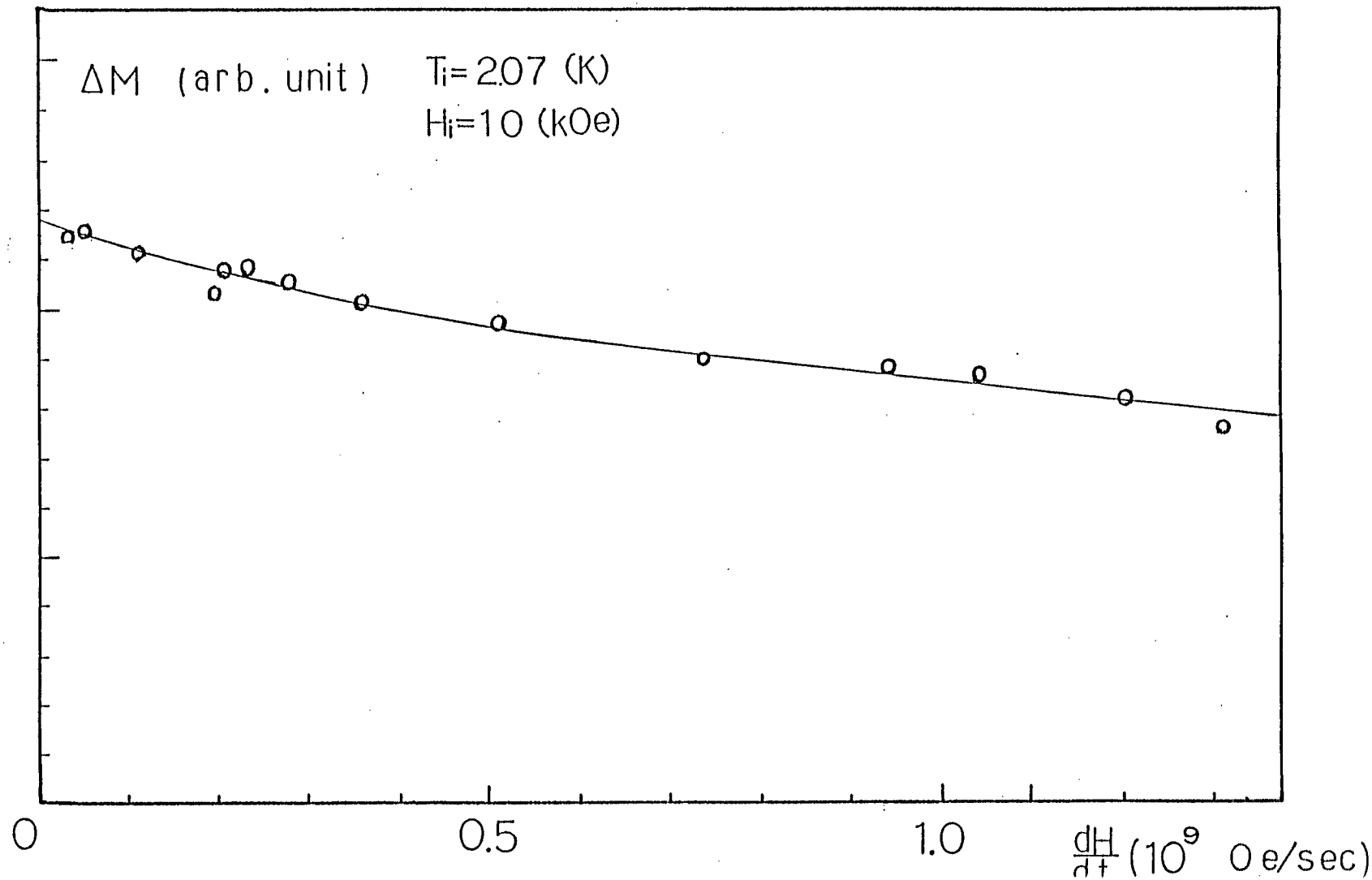

Fig. 14 ΔM vs. dH/dt

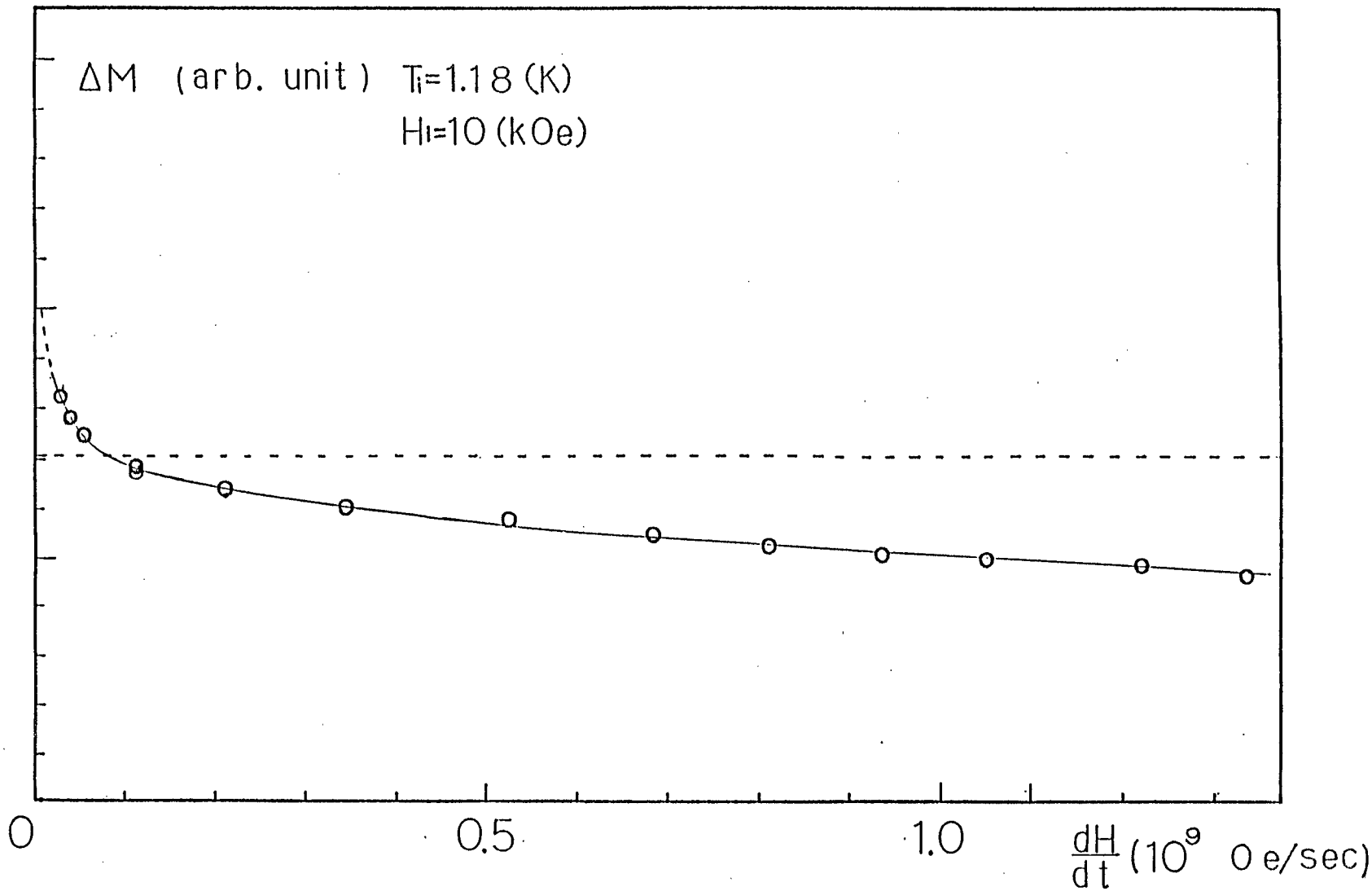

Fig. 15 M and H double pulsed magnetic field.

Time interval of two pulses is 40μsec.

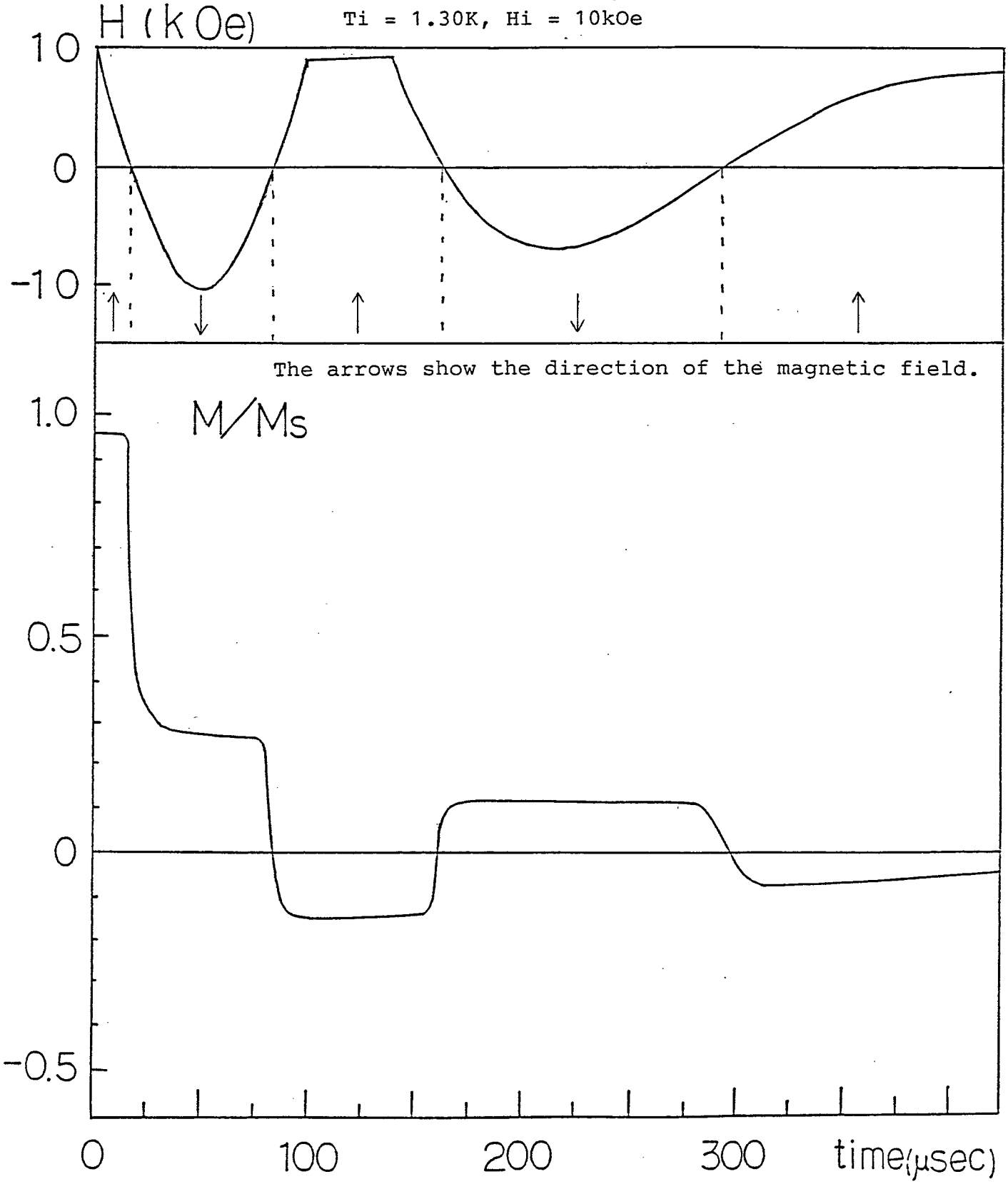

Fig. 16 M and H under double pulsed magnetic field.

Time interval of two pulses is 420μsec.

Ti = 1.30K, Hi = 10kOe

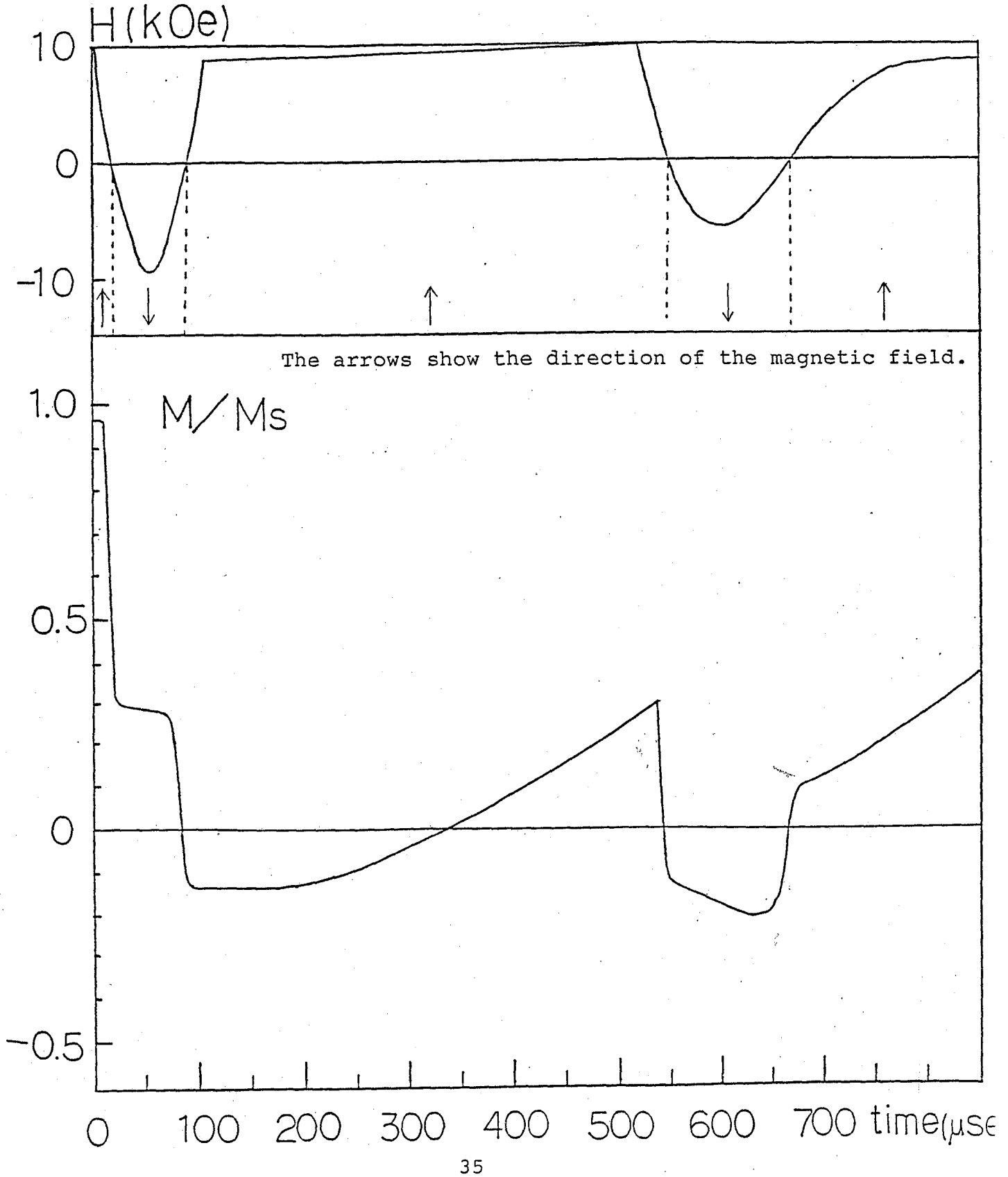

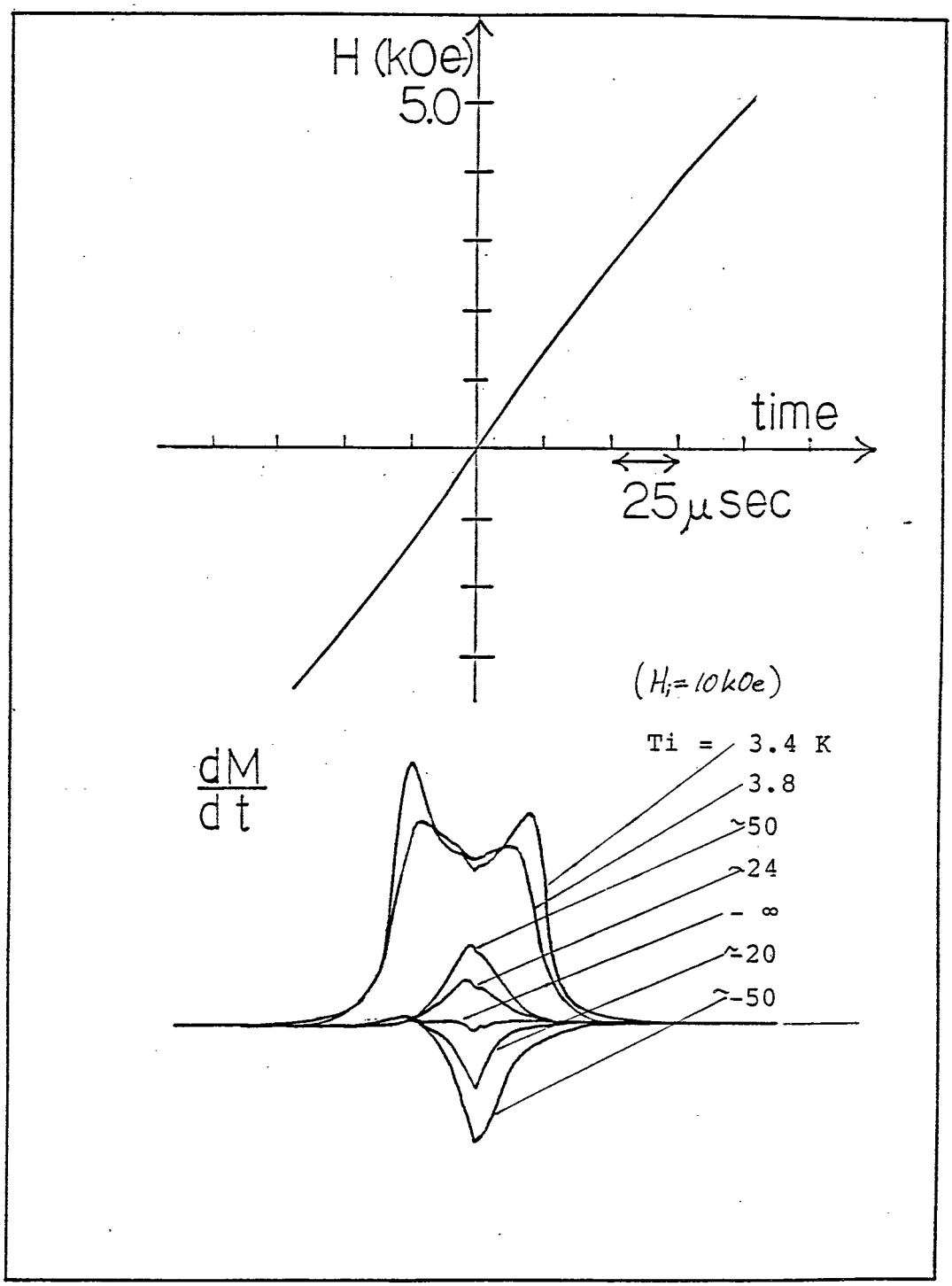

Fig. 17 dM/dt under pulsed adiabatic demagnetization. Ti is calculated from magnetization corresponds to Hi=10kOe .

2.3.3. A.C.susceptibility measurement in a static magnetic field

As we discussed in the previous section, the experiment on a pulsed adiabatic demagnetization gives direct detection of the dynamics of the spin ordering but a.c.susceptibility measurement gives a response corresponding to the small a.c.field applied to the system in thermal equilibrium. Thus a.c.susceptibility can not give direct information about time duration of the formation of ordered spin arrangement. This method, however, gives some important informations about relaxation in equilibrium state. We measured a.c.susceptibility of Cs_3CoCl_5 under static magnetic field below T_N.

A.C.susceptibility measurement is performed by using Hartshorn bridge at frequency range from 20Hz to 2kHz. A crystal is directly immersed in liq.He^3 which is cooled by the standard dilution refrigerator through Cu wires. The susceptibilities parallel to the c axis are measured in the magnetic field applied parallel to the c-axis. The susceptibility vs. H curves at several temperatures are shown in Fig.18. Results are shown only in the case of increasing field. There appears a peak of susceptibility in magnetic field of 1500 Oe at 0.392K. This peak corrsponds to a jump of a magnetization from antiferromagnetic to paramagnetic state. The obtained H_c are plotted in the phase diagram determined by Huiskamp as shown in Fig.3.

The frequency dependence of susceptibility at 0.392K in the magnetic field is shown in Fig.19. The susceptibility strongly depends on frequencies and does not give isothermal

susceptibilities in the magnetic field even at 20 Hz. We estimate roughly a spin-spin relaxation time where susceptibility recovers half of the isothermal value and obtain,

$$\tau_s \gtrsim 0.1 \quad \text{sec}$$

As described, τ_{ord} is of the order of microsecond. In comparison with τ_{ord}, τ_s is long by several orders of magnitude. τs gives roughly a time to establish a thermal equilibrium within a spin system. While τ_{ord} gives roughly a time to build up an antiferromagnetic arrangement. This arrangement is determined by a local free energy of the spin system, for this transition is of the first order. According to the above simple idea, antiferromagnetic arrangement itself may be established independently with the internal thermal equilibrium of the spin system defined by the so-called spin-spin relaxation time.

Fig. 18 $\chi_{//}$ vs. H curves at several temperatures.

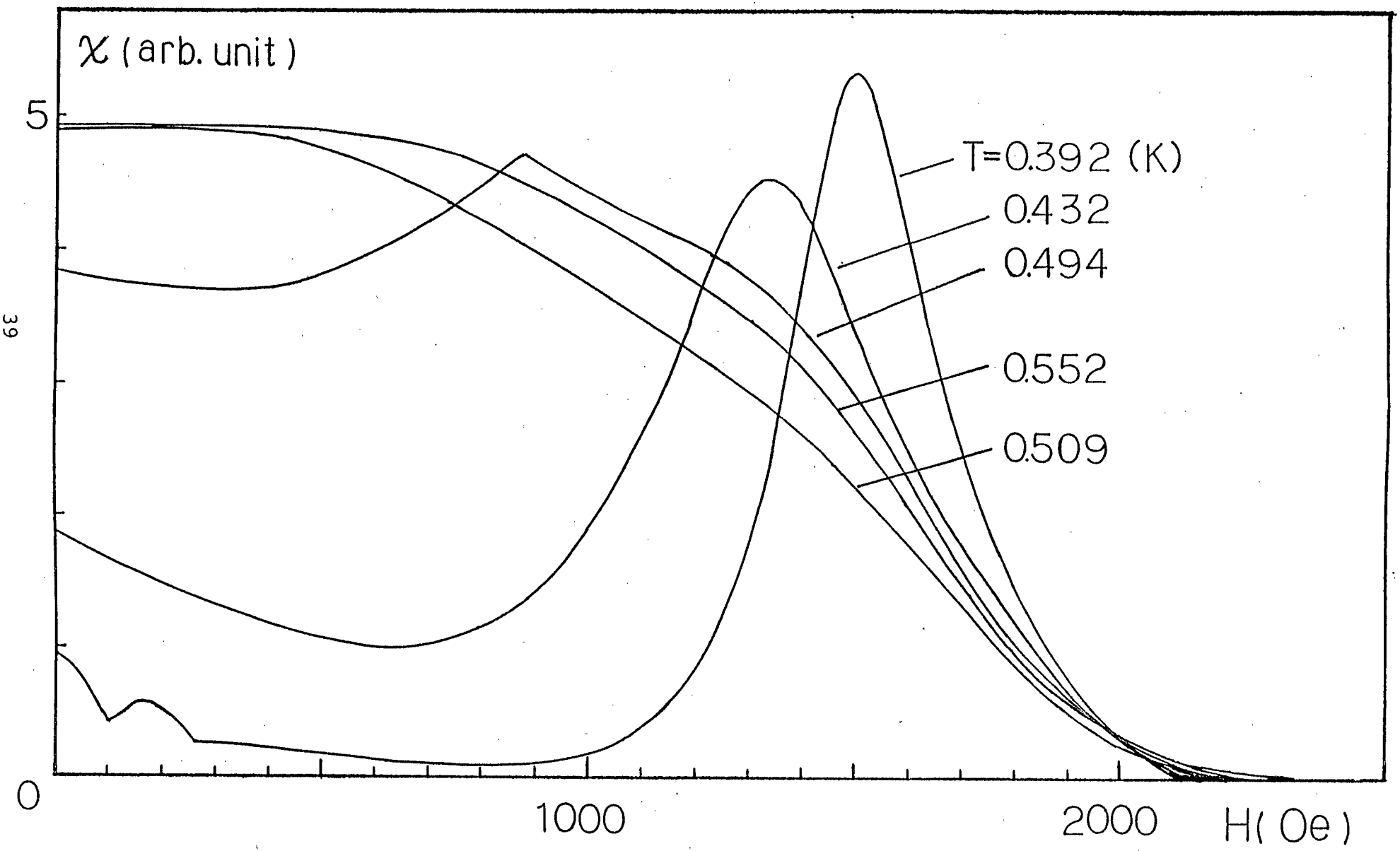

Fig. 19 Frequency dependence of $\chi_{//}$ vs. H curve at 0.392K

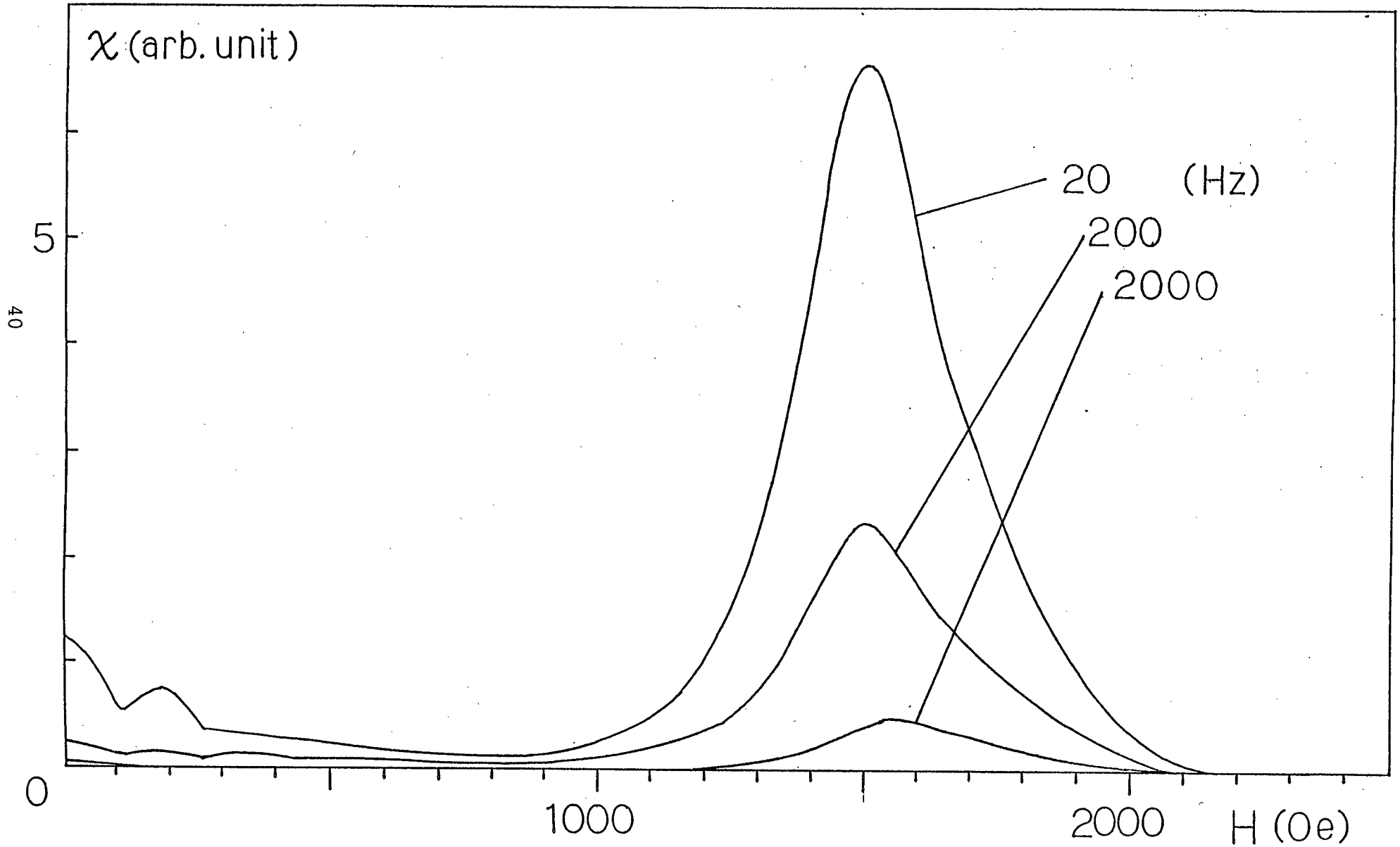

2.3.4. Relaxation measurement

In the case of sudden change of the magnetic field on the sample, the magnetization is far from thermal equilibrium value. Fig.20 shows the relxation of the magnetization and Fig.21 shows the decay in longer time scale. There appears two steps of relaxation in Fig.20 and Fig.21. The first process is due to relatively fast cross-relaxtion and the second one is due to the spin-lattice relaxation. We supposed simply that both relaxation obey the Bloch equation for small (Mz-Mo)/Mo

$$dMz/dt = -(Mz-Mo)/\tau \qquad (5)$$

where Mo is equilibrium magnetization. We can obtain both relxation times using above equation. Results are given in Fig.22 and 23.

Fig.23. showes that spin-lattice relaxation time is almost constant for the external magnetic field.

$$\tau_{ls} \cong 50 \quad \text{msec} \quad \text{at } T=1.33K$$

From A.C. susceptibility measurements, spin-lattace relaxation time at T=1.33K is given by

$$\tau_{ls} = 130 \quad \text{msec}$$

This value is about twice as large as that of our transient measurement.

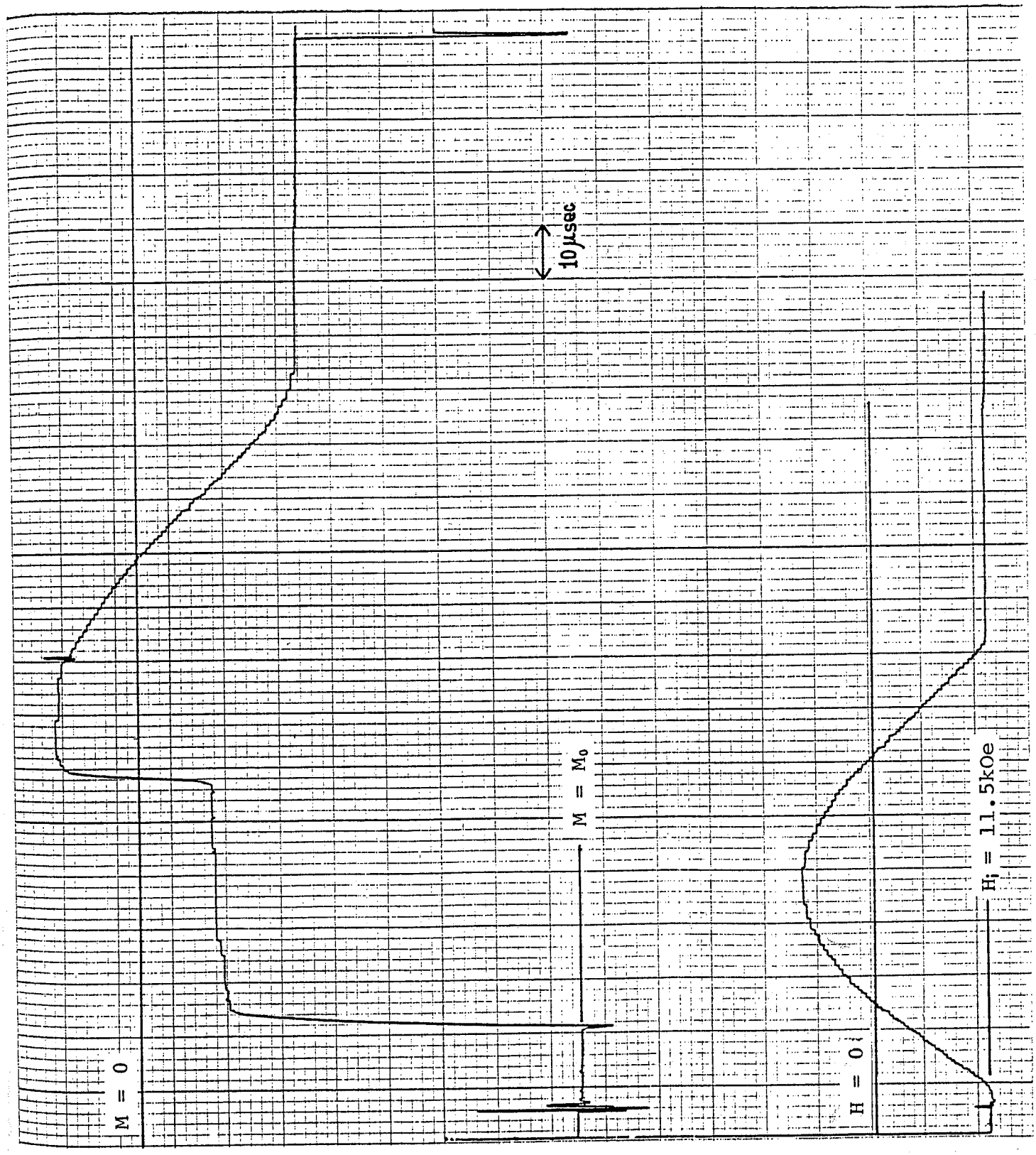

Fig. 20 Recovery of Magnetization (first step)

Ti = 1.33K and Hi = 11.5kOe

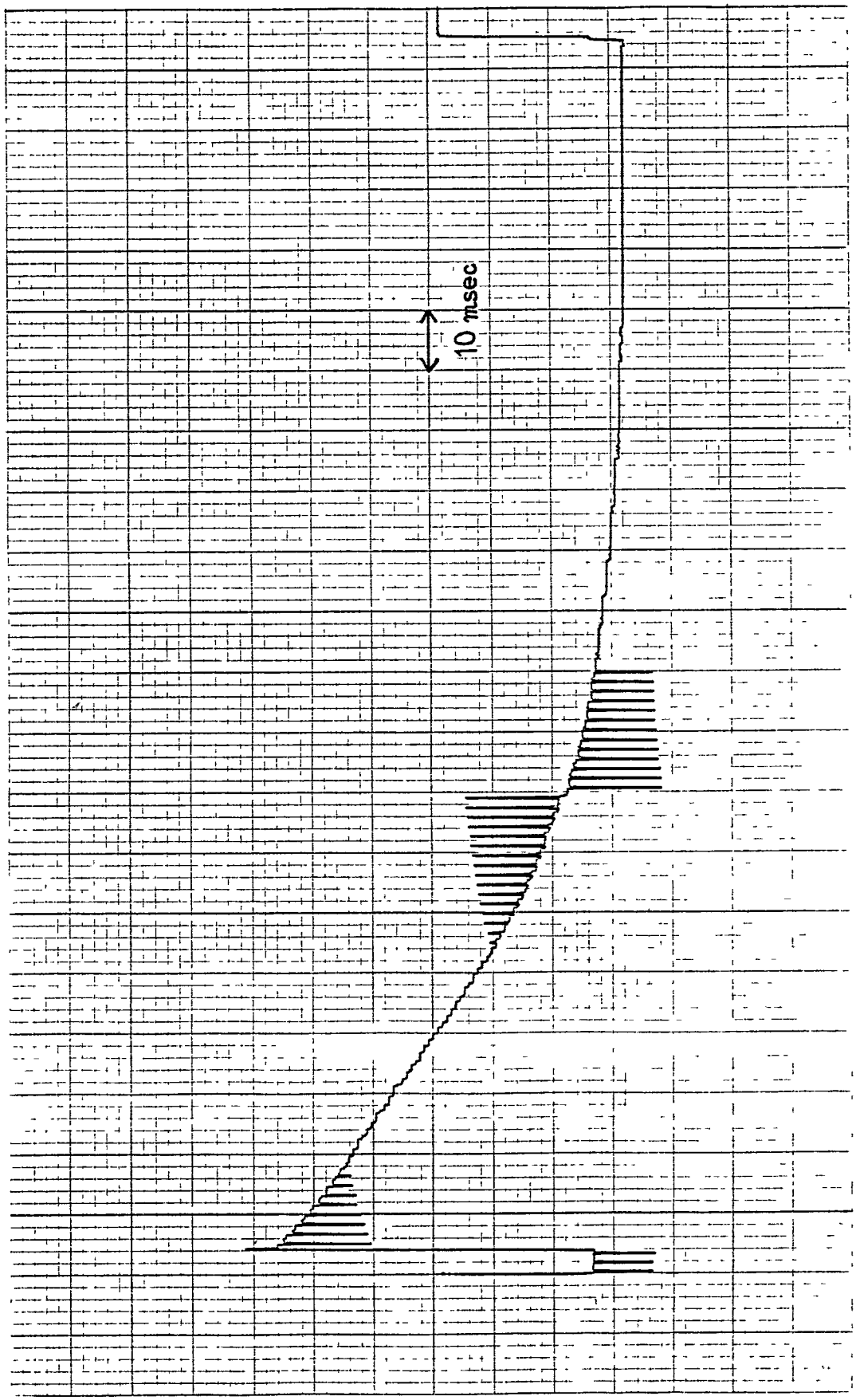

Fig. 21 Recovery of Magnetization (second step)

Ti = 1.33K and Hi = 11.5kOe

Fig. 22 τ_{ls} vs. magnetic field.

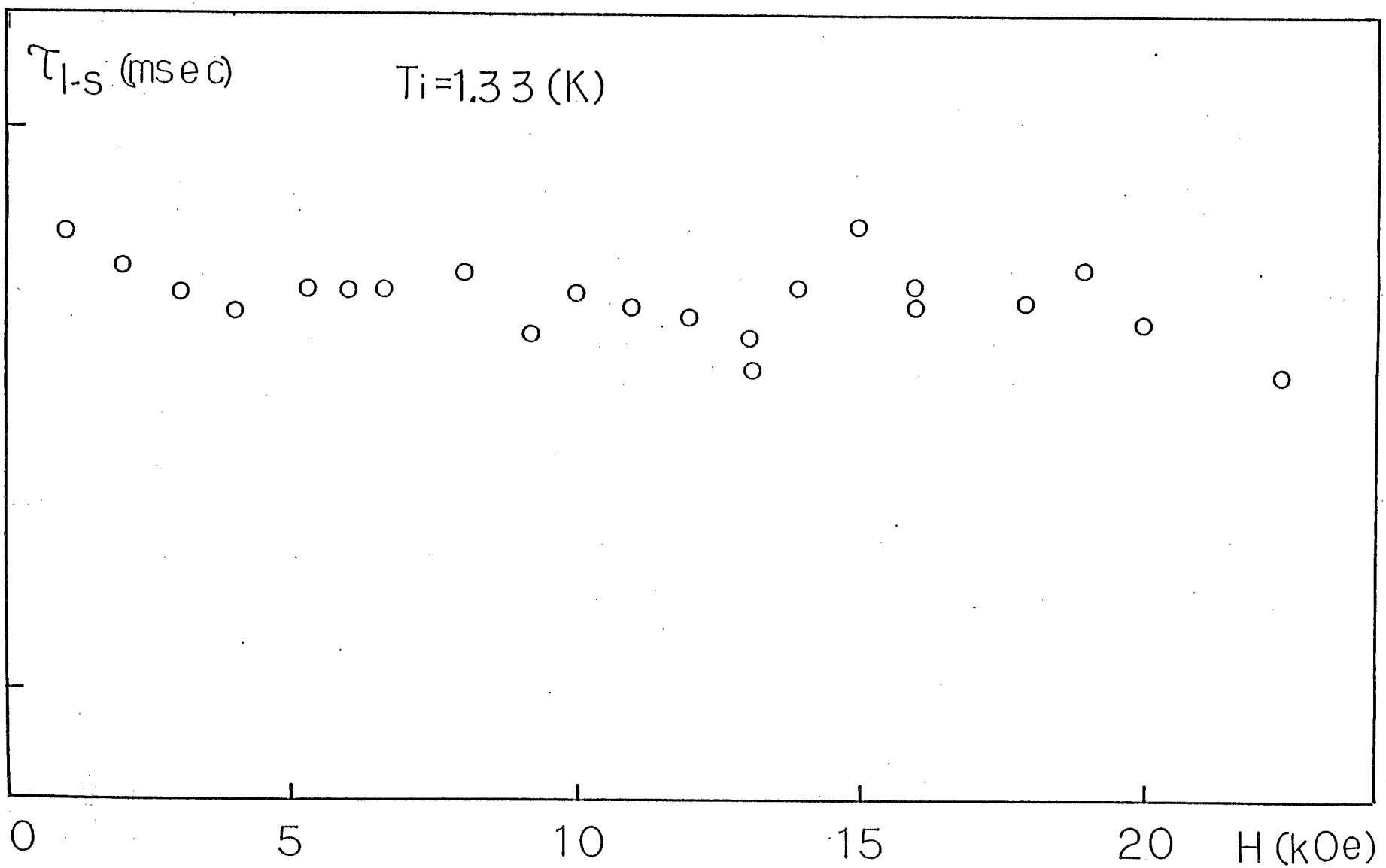

Fig. 23 τ_{cr} vs. magnetic field.

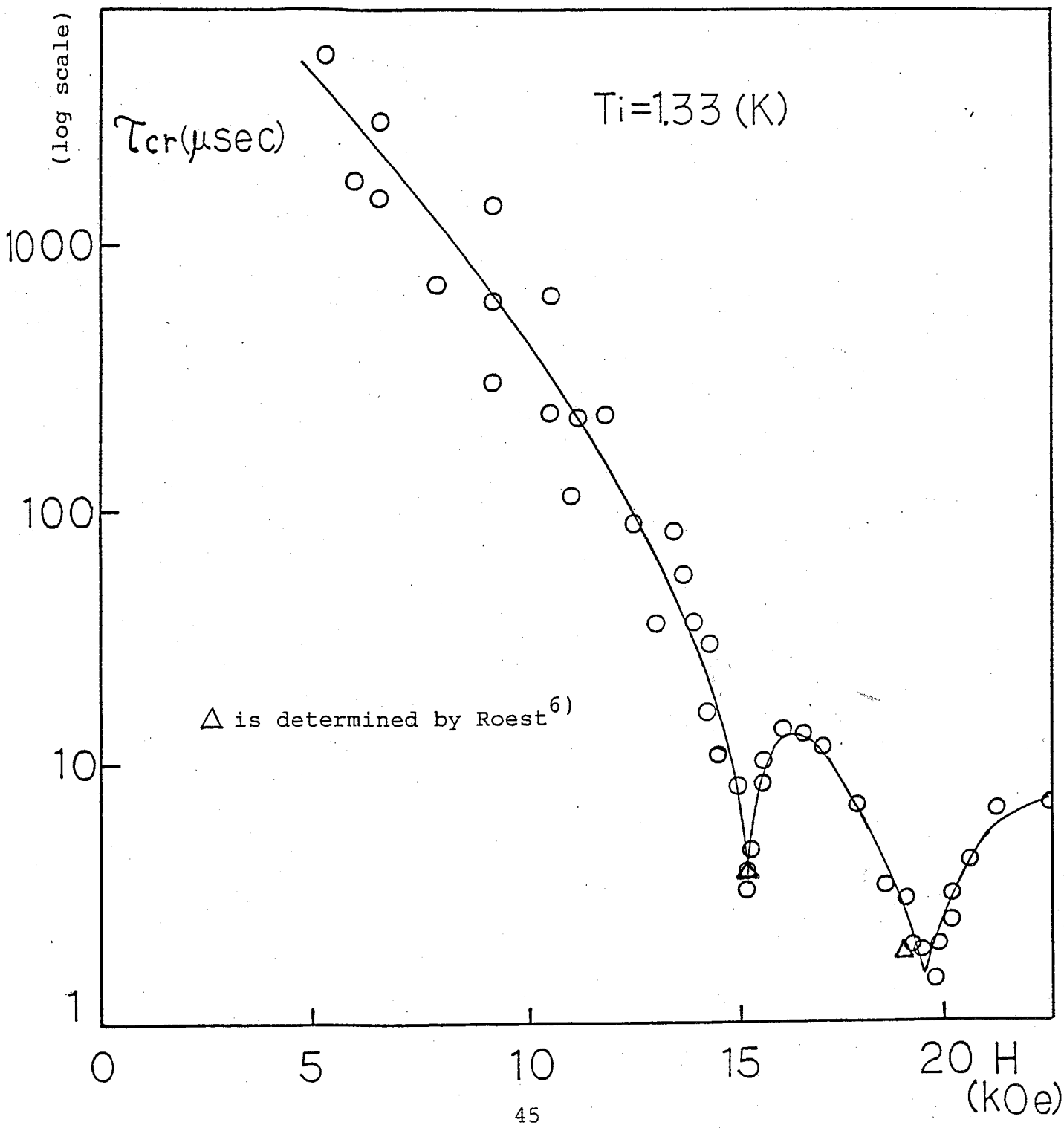

§ 2.4. Discussion

2.4.1. Ordering relaxation time

The ground state of Cs_3CoCl_5 is $S_z=\pm 3/2$. The spin can't reverse itself without thermal contact with lattice taking account of only dipole-dipole interaction of lowest order, by which only transitions with $\Delta S_z \leq 2$ are possible. Therefore, we expect that spin ordering does not occur, because the duration of the pulsed magnetic field in our experiment is much shorter than spin-lattice relaxation time. Spin ordering, however, happens as described below. An initial magnetic field is produced by superconducting magnet and a pulsed magnetic field is applied to opposite direction. Total magnetic field is not zero if direction of two coil are not completely parallel. The residual magnetic field is perpendicular to initial magnetic field or crystal c axis. The ground doublet state becomes mixed state when a magnetic field perpendicular to c axis is applied. τ_{ord} obtained for tilted pulse coil ($\theta \sim 5°$) is shorter than that of $\theta \sim 0°$ case. This shows that the mixing of ground state $|\pm 3/2\rangle$ with excited state $|\pm 1/2\rangle$ makes matrix element between ground doublet. Another mechanism of changing magnetization is dipole-dipole interaction of higher order. Higher order perturbation produce the change of magnetization. Because τ_{ord} is not changed by tilted angle so drastically, dipole-dipole interaction of higher order contributes to τ_{ord} as well as the effect of perpendicular field.

2.4.2. Relaxation time

Spin-lattice relaxation time τ_{1s} obtained in our measurement is about 50msec, while τ_{1s} obtained by a.c. susceptibility is about 130msec at T=1.33K . Our method of measurement of relaxation time is to observe recovery of magnetization far from equilibrium. The energy of spin system flows towards the lattice with the recovery of magnetization. At low temperature, the specific heat of lattice C_L is normally smaller than that of electronic spin system. This situation offen causes the phonon-bottleneck phenomena and experimental results gives the thermal relaxation time between lattice and cold helium bath. Therefore, the relaxation time obtained in our measurement is not a simple spin-lattice relaxation time but the resultant relaxation time with a lattice-bath relaxation.

Fig.22. indicates that the cross-relaxation time has minimum at 15.2kOe and 19.4kOe. These characteristic fields correspond to H_1 and H_2 in Fig.2. respectively. Under these magnetic fields the energy separations are given by the ratio of small integers. This means the equilibrium inside the spin system is attained rather easily by the mutual spin flip-flop among several spins. Therefore, the relaxation of the magnetization can occur without thermal contact with the lattice. This relaxation is called cross-relaxation. Cross relaxations times at H_1 and H_2 determined by a.c. susceptibility measurement are also shown in Fig.22. Our results is consistent with them.

2.4.3. Thermodynamical stability conditions at negative spin temperature

The most elementary form of stability criterion is that entropy of the isolated system is maximum. This is first condition.

The free energy F is given by;

$$S - \beta E = -\beta F \qquad (\beta = 1/T) \qquad (6)$$

Therefore, maximizing the entropy at constant energy amounts to looking for the unrestricted maximum of $-\beta F$. The maximizing of $-\beta F$ give the second condition. At constant temperature the stable state is that F is minimum if $T>0$, or maximum if $T<0$. Finally, using the general property that for either sign of emergy E, the entropy is a monotonic decreasing function of the absolute value of $|E|$. So that, the third condition is obtained. At constant entropy the stable state is that of lowest energy if $T>0$, and of highest energy if $T<0$.

Spin Hamiltonian of Cs_3CoCl_5 is given in eq.(1). When exchange interactions are small compared to zero field splitting $2|D|$ between two doublets and temperature is much smaller than $2|D|$, spin Hamiltonian is rewritten as a Ising model.

$$= -1/S^2 \sum_{\langle i,j \rangle} J'_{ij} S_i^z S_j^z - g\beta H/S \sum_i S_i^z \qquad (S=1/2) \qquad (7)$$

Where $J'=9/2J$. Using ESR data[7] in preceding section, the interaction coefficient for the nearest neighbors in ab plane and for the nearest neighbors in c axis is given.

$$J'/k = J'^{ex} + J'^{dip} = -0.122 \quad K$$

$$J'_c/k = J'^{ex}_c + J'^{dip}_c = 0.120 \quad K$$

In order to predict spin structures at $T=\pm 0$, we consider the cluster of 7 spins as shown in Fig.24. At positive temperature

the energy must be minimum, so the spin arrangement along c axis is ferromagnetic and that in ab plane is antiferromagnetic as shown in Fig.24(a). At negative temperature, the energy must be maximum. The predicted spin structure is shown in Fig.24(b). These structures are both antiferromagnetic structure. Neel temperature T_N is obtained from molecular field approximation.

$$kT_N = 2J'c - 4J' \qquad (6)$$

For both sign of temperature, $T_N = \pm 0.73$ K. Critical field H_c of antiferromagnetic to paramagnetic transition is also calculated.

$$T = +0, \quad H_c = -4J/g = 980 \text{ Oe}$$

$$T = -0, \quad H_c = 2Jc/g = 480 \text{ Oe}$$

Experimental values obtained by Huiskamp et al. [4] are

$$T_N = 0.523 \text{ K and } H_c = 1900 \text{ Oe}$$

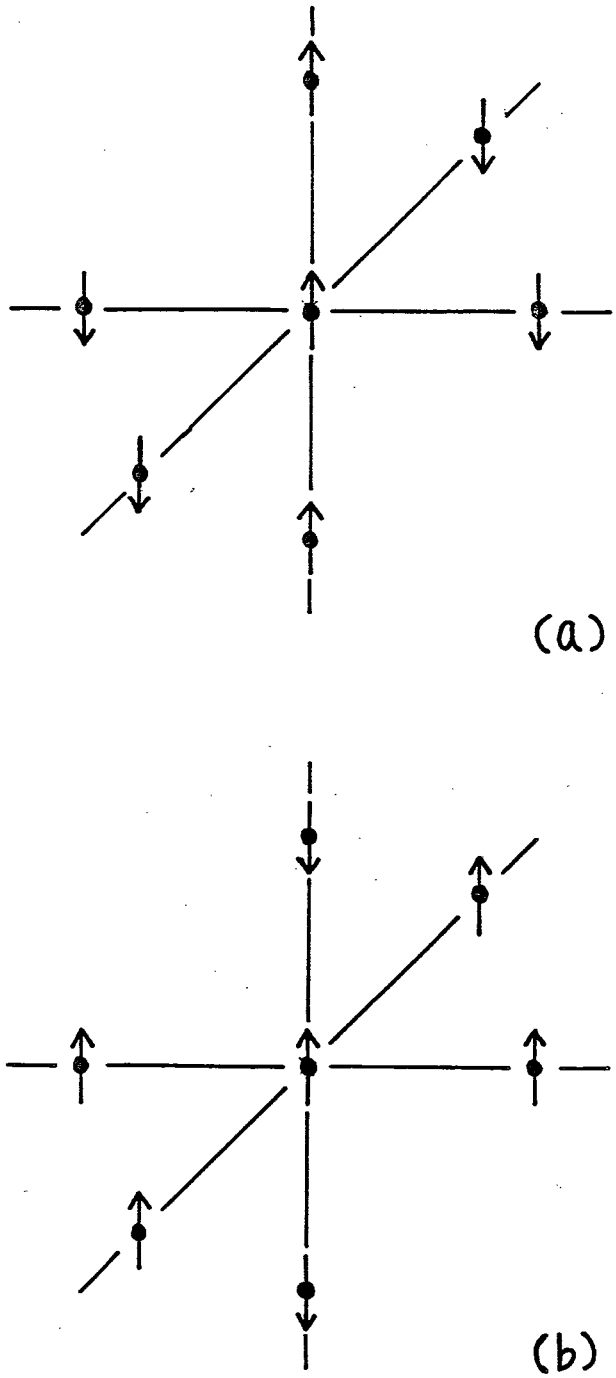

Fig. 24 Spin stractures

(a) $T > 0$, (b) $T < 0$

§ 2.5 Summary

The characteristic time τ_{ord} for antiferromagnetic ordering in Cs_3CoCl_5 is determined. τ_{ord} is 10 sec at T_i=2k and H_i=10kOe.

A negative magnetization is produced by pulsively reversal of magnetic field at T_i 1K. Is is described by a negative spin temperature if it is thermal equilibrium state.

The negative magnetization changes almost adiabatic. It is rather small, so the magnetization follows the change of a magnetic field.

References (II)

1. H.M.Powell and A.F. Wells: J. Chem. Soc. (1935)359.
2. B.N.Figgis, M.Gerloch, and R.Mason: Acta Cryst. 17(1964)506.
3. H.G.Beljers, P.F.Bongers, R.P.Bongers, R.P.Van Stapele and H.Zijlstra: Phys. Lett. 12(1964)81.
4. R.F.Wielinga, W.J.H.Blote, J.A.Roest and W.J.Huiskamp: Physica 34(1967)223.
5. K.W.Mess, E.Lagendijk, D.A.Curtis and W.J.Huiskamp: Physica 34(1967)126.
6. J.A.Roast: Thesis, Leiden (1972).
7. R.P.Van Stapele, J.C.M.Henning, G.E.G.Hardeman and P.F.Bongers, Phys. Rev. 150(1966)310.

Chap. III. Pulsed Adiabatic Magnetization of $HoVO_4$

§ 3.1. Introduction

Experiments on cooling by adiabatic magnetization have been performed quite analogously to the well know adiabatic demagnetization experiments. Non Kramer's ions such as Ni^{2+} in large crystal anisotropy [1] and spin pair system of Cu^{2+} in $Cu(NO_3)_2 2.5H_2O$ [2] are the examples. Ho^{3+} in $HoVO_4$ is the ground state singlet system with large initial splitting which results the level crossing between the ground singlet and one of the excited state relatively at high field. A field induced ordered state of Ho^{3+} electronic spin system is expected and of interest related with the magnetic ordering of enhanced nuclear system at zero field. In fact, the large hyperfine coupling is expected to give some effect on the electronic spin ordering in high field. Further, the study of ground state singlet electron spin system with high crossing field such as FeF_6Si6H_2O and the present Ho^{3+} salt is quite important from the view point of nuclear spin cooling.

§ 3.2. Sample

Crystal of $HoVO_4$ is known to have tetragonal zircon structure and belongs to space group D ($I4_1/amd$). The ground state of Ho^{3+} is I_8 in $HoVO_4$ and the lowest state (Γ_1) is a singlet. A doublet (Γ_5) and a singlet (Γ_4) plus a doublet (Γ_5) situate at $21cm^{-1}$ and at $47cm^{-1}$ above the singlet ground state. According to B.Bleaney et al.[3] the singlet is mainly $|J_z=0\rangle$ with small admixtures of $|\pm4\rangle$ and $|\pm8\rangle$ and a doublet at $21cm^{-1}$ is mainly $|J_z=1\rangle$. Level crossing with the ground state in high field, however, takes place with one of the excited state doublet at $47cm^{-1}$. The doublet Γ_5 is considered to be $|\pm7\rangle$, giving a g factor ($=2g_L J_z$) equal to 17.5.

The spin Hamiltonian is given by

$$\mathcal{H} = V_c + g_L\beta\vec{H}\cdot\vec{J} + A\vec{I}\cdot\vec{J} \qquad (1)$$

where J=8, g=5/4, I=7/2 and $A=0.027cm^{-1}$.

The splitting of Ho^{3+} spin energy level in magnetic field applied parallel to c axis is calculated and shown in Fig.1. In the experimentally obtained level scheme by Battison et al.[4], the crossing field is 11.7T.

§ 3.3. Experimental Method

The necessary experimental conditions to perform adiabatic magnetization cooling of $HoVO_4$ are to cool the Ho^{3+} spin system well below the initial splitting of $20cm^{-1}$ and also to appply the strong magnetic field up to the crossing field H_c 12T where the one of the excited state and the ground singlet crosses and the entropy of the spin system becomes maximum in isothermal condition. Thus, the magnetic cooling at the crossing field is expected by the application of magnetic field in adiabatic process.

In static experiment, steady superconducting magnet is used and adiabatic passage is performed by keeping the sample in thermally isolated cell. In transient experiment using pulsed magnet, the sample is directly embeded in liq. He^4 bath and the adiabatic cell is not necessary at all, because the spin lattice relaxation time is so slow that external heat leak during the sweep time of pulsed field is negligible. Concludingly, we simply cool the crystal in liq. He^4 bath, then apply the pulsed magnetic
field. The used pulse coil is rather compact one with inner diameter of about 5mm, coil length of 5cm and formvas insulated Cu wire of 0.6mm is wound tightly in 5 layers. The pulse duration can be changed by changing the capacity of condensor bank and normally of the order of 1msec. The detection of the magnetic cooling and ordering around H_c is possible by measuring the time derivative of the magnetization: dM/dt which appears across the pick up coil set in the pulse coil. Both the signal and pulse field is stored in the transient memory or and the

memory scope. Finally, the signal and the pulse field are written on XY recorder.

§ 3.4. Experimental Result

The dM/dt signal which is proportional to susceptibility can be plotted against the magnetic field strength. The systematic change of the signal as a parameter of initial temperature is given in Fig.2. Around the centering field of 11T, two sets of double peak in total 4 peaks are observed. In the paramagnetic region, the signal is single peak and intensity increases with decreasing the initial temperature.

Approaching the spin ordered state, where the reached spin temperature kT_f at H_c is close to the interaction energy $\langle \mathcal{H}_{int} \rangle$ among spins, the susceptibility peak becomes to saturate. For lower initial temperature, system enters the ordered state and in the case of simple 3 dimensional antiferromagnetic case, the characteristec double peak should appear as predicted by Tachiki et al.[5)]

In our case, however, the small double peak is found as well as the main double peak by which the phase boundary is determined. We expected that the Ho^{3+} spin system is antiferromagnet at low temperature around the field of H H_c with the modulation of nuclear spin system via strong hyperfine coupling. The measured lower and upper critical field are H_{c1}=11.0T and H_{c2}=12.2T. According to the simple molecular field approxination, the nearest neighbor antiferromagnitec exchange interaction J' is roughly estimated by

$$H_{c1} - H_{c2} = 6zJ'/g\beta \qquad (2)$$

that is, we obtain, J'/k =-0.021 K. This analysis gives the order of magnitude estimation of the antiferromagnetic interaction among Ho^{3+} spins, but the spin energy level scheme around H_c

given by simple Hamiltonian (1) shows a complex diagram and needs detailed analysis.

The angular dependence with respect to the misalignment between crytallographic c-axis and the field axis is studied. Fig.3. shows the result of the tendency of disappearance of the double peak with increasing the angle $\angle C \cdot H$. This may be qualitatively explained by taking the increasing anticrossing with the angle $\angle C \cdot H$ into account, but the more quantitative examination should be necessary.

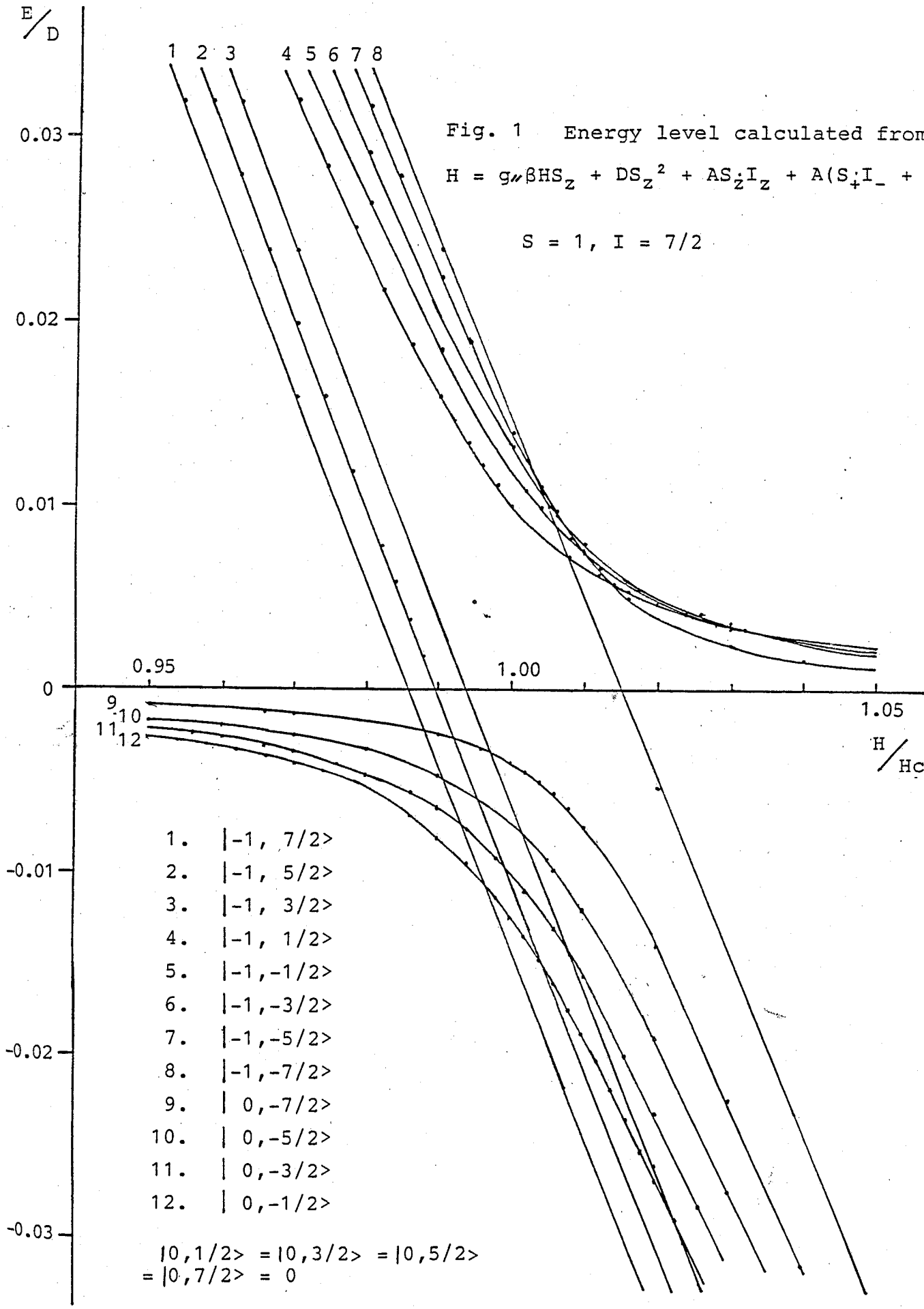

Fig. 1 Energy level calculated from

$H = g_{//}\beta HS_z + DS_z^2 + AS_zI_z + A(S_+I_- + S_-I_+)$

$S = 1,\ I = 7/2$

Fig. 2 dM/dt vs. H

Pulsed adiabatic magnetization cooling of HoVO

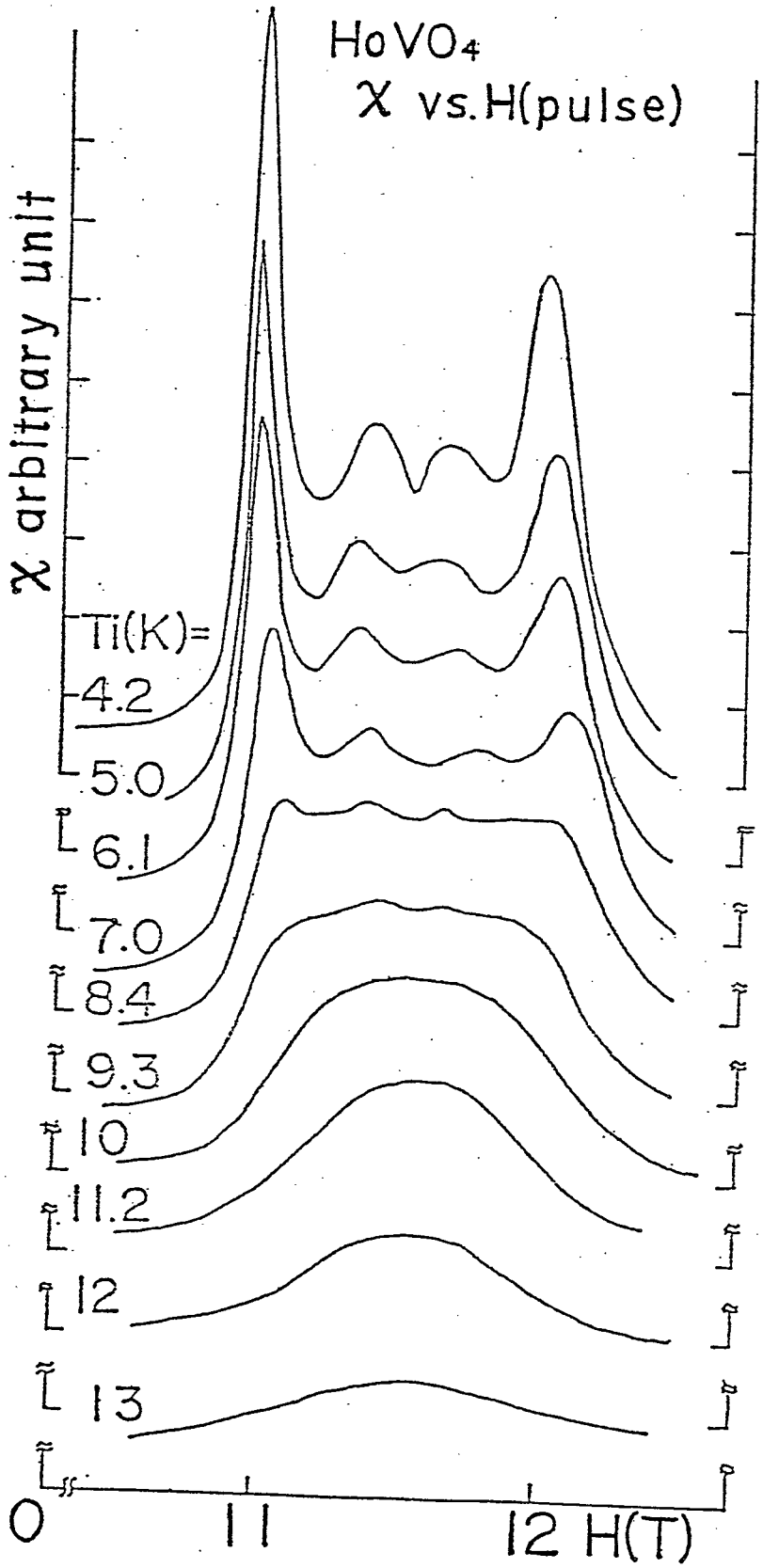

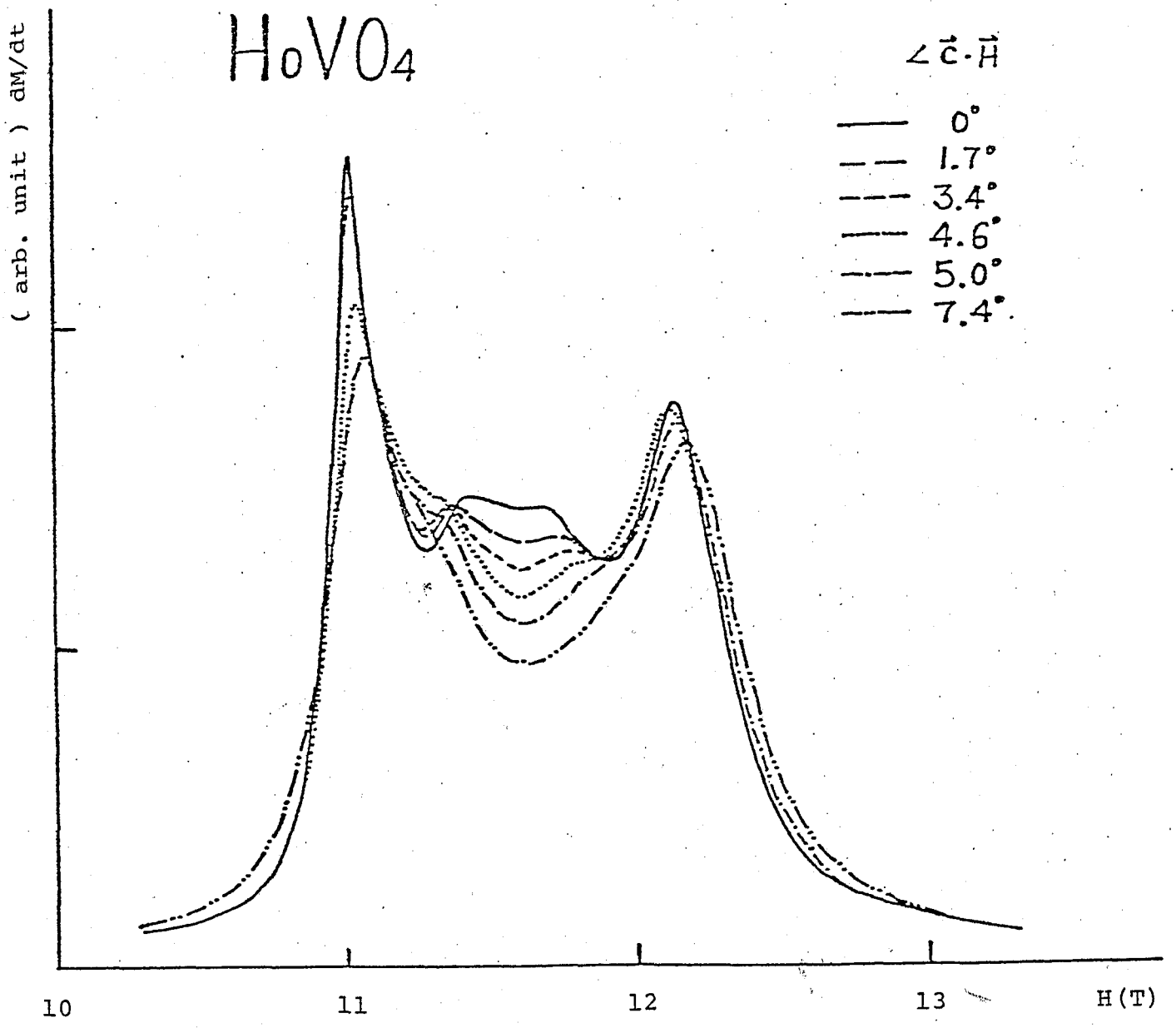

Fig. 3 dM/dt under the magnetic fields increasing the angles from c to H

§ 3.5. Summary

The study of magnetic ordering of $HoVO_4$ is now going on in our laboratory by steady method such as specific heat and susceptibility measurement assembling the strong magnetic field of 14T superconducting solenoid and powerful dilution refrigerator. Examination by steady method will be performed in the near future and the origin of the fine structure of small double peak found in pulse experiment will be made clear.

References (III)

1. N.Wada: Thesis (1980)

2. K.Amaya and N.Yamashita: J. Phys. Soc. Jpn. 42(1977)24.

3. B.Bleaney, Physica 69(1973)317.

4. J.E.Battison, A.Kasten, M.J.N.Leask and J.B.Lowry: Phys. Letters 55A (1975) 173.

5. M.Tachiki and T.Yamada: J. Phys. Scc. Jpn. 28(1970)1413.

Chap. IV. Excited State Spin Ordering

§ 4.1. Introduction

In 1927 Debye[1] and Giauque[2] proposed independentry an idea of adiabatic demagnetization cooling method in order to obtain very low temperature. This method is based on the fact that at a fixed temperature the entropy of spin system is reduced by the application of a magnetic field. If H_{loc} is the effective field that corresponds to the local interaction among spins, the final temperature T_f after adiabatic demagnetization process is given by

$$T_f=(H_{loc}/H_i)\ T_i \qquad (1)$$

where H_i is the initial field and T_i is initial temperature.

In 1958 Kittel[3] and Wolf[4] prorosed an adiabatic magnetization cooling of ions or molecules having a non-degenerate ground state. Experimental realization has been performed in $Cu(NO_3)_2 2.5H_2O$ by Haseda et al[5]. In this compound, Cu^{2+} ions(S=1/2) are coupled in pairs by isotropic antiferromagnetic exchange interaction J, and it makes ground state singlet and excited triplet with energy gap 2J/k=5.2K. If this system is put in certain magnetic field, one of the excited levels comes down to make crossing to the singlet ground level. Because of this gain of the entropy, cooling by adiabatic demagnetization can be achieved.

Tachiki and Yamada[6] have discussed the phase transition of this system in the frame of molecular field approximation. An ordered state will appear around the crossing point below certain critical temperature and there appears transverse spin components to external magnetic field in the ordered state. This theory is

in good agreement with the experiment.

Another type of ground state singlet system is that of single ion with large crystal field anisotropy. In the case of the Ni^{2+} ion, three fold spin degeneracy of ground state is removed at zero magnetic field by the combined action of spin-orbit coupling and crystal field with lower symmetry. Tsuneto and Murao[7] investigated theoretically a spin ordering of such a crystal field system. Wada et al.[8] found the spin ordering of this spin system in some nickel compounds.

Amaya et al.[9] have made an experiment about the adiabatic magnetization cooling and spin ordering of $Cu(NO_3)2.5H_2O$. The merit of using a pusled magnetic field is described in the following. Because the sweep rate of a pulsed magnetic field is sufficiently fast compared with spin-lattice relaxation rate and slow enough to spin-spin relaxation rate, in usual case, the adibatic condition between spin and lattice system is normaly attained. Therefore, only the spin system is cooled in this pulsed magnetization process and the spin ordering is established below a certain spin temperature defined within spin system.

Now, we propose an idea of the possibility of the ordering among the level systems of the excited state[10]. This will be realized quite analogously with the ground state singlet system, but to make this ordering pulsed magnetic field plays an essential role. Pulsed magnetic field is necessary to make populations in the excited state. If excited state makes an quasi-thermal equilibrium around H_c, we expect an excited state spin ordering. The quasi-equilibrium state, however, breaks down

in a certain time called relaxation time . Therefore, sample must have large relaxation time in comparison with measurement interval. $NaNiAcac_3$benzene is suitable for this experiment. We discuss at the latter section the experimental conditions necessary for excited state spin cooling and ordering.

§ 4.2. Sample

4.2.1. Sample preparation

$NaNiAcac_3$benzene is a member of $M^{I}M^{II}Acac_3$benzene series, where Acac represents acetylacetonate, M^{I} = Na, K or M^{II} = Mg, Mn, Fe, Co, Ni or Zn. Similar series of salt can be made when benzene is replaced by p-dioxane , fluorobenzene, ethanol, methanol, acetone, glycerin or phenol.

The single crystal is obtained by a benzene vapor diffusion process into a $NaNiAcac_3$ aquenous solution. This technique is given by Treuting and Van Uitert[11].

4.2.2. Characteristics of $NaNiAcac_3$benzene

An X-ray study on the crystal structure of $NaNiAcac_3$benzene was performed by Treuting[11]. The crystal belongs to space group P31c and has a unit cell with a=10.23±0.02, c=12.20±0.02 A. The Ni^{2+} ions form a triangular lattice in the hexagonal plane perpendicular to the c axis as shown in Fig.1(a).

The F ground state of the d^8 configuration of free Ni^{2+} ion is split by the cubic field ($Vc \sim 10^4$ cm^{-1}) of the oxygen octahedron into a $^3A_2$ orbital singlet and two excited $^3T_1$ and $^3T_2$ triplets. Since neither these two nor the low-lying state ^1E of the next orbital multiplet can be admixed with $^3A_2$ by spin-orbit coupling in the first order, the properties of the Ni^{2+} ions are well described by a spin Hamiltonian with S=1 . According to the study of E.P.R . by Peter[12], the spin Hamiltonian under a magnetic field applied parallel to c axis is well described as follows :

$$\mathcal{H} = g\beta H S_z + D(1-S_z^2) \qquad (2)$$

$$g_{/\!/} = 2.20 \quad , \quad D/k = 3.15 \quad K$$

The energy level is shown in Fig.1(b).

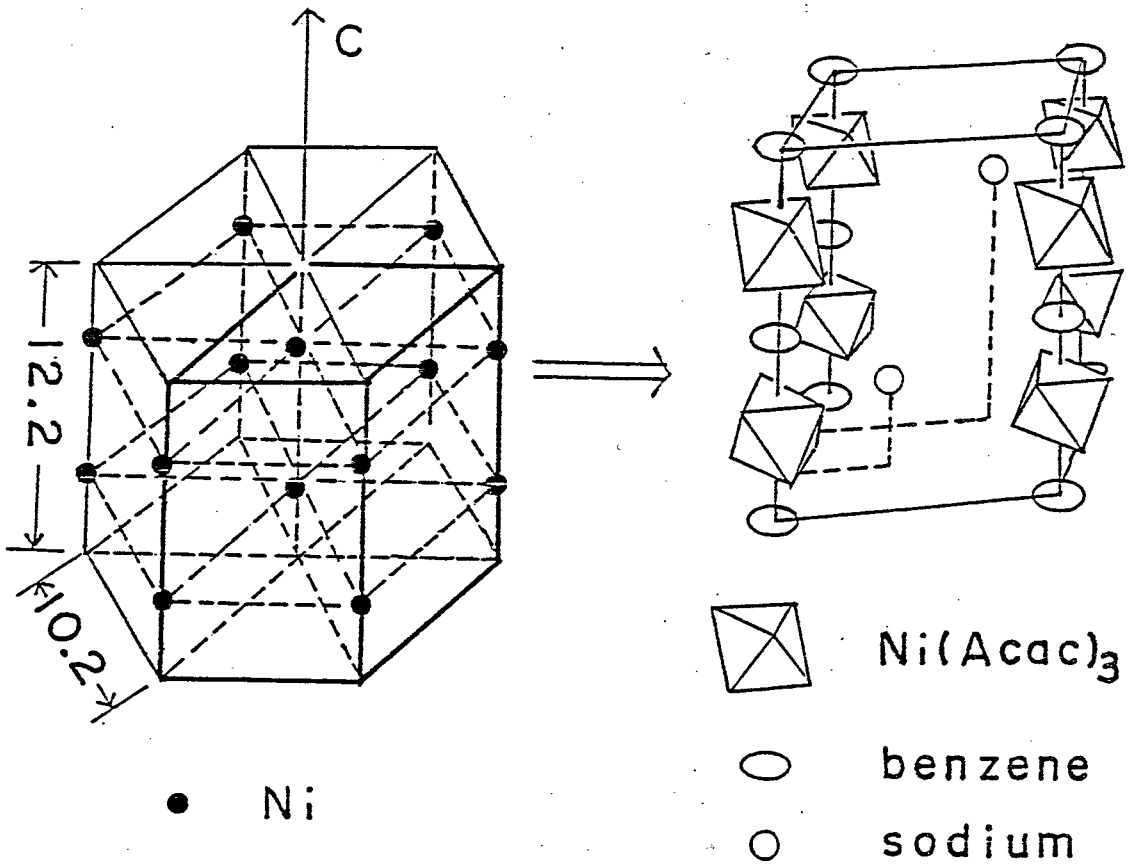

Fig. 1 (a) Crystal structure of $NaNiAcac_3benzene$.

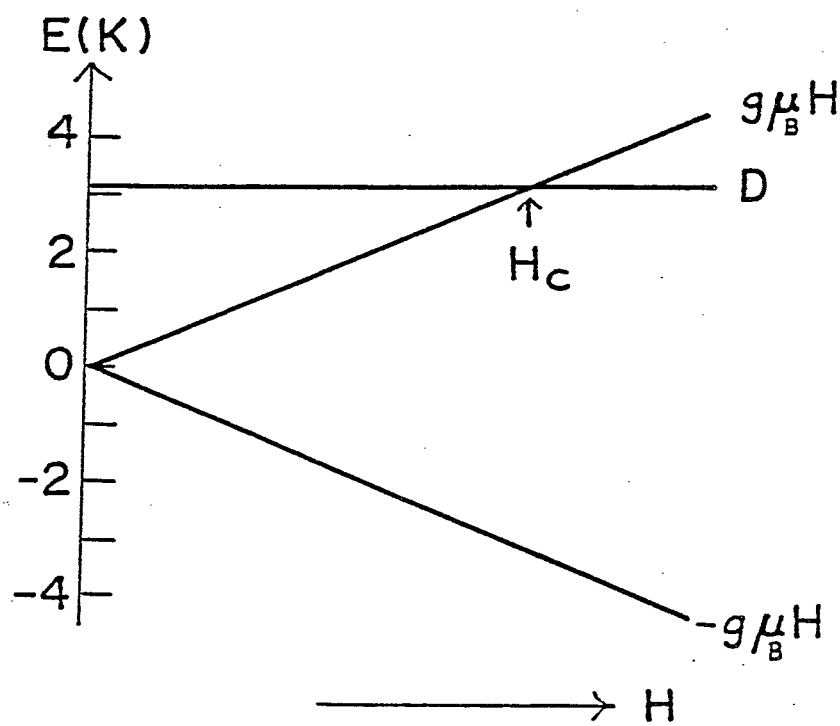

Fig. 1 (b) Energy level splitting of Ni^{2+} in $NaNiAcac_3benzene$.

§ 4.3. Magnetic Transitions: Ground state doublet

4.3.1. Introduction

A simple antiferromagnetic structure does not fit into a triangular Ising lattices. In the theoretical study of the spin ordering of the triangular Ising lattice with antiferromagnetic nearest neighbor interaction, Wannier[13] pointed out the multiplicity of the spin structure with the lowest energy and evaluated the residual entropy at T=0 K.

Mekata[14] studied the spin ordering in the triangular Ising lattice with antiferromagnetic nearest neighbor interaction J and ferromagnetic second nearest neighbor interaction J'. on the basis of a molecular filed approximation with the 3-sublattice model. The existence of the partially disordered antiferromagnetic state between the paramagnetic and the ferrimagnetic states and of the direct phase transition from the paramagnetic to the ferrimagnetic state, are predicted in the cases of $0 > 2J'/J > -0.8$ and $2J'/J \leq -0.8$.

Expecting to detect the partially disordered antiferromangetic state, we tried the A.C. susceptibility and the specific heat measurements[15] of $NaNiAcac_3$benzene which is considered to be an example of the triangular Ising lattice, although the system is not two dimensional but actually three dimensional one.

4.3.2. Experimental apparatus

The apparatus for the measurement of the A.C, susceptibility is shown in Fig.2. The measurement was performed by the Hartshorn bridge method with the frequency mostly of 200 Hz. The dilutuon refrigerator used in the experiment is capable enough to reach the lowest temperature of 6 mK. The crystal is placed on the small piece of Cu wire foil to fix the crystal in the cell and protected from the moisture by the thin layer of GE 7031 varnish. This sample unit is packed in a He^3-sample cell made of stycast 1266. The crystal has thermal contact with pure liquid He in the cell, which is cooled through Cu wire bundle. The bundle consists of 4500 Cu wires of the diameter 0.05 mm and the ends of them are hard soldered to the Cu disk screwed to the mixer.

As a thermometer for sample specimen, we used MATSUSHITA carbon resistor ERC 18GJ 51 ohms which is calibrated by a standard Ge resistance thermometer and a nuclear orientation thermometer of ^{60}Co in hexagonal cobalt crystal, at temperatures above and below 50 mK respectively. The sample thermometer is immersed directly in liquid He^3 cell. The resistance was measured by the use of a potentiometric conductance bridge specially designed so as to reduce excitation power to less than 10^{-14} watts below 50 mK.

The apparatus for the measurement of the specific heat is shown in Fig.3. The sample is sandwiched in, with Apiezon N glease, between two plates made of about 60 Cu wires of the diameter 0.14 mm. The sample unit is shielded against radiation by a Cu bobbin and a coil is reinforced by silk threads and

Araldite. The whole assembly is screwed to the mixer. The measurement was performed by the conventional method using Tin thermal switch.

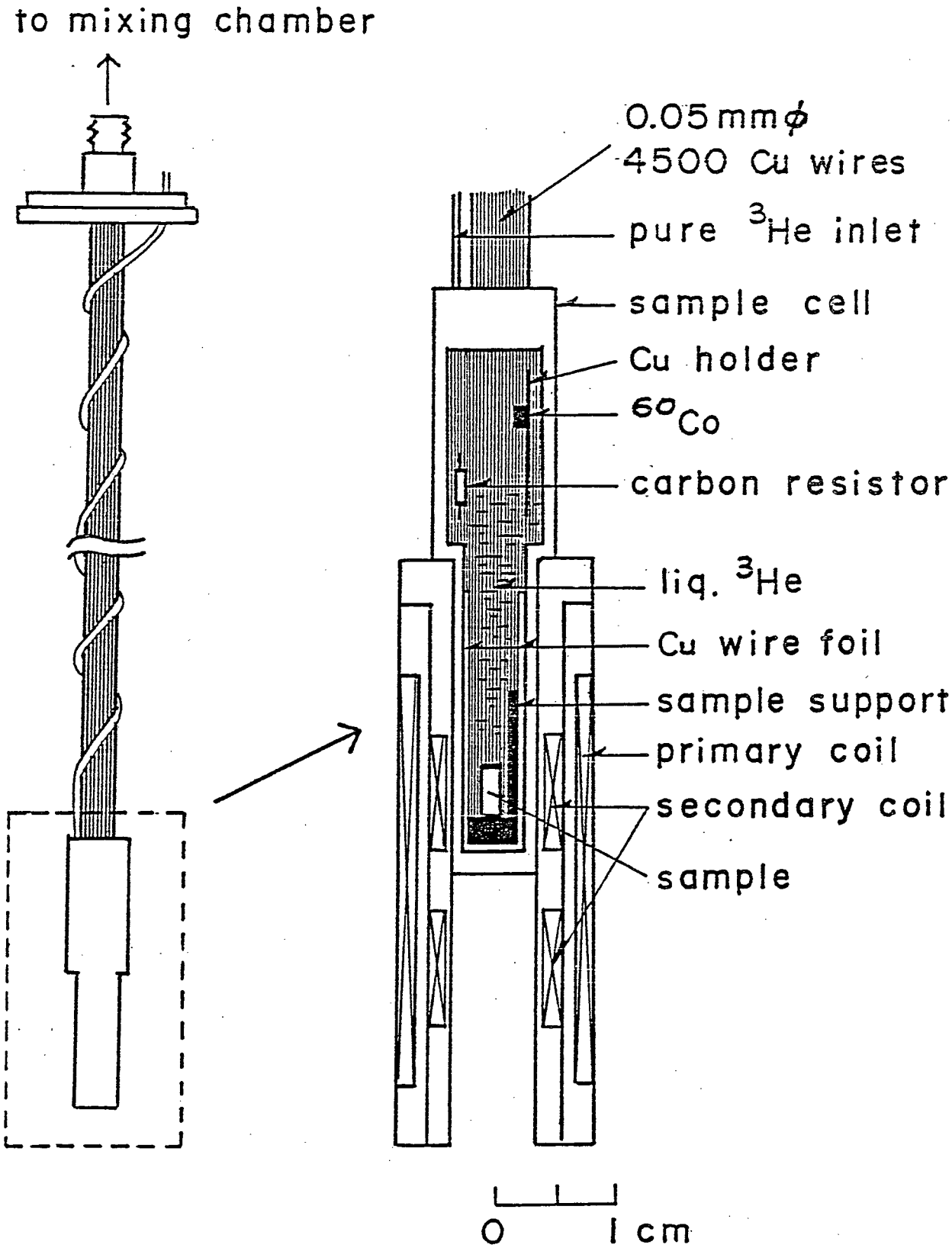

Fig. 2 Apparatus for measurement of susceptibility.

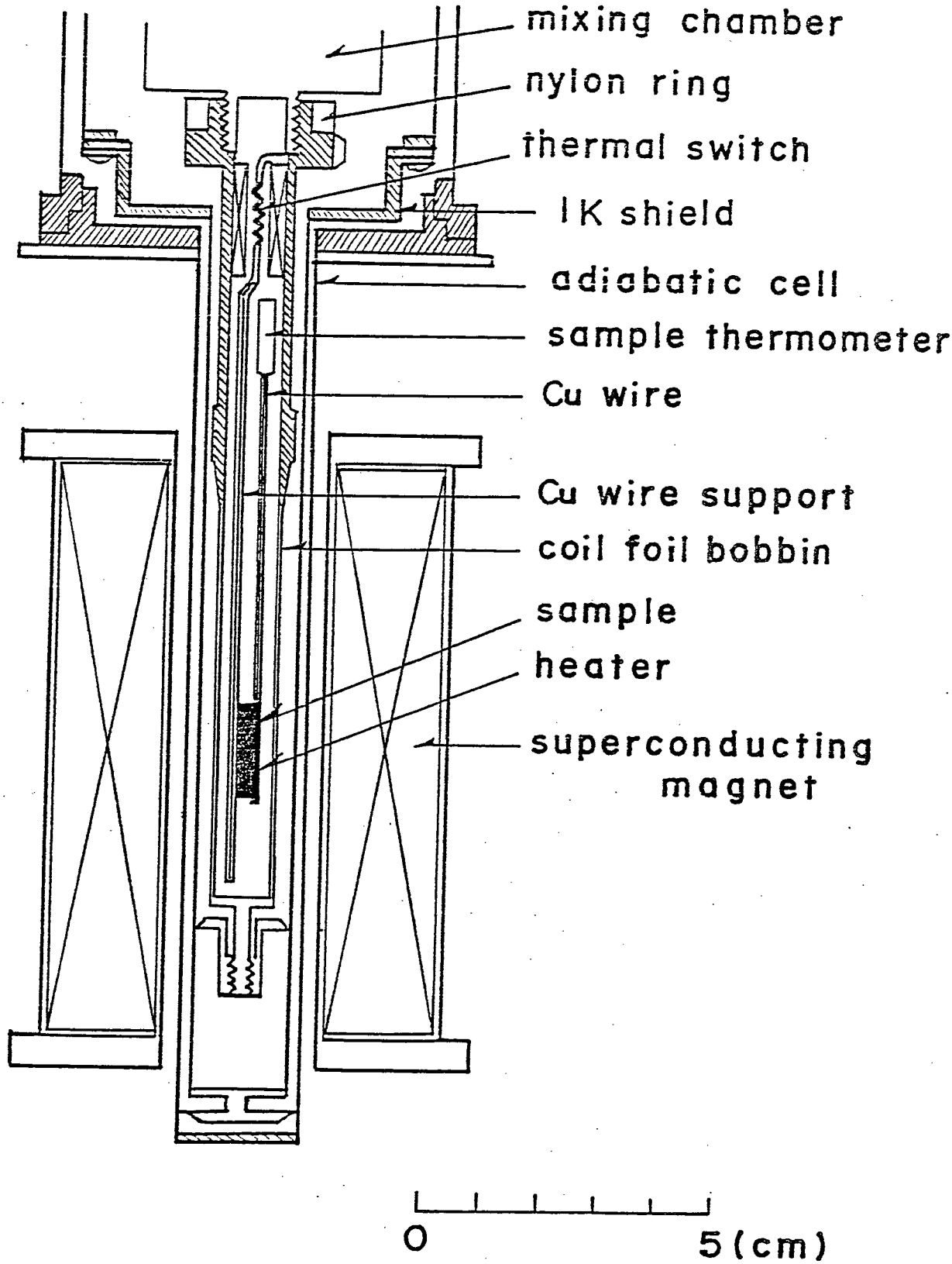

Fig. 3 Apparatus for measurement of specific heat.

4.3.3. Experimental results

4.3.3-1. χ vs. T under zero magnetic field

The differential susceptibilities parallel ($\chi_{//}$) and perpendicular ($\chi_{\perp}$) to c axis are measured under zero magnetic field. The temperature dependences of $\chi_{//}$ and $\chi_{\perp}$ between 2 K and 60 mK are shown in Fig.4. The dotted and solid lines show the theoretical $\chi_{//}$ and $\chi_{\perp}$ for non-interacting spins. The inverse of $\chi_{//}$ at the lowest temperature region is shown in Fig.5. The solid line shows the Curie-Weiss law with antiferromagnettic Weiss temperature of $\Theta \simeq 18$ mK. The deviation from the Curie-Weiss law becomes appreciable below about 70 mK.

4.3.3-2. $\chi_{//}$ vs. H and M vs. H

$\chi_{//}$ is measured under the magnetic field applied parallel to c axis. The $\chi_{//}$ vs. H curves at several temperatures below 70 mK are shown in Fig.6. In the temperature region higher than 32 mK, $\chi_{//}$ decreases monotonically with increasing magnetic field. However, an anomalous behavior is observed below 32 mK. For example, at 20 mK, $\chi_{//}$ has a peak at about 265 Oe. The spin system is presumably in some ordered state below this critical magnetic field.

The frequency dependence of $\chi_{//}$ at 22 mK under the magnetic field, is given in Fig.7. The $\chi_{//}$ vs. H curves for three different frequencies (20,200 and 1000 Hz) are almost identical except some slight deviation in the field range between 70 Oe and 200 Oe. So, we can take the measured $\chi_{//}$ as static one, we obtain the magnetization curve by the integration of $\chi_{//}$ with respect to the magnetic field. We show the M vs. H curve at 20 mK in Fig.8.

The magnetization increases abruptly threefold at about 265 Oe.

4.3.3-3. Specific heat C vs. T under zero magnetic field

The temperature dependence of the specific heat under zero magnetic field was observed in reference with the origin of the deviation from Curie-Weiss law below about 70 mK. The C/R vs. T and the C/R vs.$1/T^2$ curves are shown in Figs.9 and 10. As is apparent in these Figs., no anomaly of C/R is observed above 45 mK and the simple paramagnetic b/T^2 dependence with $b = 1.2 \times 10 \cdot R$ is observed above 0.1 K. If we assume the paramagnetic state having the entropy S=Rln2 above 0.2 K, the entropy reduction by the development of spin correlation can be calculated using the specific heat data as is shown in Fig.11. The amount is about 38 % at 45 mK.

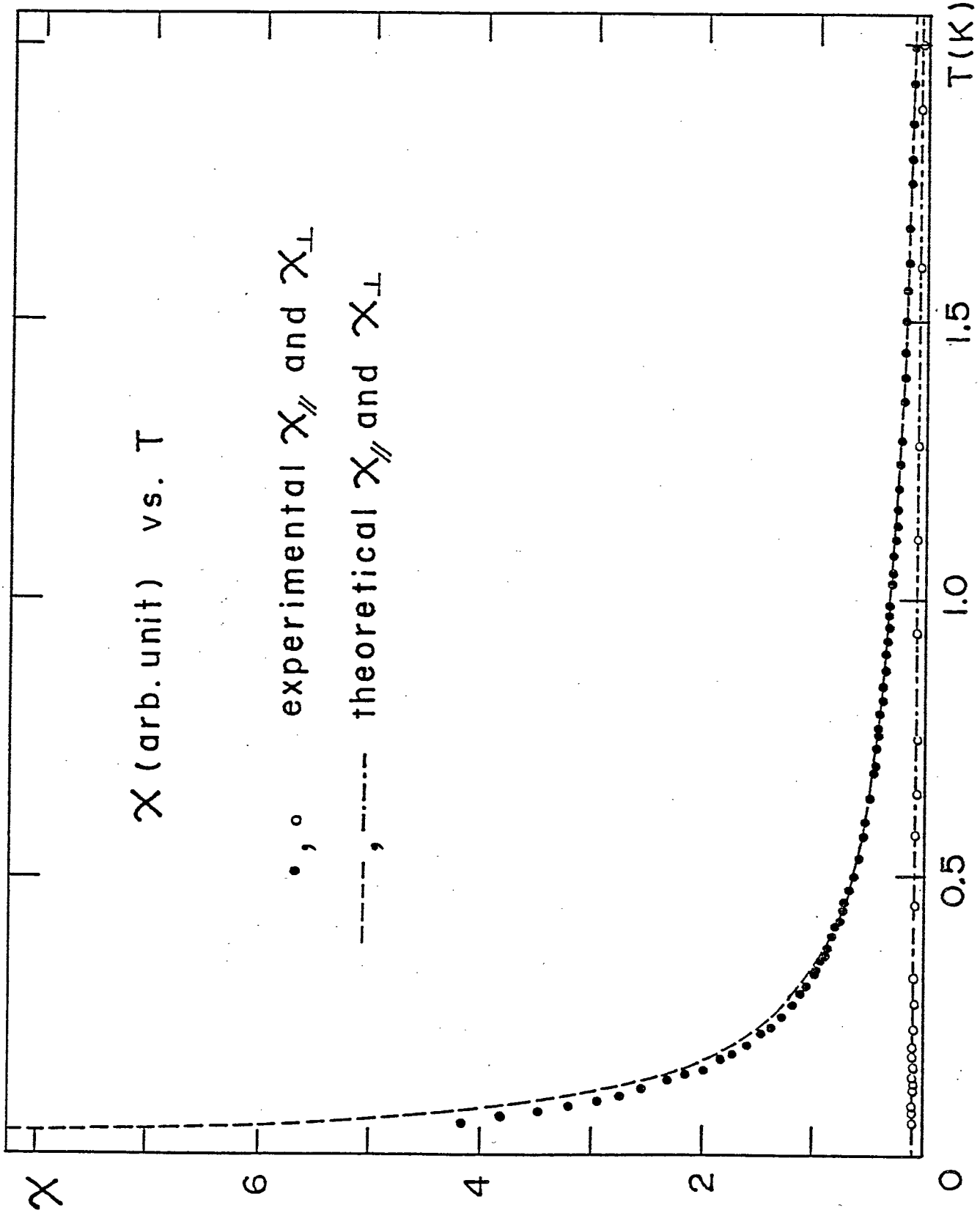

Fig. 4 Susceptibility parallel and perpendicular to c-axis.

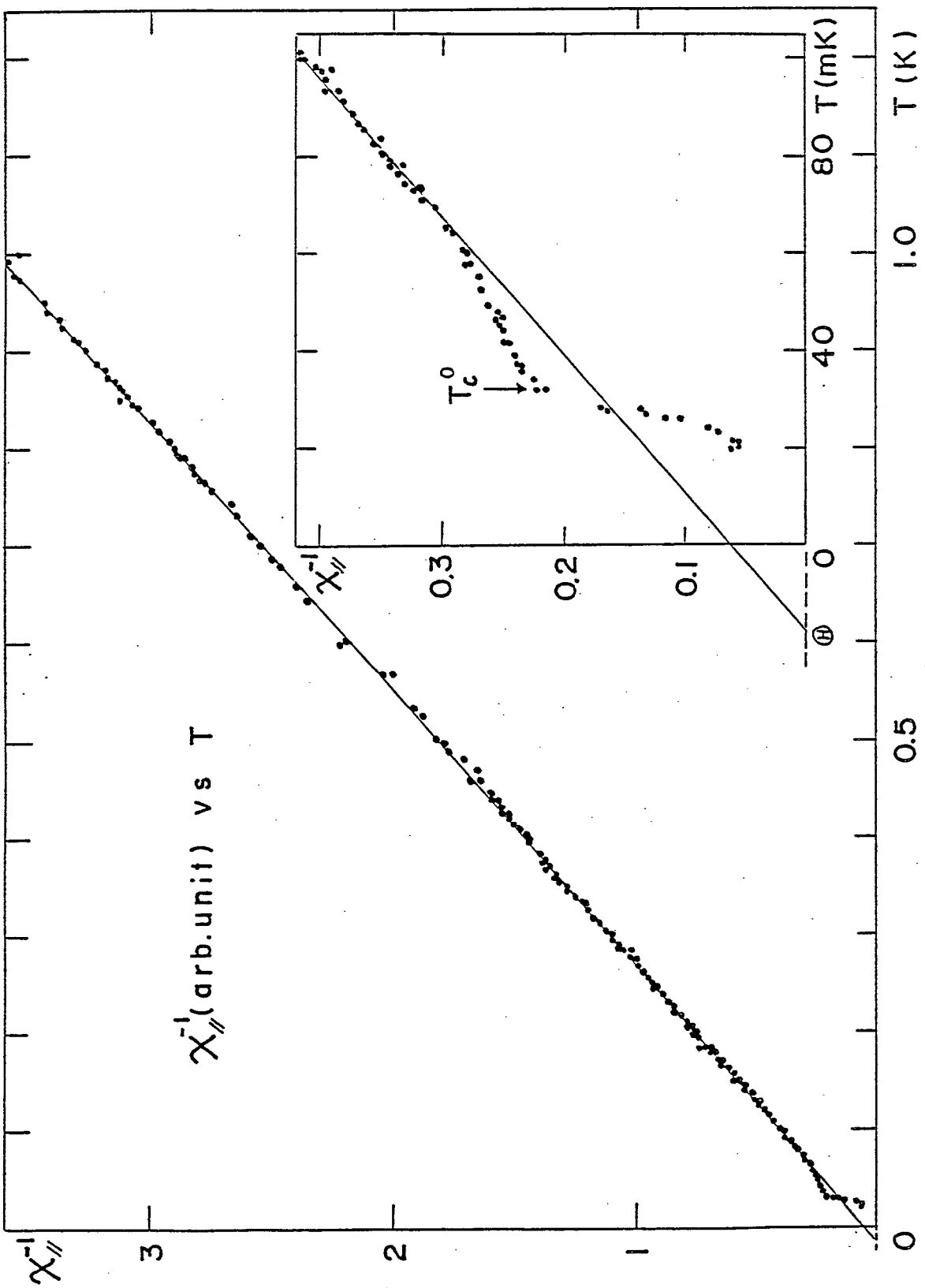

Fig. 5 Inverse of $\chi_{//}$ below 1 K under zero magnetic field.

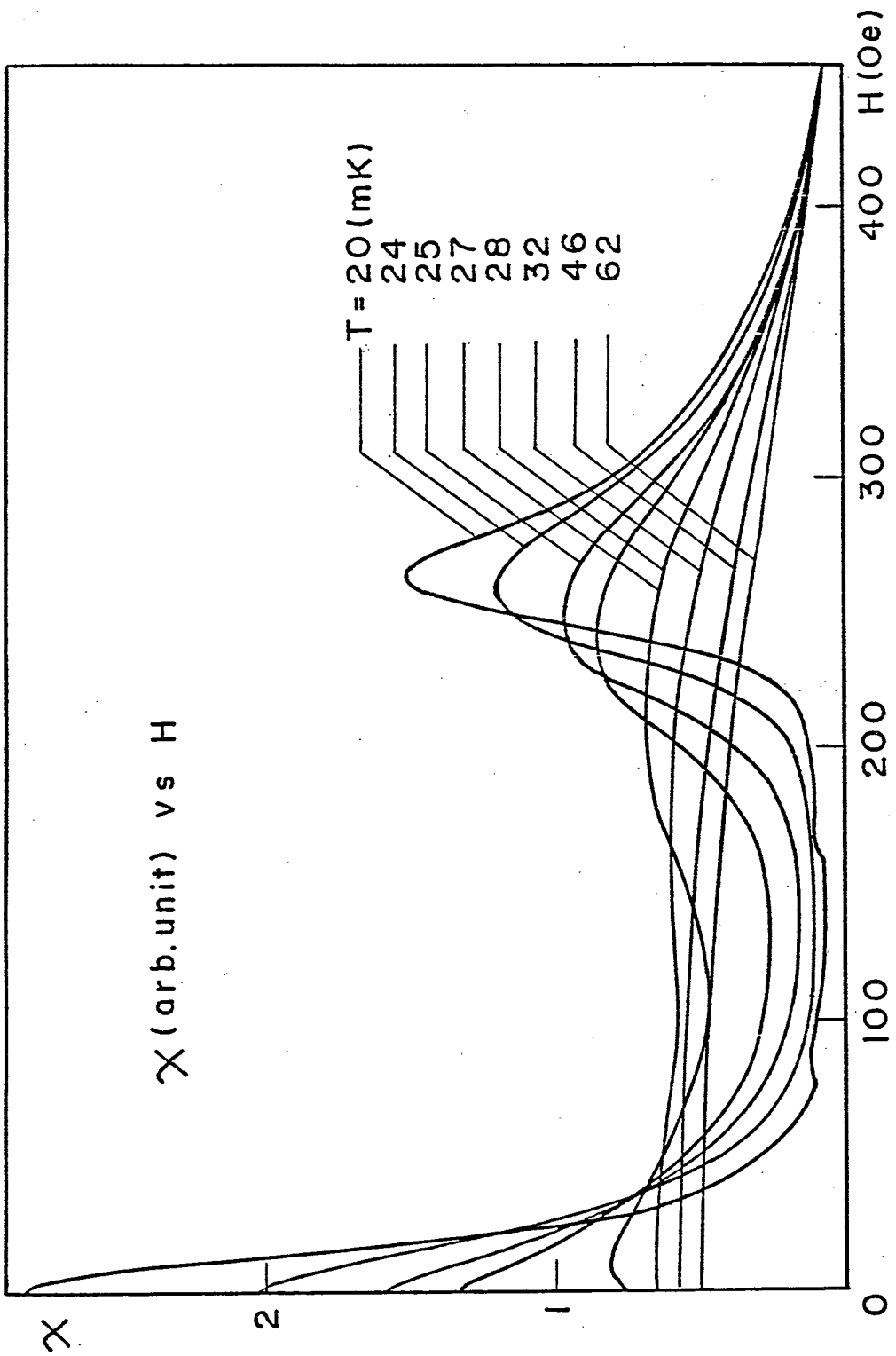

Fig. 6 $\chi_{//}$ vs. H curves at several temperatures below 70 mK.

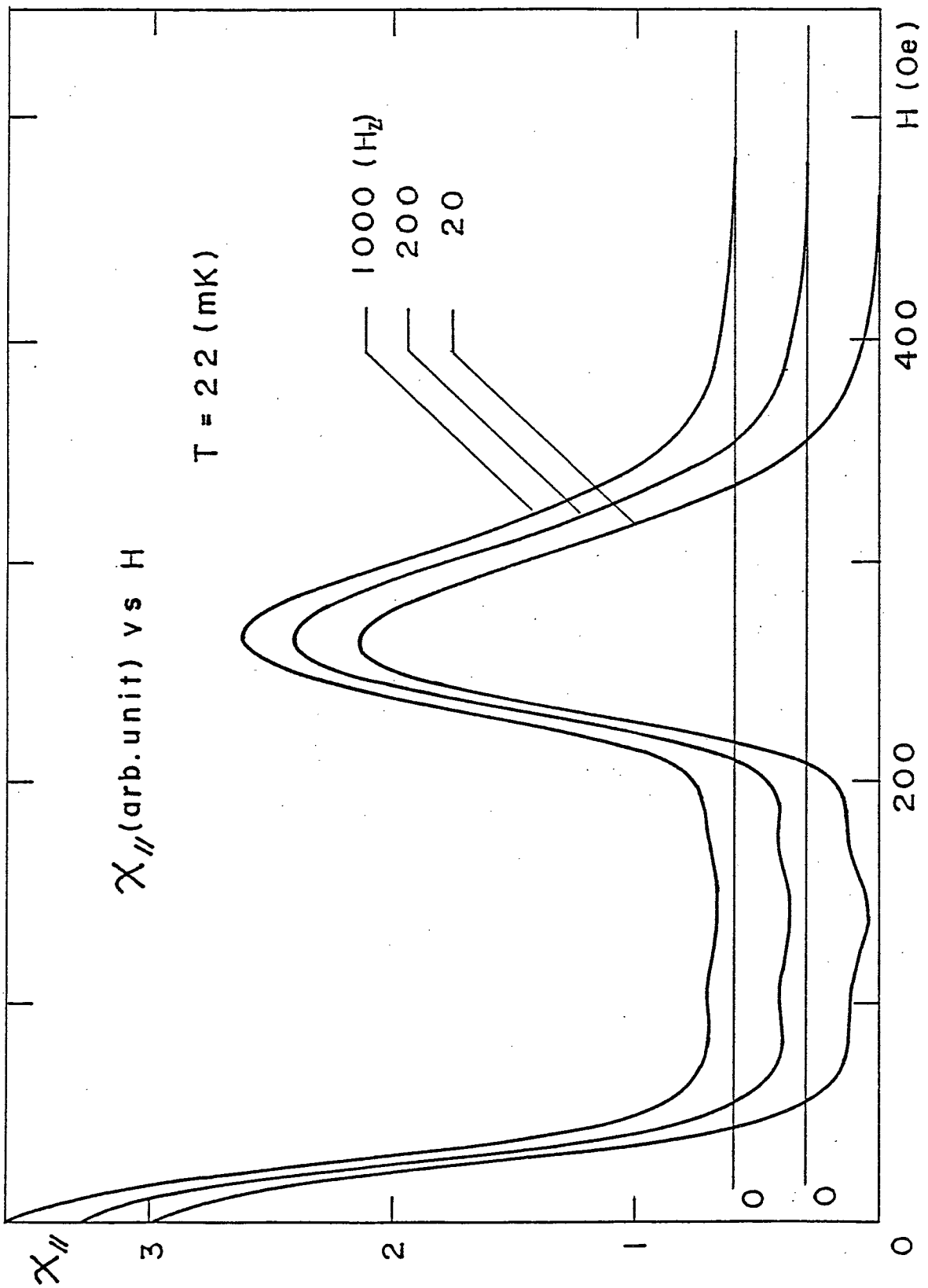

Fig. 7 Frequency dependence of $\chi_{//}$ vs. H at 22 mK.

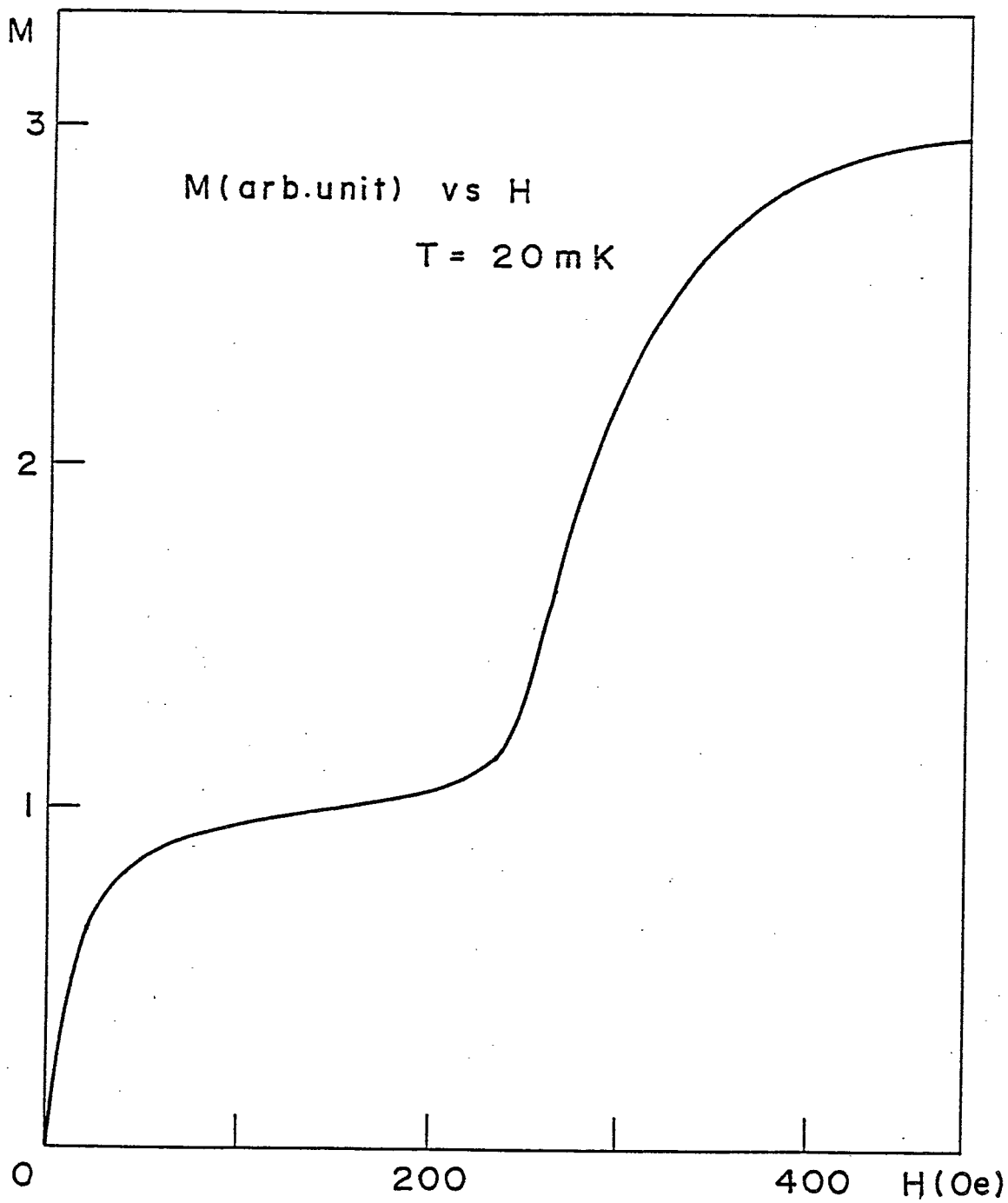

Fig. 8 Magnetization M vs. H curve at 20 mK.

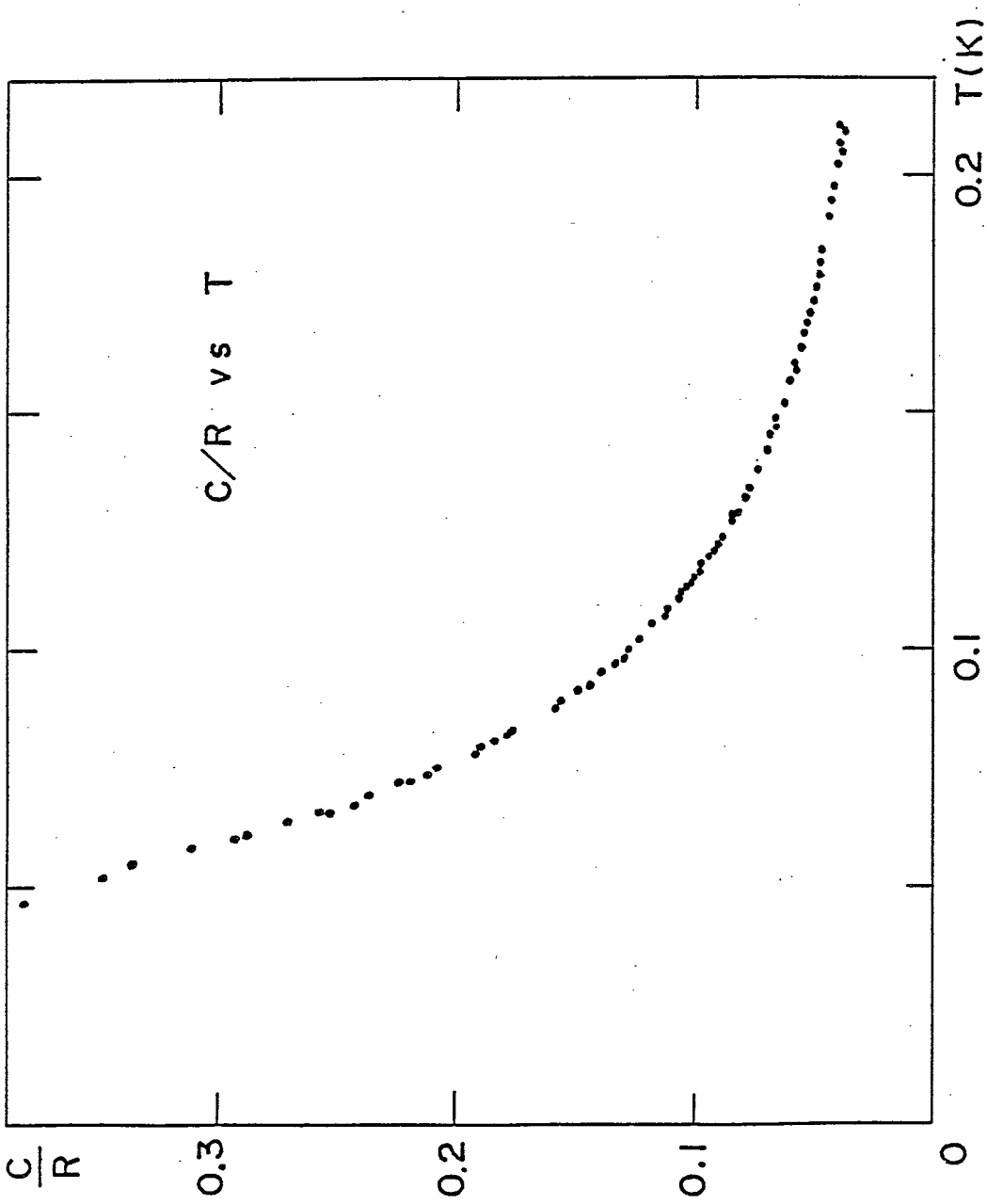

Fig. 9 Specific heat C/R vs. T.

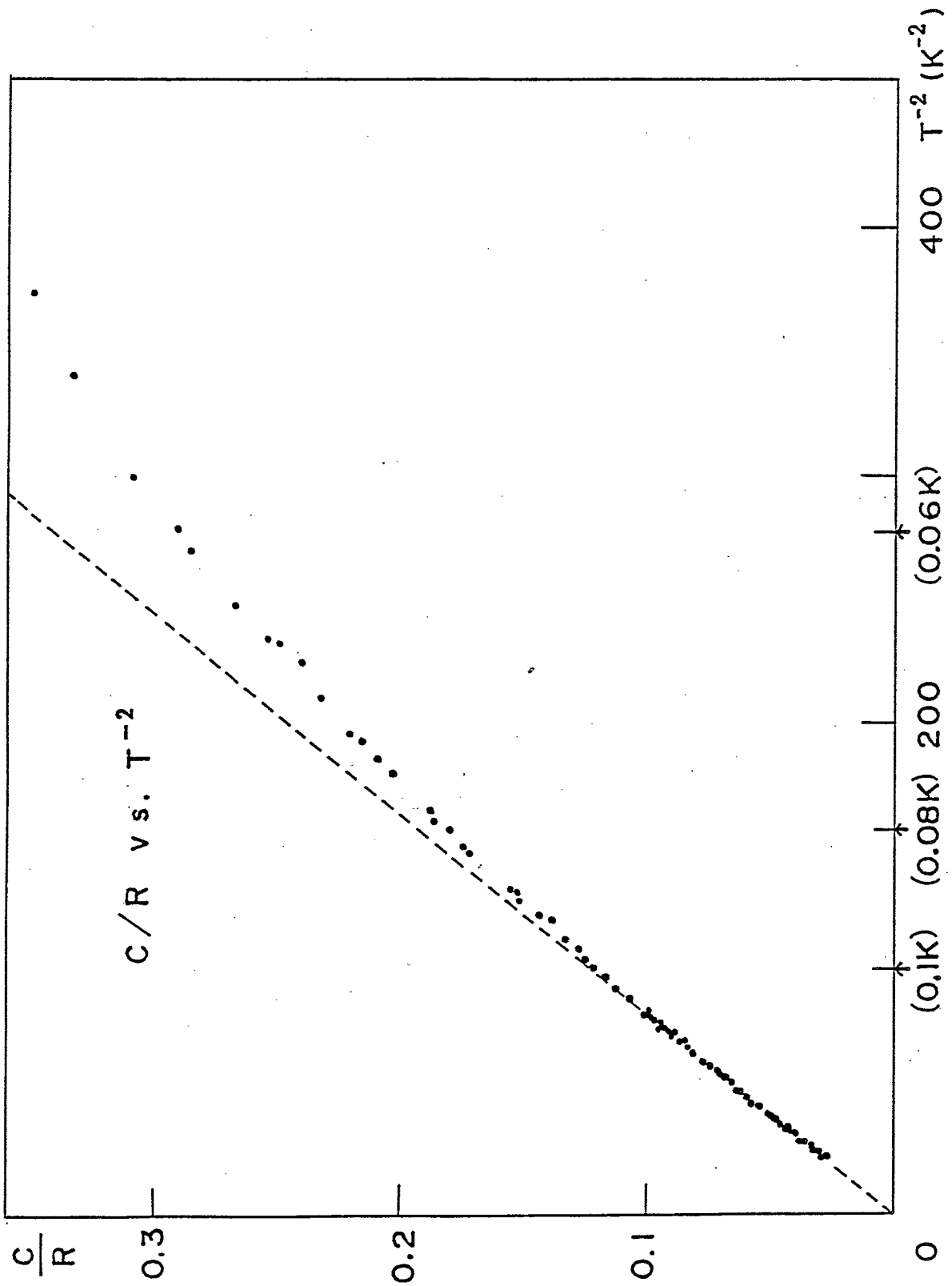

Fig. 10 Specific heat C/R vs. T^{-2}.

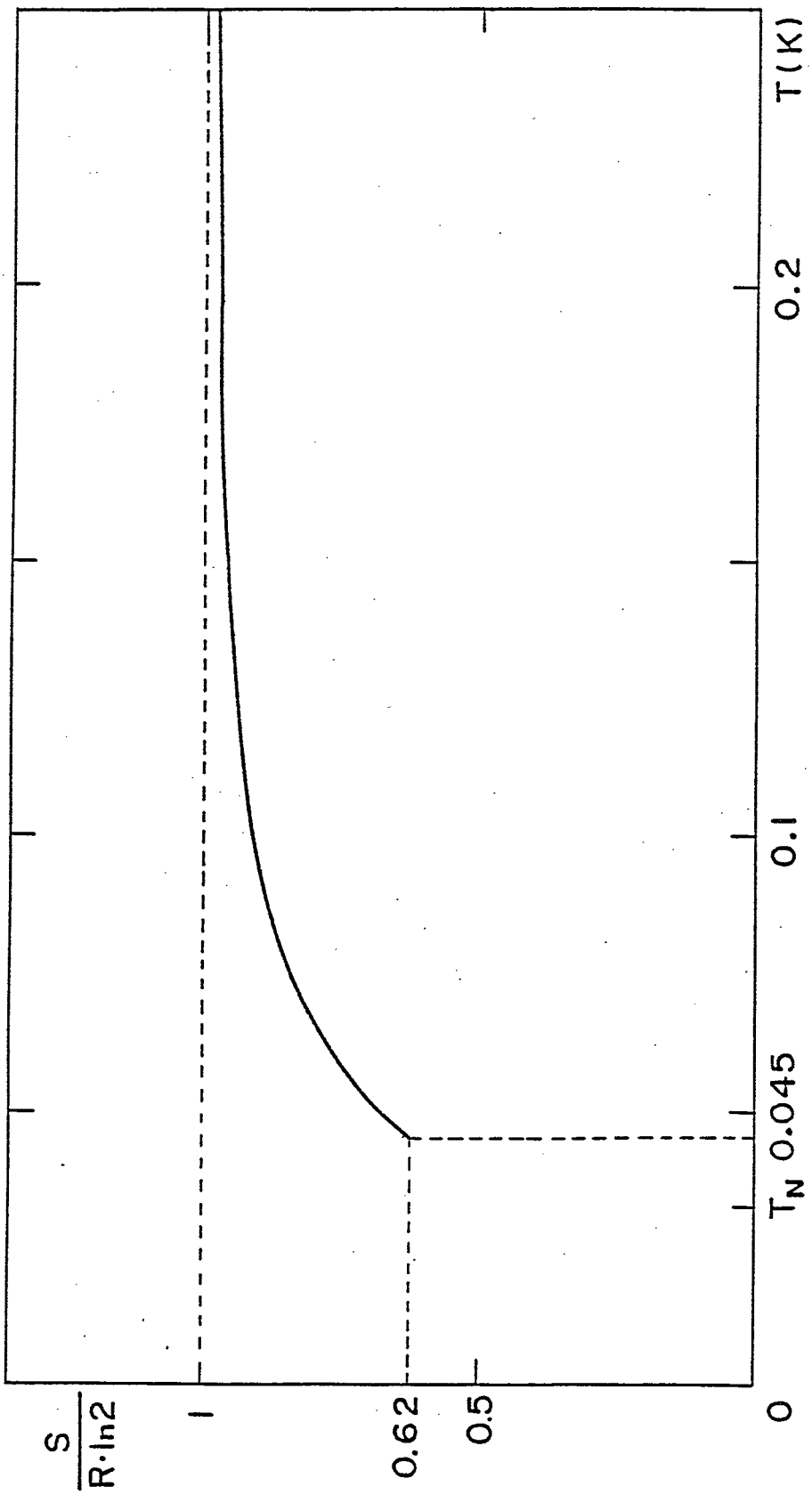

Fig. 11 Entropy calculated using the specific heat data.

4.3.4. Discussions

4.3.4-1. The characteristics of the phase transition

Among the experimental results, the M vs. H curve at 20 mK suggests that the spin system is in the ferrimagnetic state below the temperature indicated by T_c^o in Fig.5, and the C vs. T curve under zero magnetic field suggests that the deviation of $\chi_{//}$ from the Curie-Weiss law is attributed to the development of spin correlation in short range ordered state. Therefore, T_c^o is considered to be the ferrimagnetic transition point directly from the paramagnetic state. However, the antiferromagnetic deviation of $\chi_{//}$ from the Curie-Weiss law is observed in the temperature range 70 mK > T > T_c^o. The susceptibility does not diverge to infinity at T_c^o, and it increases with decreasing temperature below T_c. The properties such as these have not been obseved in the ferrimagnetic substances which were reported before. The magnetic phase diagram determined by the susceptibility measurement is shown in Fig.12. The dotted line shows the magnetic phase boundary obtained by the assumption that it is written by the following form,

$$(H_c/H_c^o)^{\lambda} = 1-(T_c/T_c^o)^2 \qquad (3)$$

The best fit with the experimental data gives H_c = 320 Oe and $\lambda \cong 3.5$.

4.3.4-2. A molecular field approximation

We will show in the following that the magnetic behaviors mentioned above are qualitatively explained by a molecular field approximation with the 3-sublattice model.

The energy level diagram of a single Ni^{2+} ion under a

magnetic field parallel to c axis is given in Fig.1(b). In the temperature region kT << D, the excited state can be neglected. Therefore, the total spin Hamiltonian for interacting spins is written as follows :

$$\mathcal{H}_T = \sum_i g\beta H S_z^i - \sum J_{ij} S_z^i S_z^j \quad , S_z = \pm 1 \ (H /\!/ c /\!/ z) \quad (4)$$

because the contribution of $S_x S_x$ and $S_y S_y$ are dropped out by neglecting the excited state. So, this spin system is Ising one, which is induced by crystal fields.

4.3.4-3. Simple analysis

We take the 3-sublattice model shown in Fig.13(a). Then the Hamiltonian for the 1-th sublattice is written in the molecular field approximation as

$$\mathcal{H}_1 = -3J(\alpha\langle S_{z1}\rangle + \langle S_{zm}\rangle + \langle S_{zn}\rangle - \gamma)\sum_i S_{z1}^i \quad (5)$$

$$\alpha = (6J' + 2J_c)/3J \ , \ \gamma = g\beta H/3J$$

where subscripts 1, m and n specify the sublattice and i the unit cell, J and Jc are interaction coefficients for the nearest neighbor in the c plane and on the c axis respectively, and J' is for the next nearest neighbor in the c plane. This Hamiltonian is equivalent to the starting Hamiltonian used by Mekata for the study if the magnetic behavior at finite temperatures. So, the results obtained by Mekata can be used in our case. The α vs. T phase diagram obtained by Mekata is shown in Fig.14. The structures of the partially disordered antiferromagnetic stste and the ferrimagnetic state in the diagram are shown in Fig.13 (b) and (c).

Referring to the experimental resuts in $NaNiAcac_3$benzene, it

is strongly suggested that only the transition from paramagnetic to ferrimagnetic state is observed. Therefore, we consider the magnetic behavior corresponding to the condition $\alpha \leqq -0.8$. The temperature dependencies of the susceptibility for α =-0.8,-0.9 and -1.0 is shown in Fig.15. And the temperature dependence of sublattice magnetization and of magnetization per unit cell for α=-0.9 are shown in Fig.16 and Fig.17, respectively. According to these theoretical results, it is noteworthy that the susceptibility does not diverge at T_c^o in contradiction to the usual ferro- or ferri-magnetic transition where the spontaneous magnetization $\langle S_z \rangle$ starts to increase sharply. The reason is the following. Although the temperature derivative of $\langle S_z \rangle$ for each sublattice $\partial \langle S_{z1} \rangle / \partial T$, $\partial \langle S_{zm} \rangle / \partial T$ and $\partial \langle S_{zn} \rangle / \partial T$ are infinite at T_c^o respectively, the net change $\partial / \partial T(\langle S_{z1} \rangle + \langle S_{zm} \rangle + \langle S_{zn} \rangle)$ is zero at T_c^o. This is consistent qualitatively with the experimental results shown in Fig.5.

Now, we give the representation of the Curie-Weiss law. The susceptibility for the paramagnetic state is written as follows :

$$\chi_{//} = \frac{(g\beta)^2}{k} (T - \Theta)^{-1}$$
$$k\Theta = 6J + 6J' + 2Jc + k\Theta_{dip} \quad . \tag{6}$$

And, if we include the external the excited level, the susceptibility is written as follows :

$$\chi_{//} = \frac{(g\beta)^2}{k} [(1 + e^{-D/kT})T - \Theta]^{-1} \tag{7}$$

where $\Theta_{dip} = \sum_i J_{ij}^{dip}$. J_{ij}^{dip} is dipole-dipole interaction coefficient, and written as follows :

$$J_{ij}^{dip} = \frac{(g\beta)^2}{a^3} \frac{2\Gamma^2\zeta^2 - \xi^2 - \xi\eta - \eta^2}{(\Gamma^2\zeta^2 + \xi^2 + \xi\eta + \eta^2)^{5/2}} \tag{8}$$

$$\vec{R}_i - \vec{R}_j = a(\xi\vec{a}_1 + \eta\vec{a}_2) + c\zeta\vec{c} \quad \Gamma = c/a$$

where a and $\vec{a}_1$ and $\vec{a}_2$ represent the distance of nearest neighbor spins and unit vectors in the c plane, and c and $\vec{c}$ represent the distance of nearest neighbor spins and a unit vector on the c axis, respectively. And the vector $\vec{R}_i - \vec{R}_j$ describes the relative postion between i and j spins, and ξ, η and ζ are integers.

4.3.4-4. The critical magnetic field

The critical magnetic field is arised from two parts. the one is super exchange interaction , and the other is the dipole-dipole interaction. Owing to strong dipole-dipole interaction along c axis, spin structure of c axis is ferromagnetic. The dipole-dipole interaction energy between c chains in the ordered state are calculated. The dipole energy between two chain is . The dipole-dipole energy is very small. The reason is that the interaction between neighboring spin in the chain is antiferromagnetic and strong but a number of interacting spin is small, while the interaction between distant spin in the chain is ferromagnetic and mumber is large, so total energy becomes very small. Therefore the critical magnetic field at T=0 is determined dy only exchange interaction:

$$H_c^o = 6|J|/g\beta . \qquad (9)$$

Experimental value of H_c is 320 Oe, so J = -7.9 mK.

4.3.4-5. The small susceptibility peaks in ordered state

The magnetic field dependence of the susceptibility measured at 22 mK shows the existence of two small peaks below H_c in the course of increasing and decreasing the field. The phenomenon is

considered to be analogous to phenomenon detected in the ferrimagnetic state in $CoCl_2\ 2H_2O$, which is caused by the rearrangement of the ferrimagnetic boundaries in the course of change of a magnetic field. In our case, there might also exist some excited configulation because of the triangular Ising lattice of the present crystal. That is, small auount of spins in the excited state is considered to be remained around the boundaries. The two peaks observed below H_c are attributed to the spin rearrangement at the energy crossing point between expected configulations. We suppose the five spin structure (see Fig.18). The Zeeman and exchange energy in each spin structure in the external magnetic field ($H /\!/ C$) is

$$E(A.F.1) = -|J| - J' - J_c \qquad (10)$$

$$E(A.F.2) = -|J| + J' - J_c \qquad (11)$$

$$E(F.O) = 3|J| - 3J' - J_c - g\beta H \qquad (12)$$

$$E(F.I.1) = -|J| - 3J' - J_c - g\beta H \qquad (13)$$

$$E(F.I.2) = -J_c - \tfrac{1}{2}g\beta H \qquad (14)$$

Fig.19 shows E-H curve. We consider only exchange interaction as described in 4.3.4-4. The energy crossing points at the lowest excited state are H_α and H_β as shown in Fig.19. H_α and H_β is

$$H_\alpha = 2(|J| + J')/g \qquad (15)$$

$$H_\beta = 6(|J| - J')/g \qquad (16)$$

Experimental value is

$$H_\alpha = 120 \pm 20 \text{ Oe}$$

$$H_\beta = 210 \pm 20 \text{ Oe}$$

Therefore, $J' = 2.5 \pm 1$ mK.

4.3.4-6. Estimation of the exchange interaction coefficients

From nummerical calculation of dipole-dipole interaction and eq.(5), J_c is obtained.

$$J_c = -13.2 \quad mK$$

b is given by high temperature appoximation:

$$b/R = 3(J/K)^2 + 3(J'/K)^2 + (Jc/K)^2 + b_{dip} \qquad (17)$$

Using calculated b_{dip} and obtained exchange coefficient, b is

$$b = 1.3 \times 10^{-3} \cdot R$$

This is agree with experimental value $b = 1.2 \times 10^{-3} \cdot R$

The value of α calculated by these data is -1.2 and corresponds to the case of $\alpha \leq -0.8$. According to these estimations, the dipole-dipole interaction is comparable order to the super exchange one.

4.3.4-7. Some features of ordered state

Now, we consider the increasing susceptibility with decreasing temperature below Tc^o. In 4.3.4-3., it is described that $\partial/\partial T(\langle S_{zl}\rangle + \langle S_{zm}\rangle + \langle S_{zn}\rangle)$ is zero at T_c^o. Where the spontaneous magnetization per unit cell starts to appear. Therefore, it can be considered that the spin system behaves like antiferromagnetic at T_c^o and like ferromagnetic below T_c^o. It is expected that some kind of domains will be formed with appearence of spontaneous magnetization, and that the susceptibility corresponding to some kind of rearrangement of magnetic domains is observed. This is supported by the fact that the temperature dependence of the observed susceptibility under the magnetic field which is strong enough to aligen the ferrimagnetic moments leaving various type of mismatch boundaries between domains is

consistent qualitatively with the theoretical result obtained for the uniform ferrimagnetic state under zero magnetic field (see Fig.17).

According to this interpretation, the temperature dependence of the susceptibility below T_c^o reflects the temperature dependence of the magnetization. If we assume that H^*, where $\chi_{//}(H^*) = \chi_{//}^o/2$, corresponds to the magnetic field necessary to aligen the ferrimagnetic moments, this is about 20 Oe at 20 mK.

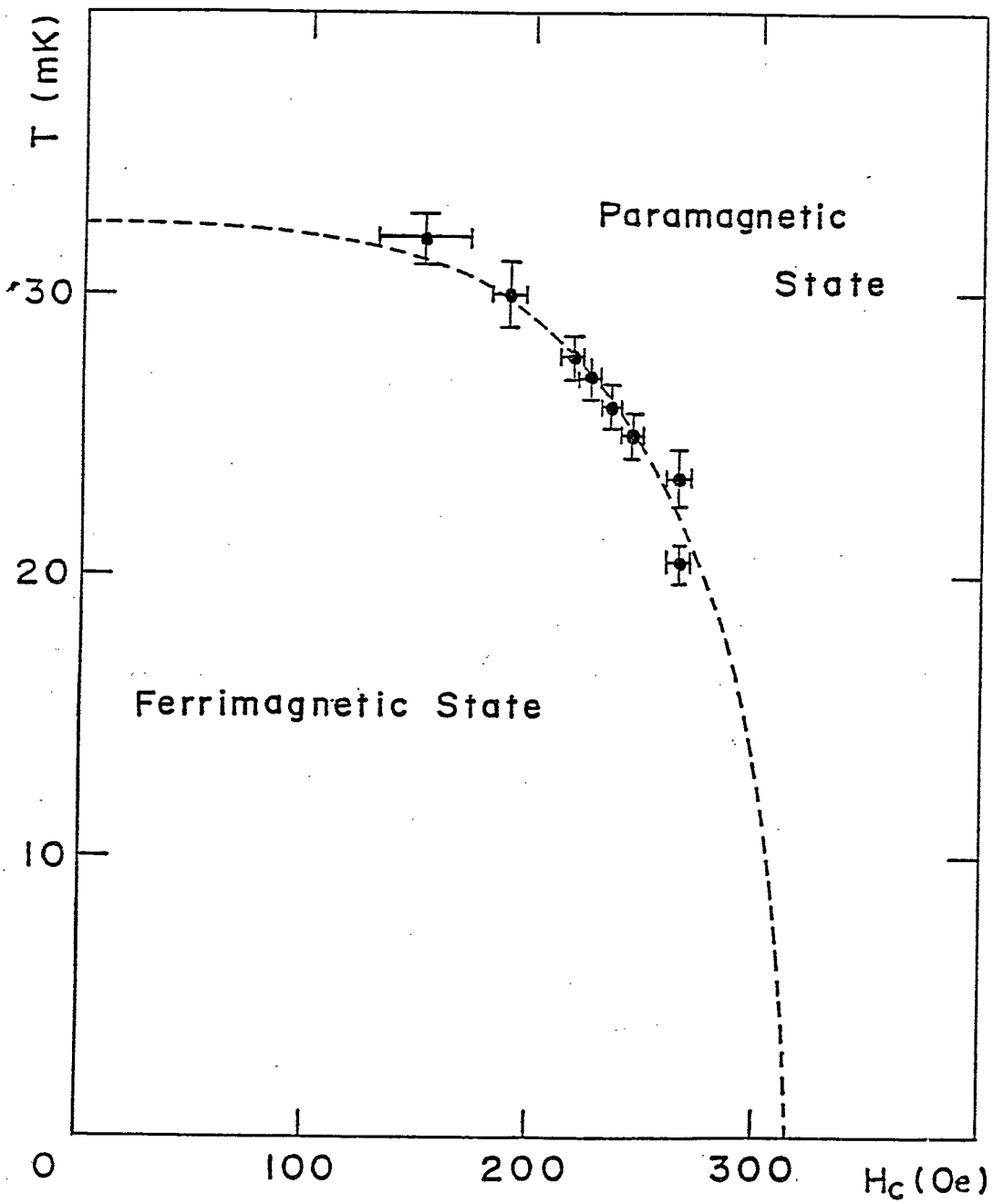

Fig. 12 H vs. T phase diagram. The parameters for the dotted line is given in the text.

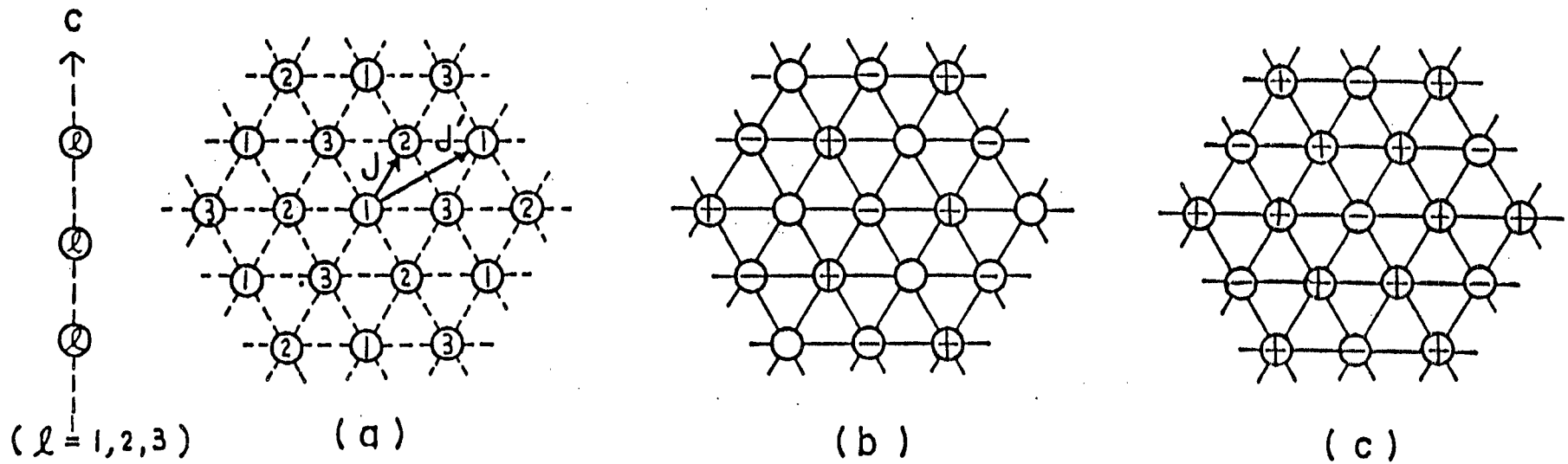

Fig. 13 (a) 3-sublattice model. ($J < 0$, $J' > 0$ and $Jc > 0$).
(b) The structure of partially disordered antiferromagnetic state.
(c) The structure of ferrimagnetic state.

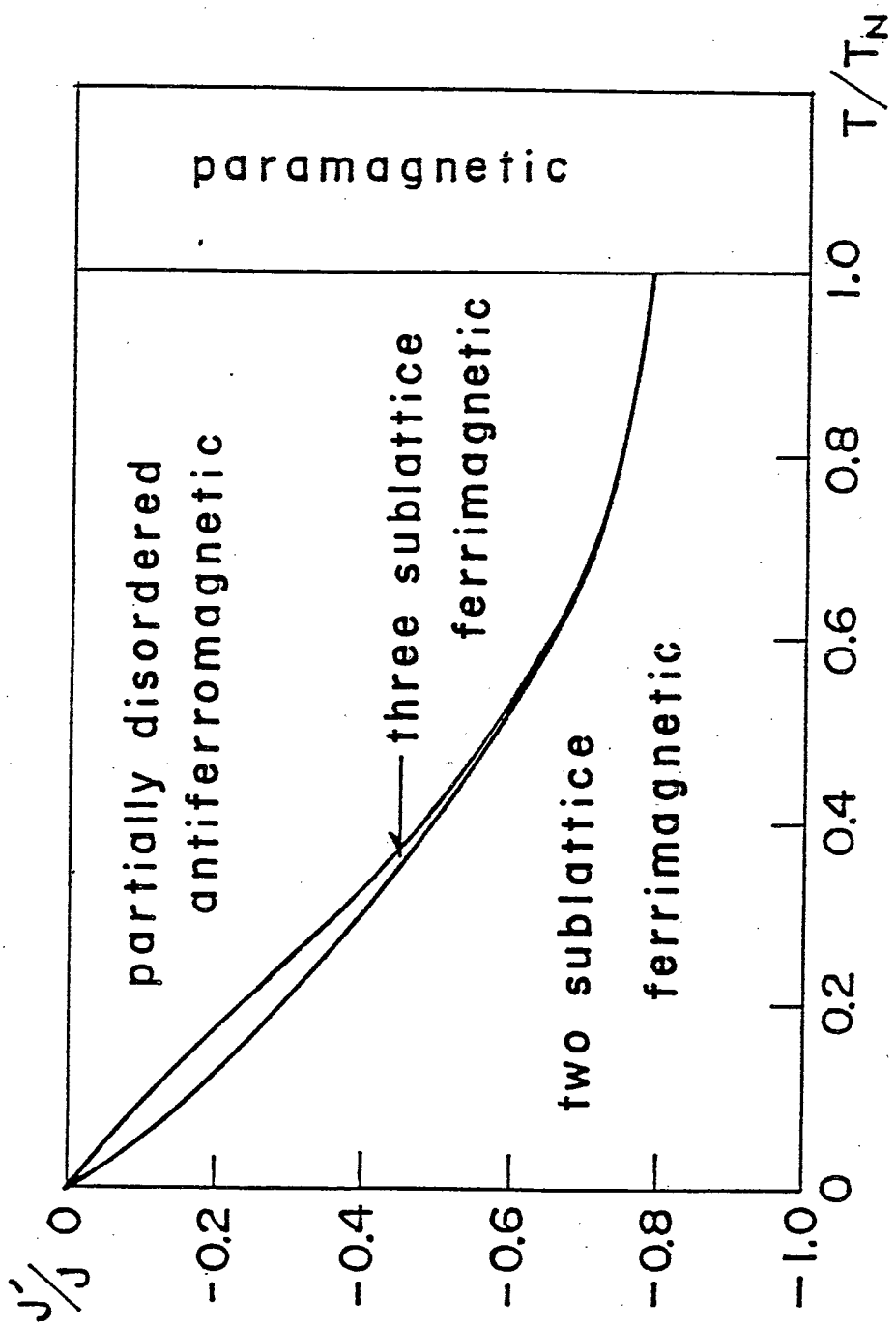

Fig. 14 α vs. T phase diagram.

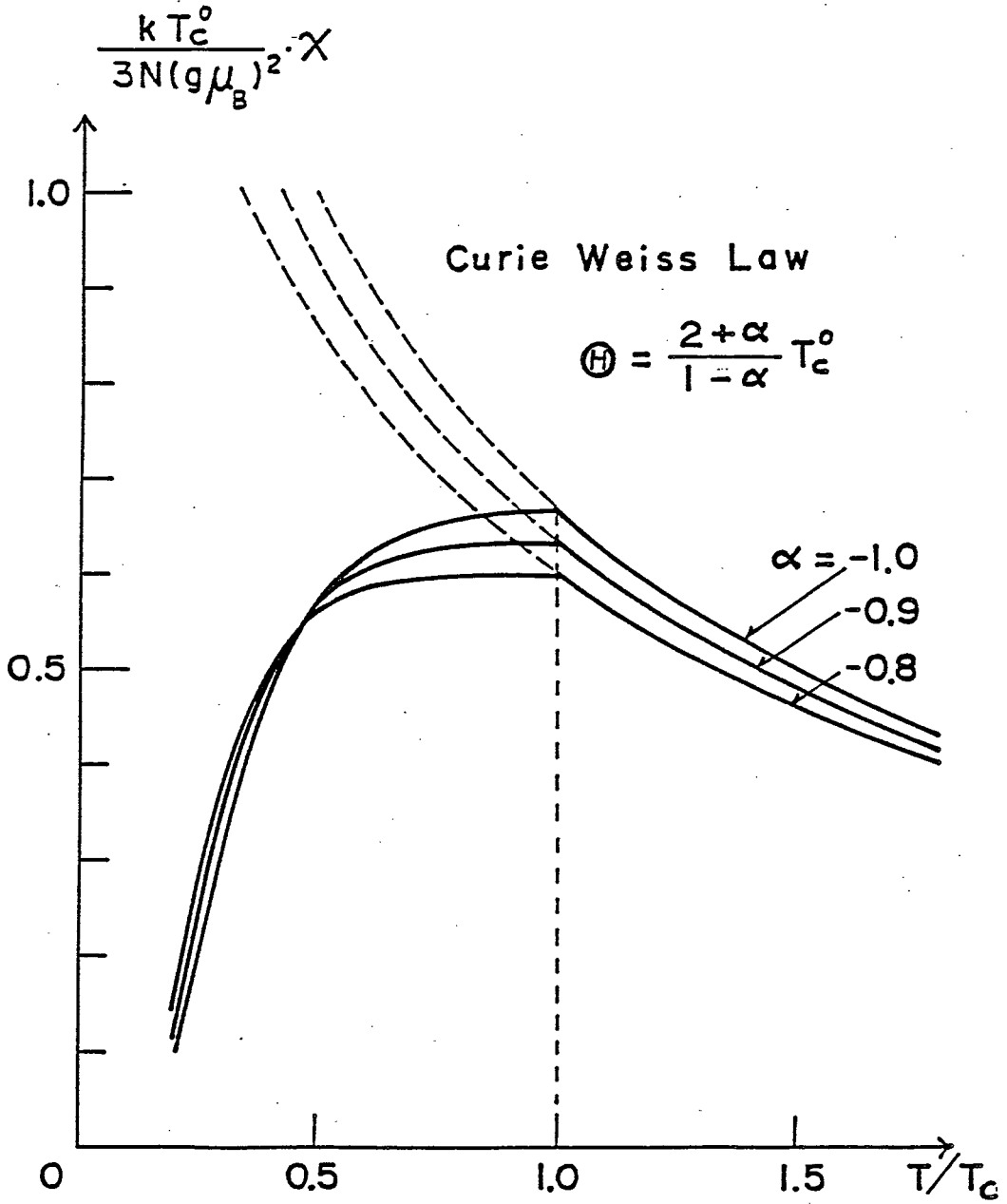

Fig. 15 Temperature dependence of susceptibility calculated for α = -0.8, -0.9 and -1.0.

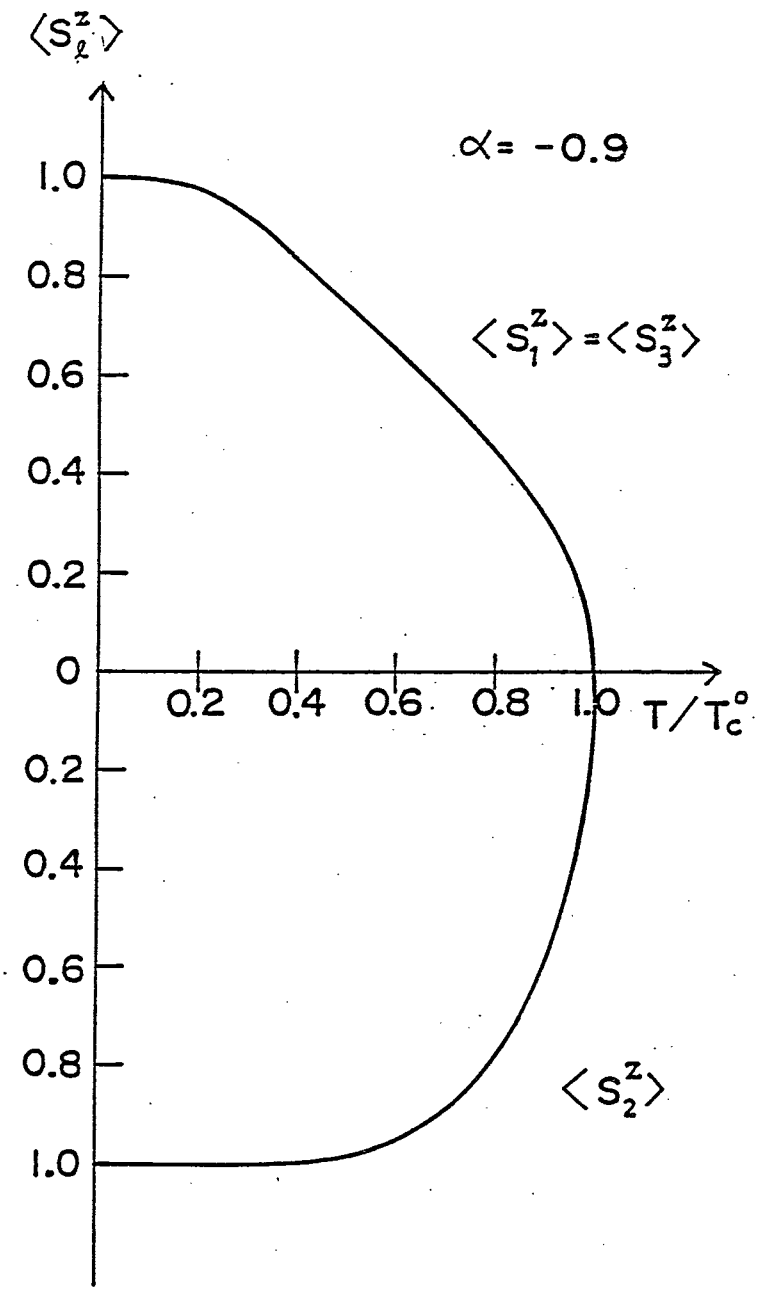

Fig. 16 Temperature dependence of sublattice magnetization calculated for $\alpha = -0.9$.

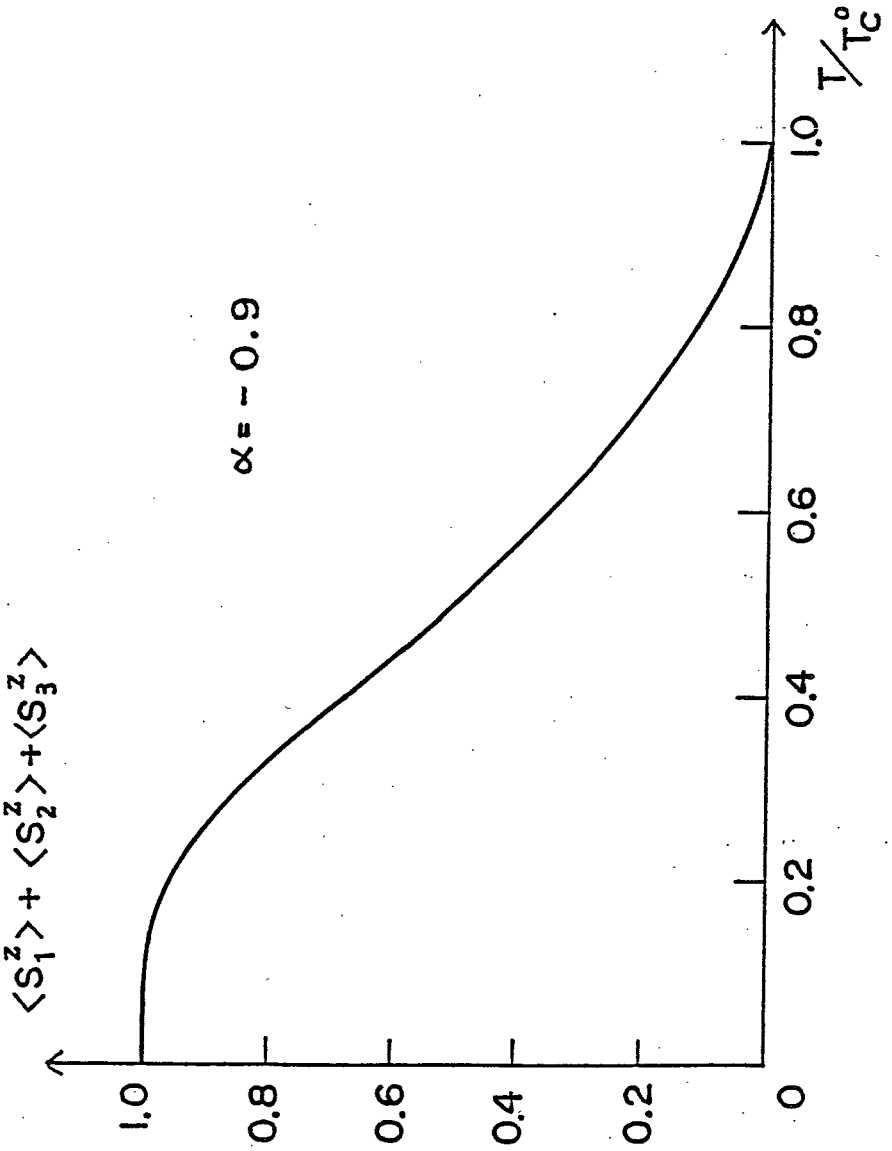

Fig. 17 Temperature dependence of magnetization per unit cell calculated for $\alpha = -0.9$.

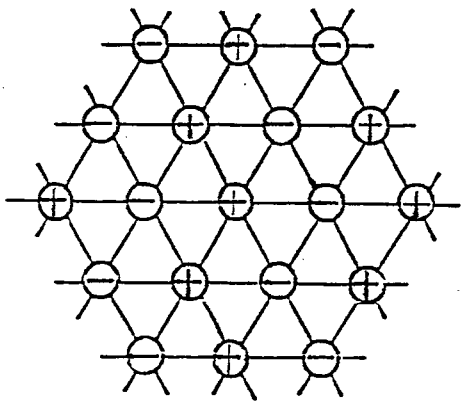

A.F.1

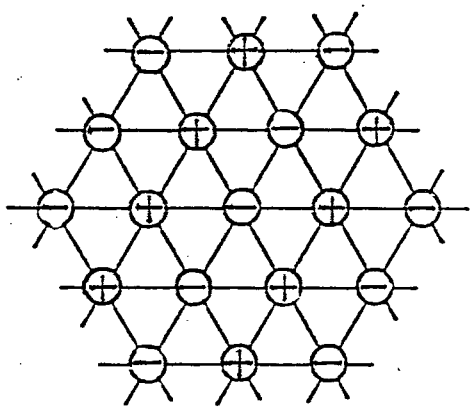

A.F.2

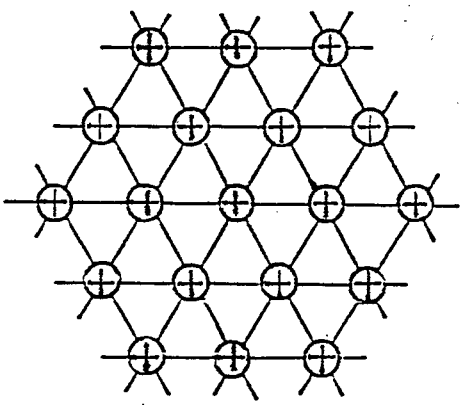

F.O.

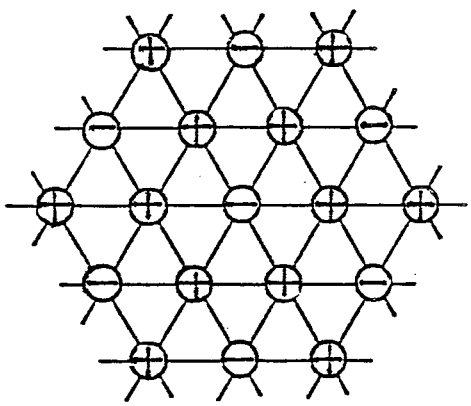

F.I.1

F.I.2

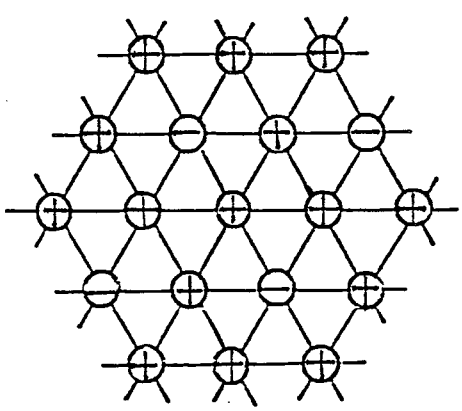

Fig. 18 Spin structures given in eq. (10) ∿ (14)

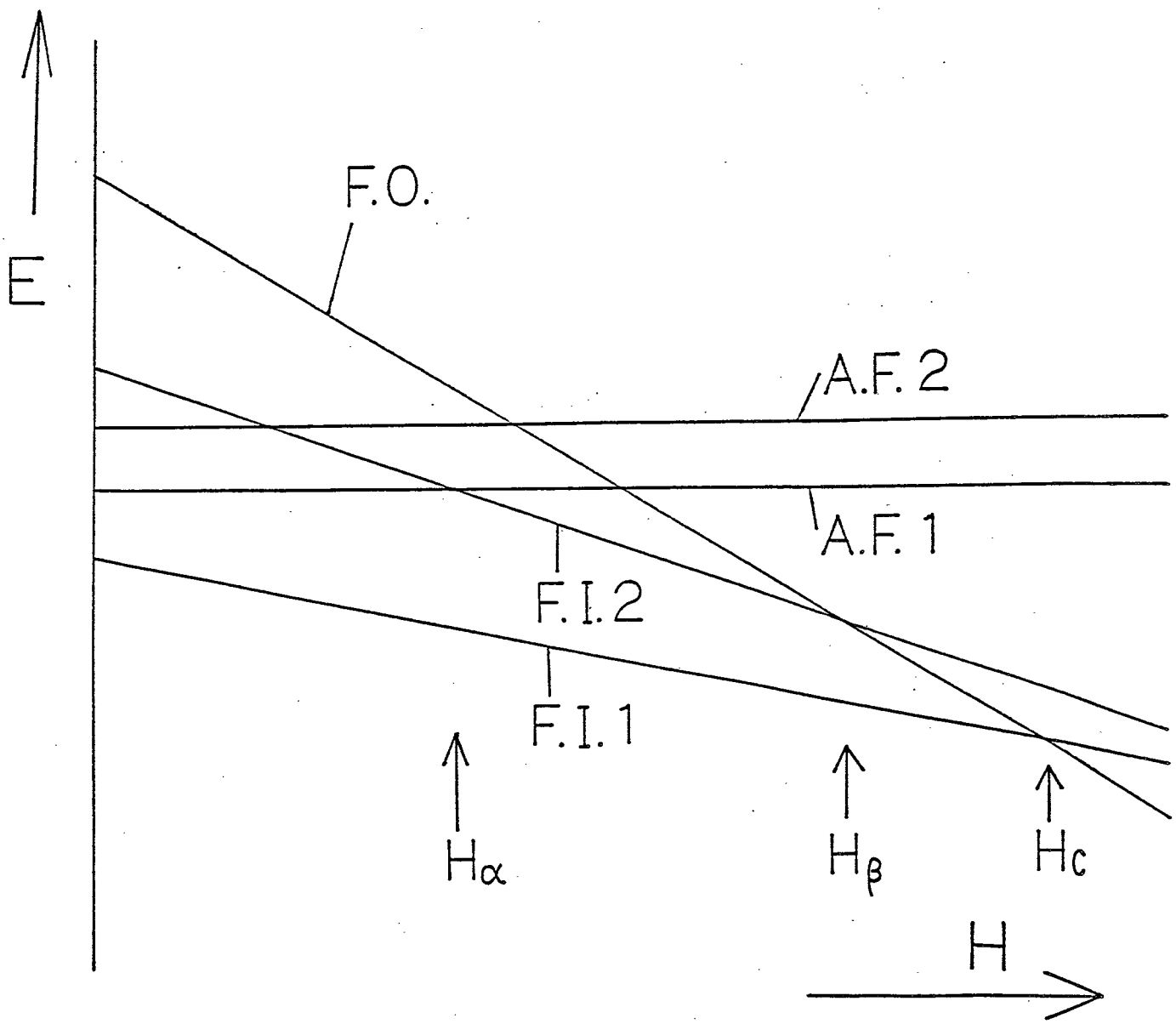

Fig. 19 E-H curves showing the eq.(10)~(14)

4.3.5. Summary

From the A.C. susceptibility measurement, it is concluded that the system is the ferrimagnetic state below 32.5 mK. We expected, at first, the partially disordered antiferromagnetic state in the temperature region where the deviation of the susceptibility from the Curie-Weiss law was notable below about 70 mK. But the specific heat measurement shows that this deviation is due to the development of spin correlation of short range order. Therefore, the observed ferrimagnetic phase transition corresponds to the case of $\alpha \leq -0.8$ in the antiferromagnetic triangular Ising lattice. This ferrimagnetic phase transition is characterized by the finite susceptibility at the phase transition point in spite of the appearance of the total spontaneous magnetization. The characteristics have not been observed up to now in ever-known ferrimagnets.

§ 4.4. Magnetic Transition: Excited state

4.4.1. The experimental conditions of excited state spin ordering

The spin Hamiltonian of Ni^{2+} (S=1) in trigonal crystal field is described by

$$\mathcal{H} = D(1-S_z^2) + g\beta HS_z \quad (s=1) \qquad (18)$$

In the case of D>0, the upper level $|+1\rangle$ of the ground doublet $|\pm1\rangle$ crosses the excited singlet state $|0\rangle$ at the field of $H_c=D/g\beta$ as shown in Fig.1(b).

Experimantal procedure is as below. First of all, we cool the spin system well below the crystal field splitting D at zero field, then we apply magnetic field with the sweep rate faster than such spin relaxation rate that changes the population of each level. This is the second condition and the spin relaxation in question is so called "cross-relaxation". The shortest cross-relaxation time below H_c of $NaNiAcac_3$benezene is 6μsec at $H_c/3$. At this field, the three spin levels make a equal spacing and cross- relaxation time is minimum here.

If we suppose that the population of each level does not change in the course of increasing magnetic field and only thermal equilibrium within two levels $|0\rangle$ and $|+1\rangle$ is attained near the crossing field H_c, the the adiabatic magnetization cooling may be achieved. Namely, we expect

$$T_f^e=(H_{loc}^e/H_c)T_i^e \qquad (19)$$

is valid. Where a superscript ^{e} means excited state and $H_c=D/g\beta$. The spin ordering may happen when $T_f^e \lesssim g H_{loc}^e/k$ or $T_i \lesssim D/k$. The character of this spin ordering is expected to be the same as that of ground state singlet spin system.

The energy level separation near Hc depends on the direction of external magnetic field with respect to the crytal c axis. The misorentation of the field axis of angle θ from c axis couses an anticrossing between $|+1\rangle$ and $|0\rangle$ level at H_c with energy gap ΔE of

$$\Delta E = \sqrt{2}D\theta \qquad (20)$$

The spin ordering does not occur when E is larger in comparison with spin-spin interaction. This is already discussed by Tachiki in the case of the ground state singlet system. This is third condition.

4.4.2. Experimental apparatus for pulsed magnetic field

The three condition in order to observe an excited spin ordering are

1. $T_i \lesssim D/k$
2. $dH/dt \gg \Delta H_{cr} / \rho_{cr}$ $\left[\Delta H_{cr} \sim 300\,Oe,\ \rho_{cr} \sim 6\mu sec \text{ at } H_c/3 \right]$
3. $\sqrt{2} D\theta \lesssim \langle \mathcal{H}_{s-s} \rangle$ $\left[\langle \mathcal{H}_{s-s} \rangle \sim 30\,mK \right]$

where D is uniaxial crystal field splitting, ΔH_{cr} is the half width of the cross-relaxation, ρ_{cr} is cross-relaxation time and $\langle \mathcal{H}_{s-s} \rangle$ is spin-spin interaction energy.

Now, we estimate above condition numerically for $NaNiAcac_3$benzene. To cool the sample below 3K is easy. Using standerd He^3 or He^4 cryostat, we control the initial spin temperature between 0.4K to 4.2K. The second condition claim that the sweep rate of a pulsed magnetic field should be faster than 10^8 Oe/sec at Hc/3. Also the angle between the direction of a magnetic field and c axis must be smaller than 0.4° to fill the third condition.

We designed a single layer coil with small inductance. The size is 30mm long and 6mm in diameter. This coil producies a pulsed magnetic field with peak value of 50kOe at quartor period of 50 sec and the coil can be tilted by few degrees. In order to cool the crystal at liq.He^3 temperature, we make a small adiabatic cell and He^3 pot to set in the puls coil. The adiabatic cell is made of 5mm stainless pipe and He^3 pot is made of 3mm Cu-Ni pipe. The cryostat is shown in Fig.20. The block diagram of the experimental apparatus is shown in Fig.21. The sweep rate can be changed by charging voltage and capacitance of condenser.

The signal dM/dt is measured by usual pick up coil method and the magnetic field is monitored by integration of the voltage of the search coil. Both signal is stored in a digital memory and recorded by X-Y recorder.

We use MATSUSHITA carbon resistor ERC 18 SGJ 510 ohms as a resistance thermometer. The thermometer is calibrated by Ge resistance thermometer.

In order to obtain higher sweep rate of a magnetic field, we made a miniature pulse coil with very small inductance. The bobbin of this coil is made of thin glass pipe with outer diameter 1.3mm and inner diameter 0.8mm. The crystal is put into the glass pipe and fixed by G.E. vanish. The pulse coil is made of one layer of Formex copper wire with diameter of 0.06mm. The pick up coil is wound around the pulse coil. The pulse coil produces about 40kOe with a quarter period of 10μ sec with combined use of capacitors (4μ~14μF). Conventional ignitron switch is used for discharge. This results the maximaum sweep rate of $dH/dt=5\times10^{9}$ Oe/sec. The pulse coil and cryostat is shown in Fig.22. In this system, the pulse coil and the crystal are fixed together and the small misalignment of a magnetic field can not be adjusted.

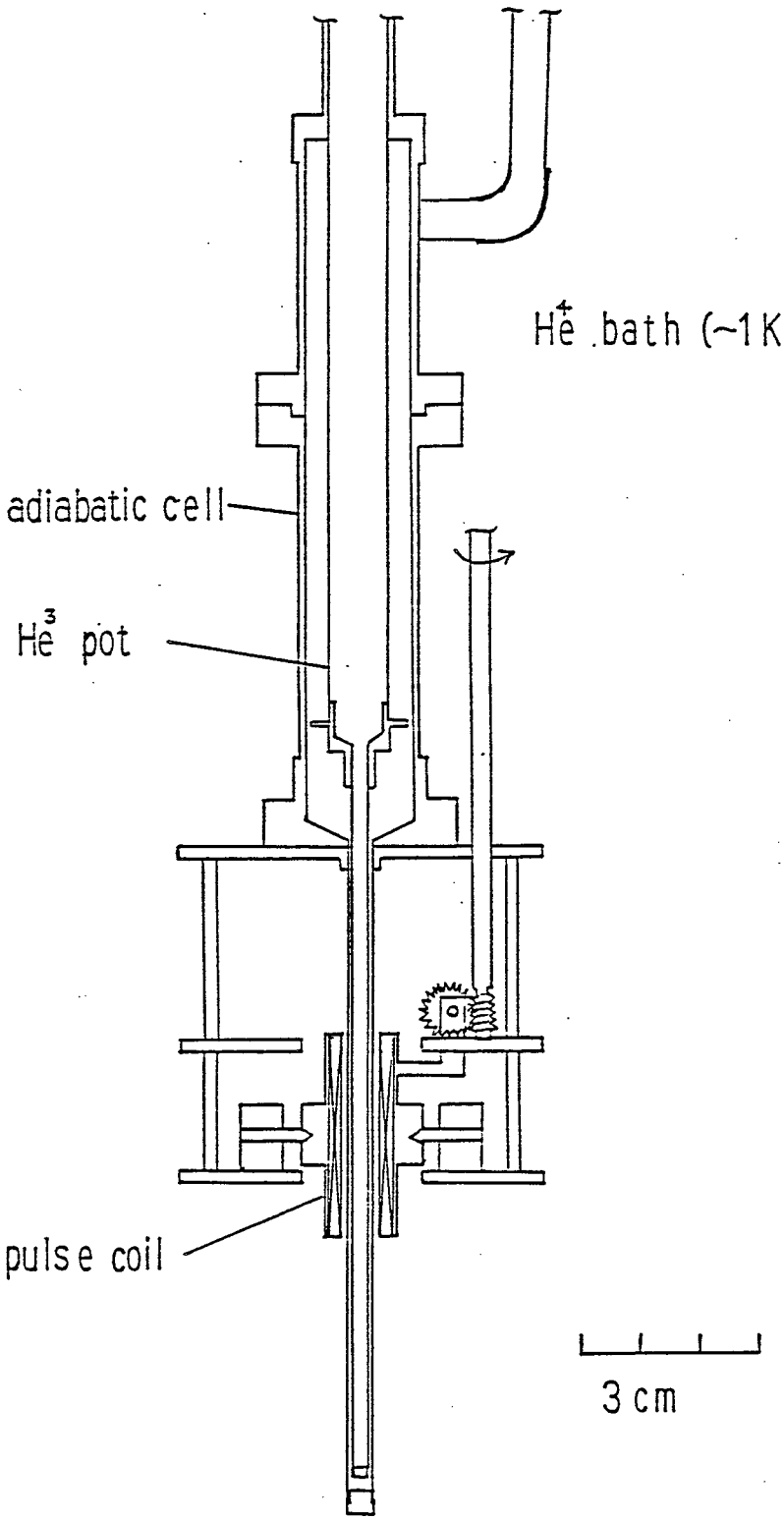

Fig. 20 Pulse coil and liq. He^3 cryostat

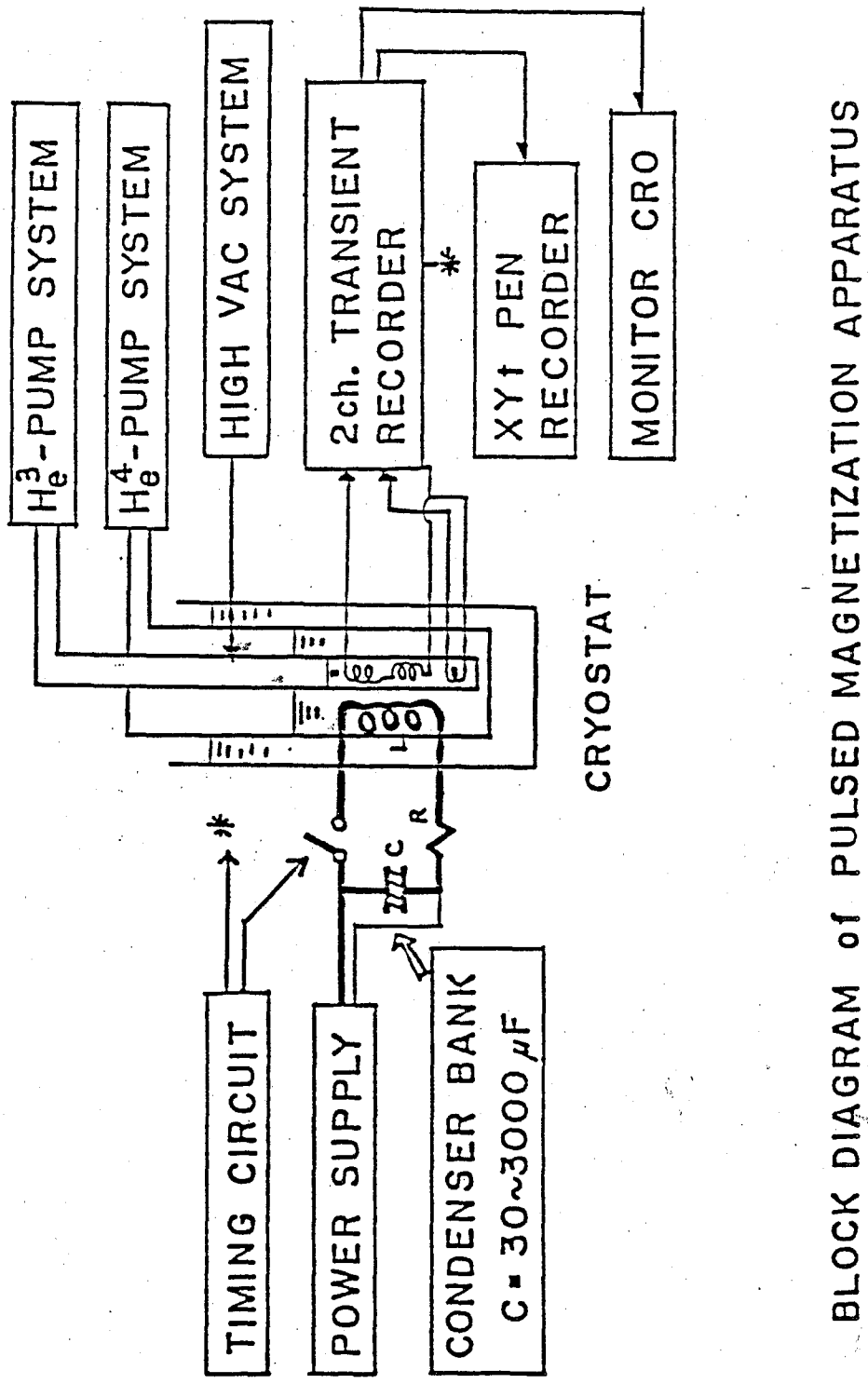

BLOCK DIAGRAM of PULSED MAGNETIZATION APPARATUS

Fig. 21 Block diagram of pulsed adiabatic magnetization.

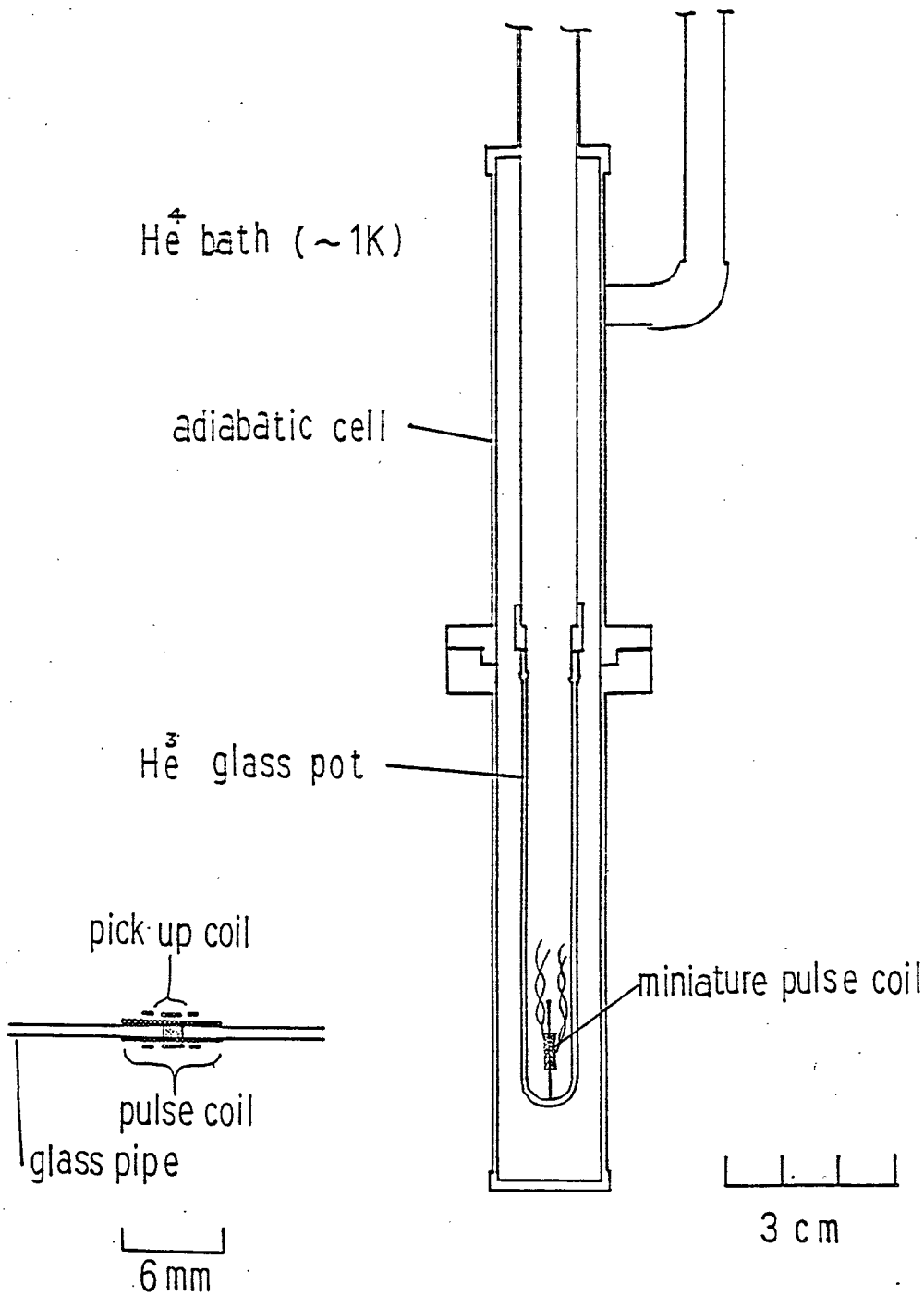

Fig. 22 Miniature pulse coil and liq. He^3 cryostat

4.4.3. Experimental results

4.4.3. Observation of excited state spin ordering

Fig.23 shows the example of experimental results on $NaNiAcac_3$benzene in the case of pulsed magnetic field applied parallel to the crystallographic c axis; H//c. Fig.24 shows initial temperature T_i dependence of the dM/dt around H_c in the increasing mode of pulse field . The systematic development of the signals obvserved by decreasing the initial temperature shows the antiferromagnetic spin ordering just like the ground state singlet system. In Fig.24 there is a small plateau between $T_i \cong 3.00$ and 2.08K and it becomes very sharp below 1K. Therefore, a certain spin ordering occurs below $T_i \approx 3K$. This is consistent with the condition 1. The angular dependence of signal on the direction of the magnetic field with respect to c axis is shown in Fig.25. The double peak becomes single by changing angle about 0.7°. This suggests that spin ordering is destroyed by anticrossing caused by misalignment of the order of θ 0.7 .

4.4.4. Results of the experiments on the miniature pulse coil

The miniature pulse coil is fixed with the sample, so the direction of the magnetic field cannot be changed. We already know the resulting signal due to misalignment of the magnetic field from c axis as shown in Fig.25. Thus we make a lot of miniture pulse coils with sample and examine the signal dM/dt around H_c. Results of pulse coil with the smallest misalignment are shown. The dM/dt around H_c are shown at three sweep rates. The results for different sweep rates of $dH/dt=4.06\times10^9$ Oe/sec, $dH/dt=2.44\times10^9$ Oe/sec and $dH/dt=1.64\times10^9$ Oe/sec are given in Fig.26-28. When the sweep rate becomes large, the double peak tends to disappear as shown in Fig.28. The dM/dt in decreasing field ($dH/dt=4.0\times10^9$) does not show double peak.

4.4.5. The case of mixed crystal $NaNi_{1-x}Co_xAcac_3$benzene

So far we have described the results on pure $NaNiAcac_3$benzene. The pure crystal means that Co^{2+} ions are contained less than 0.02%. In this section we describe the effect of Co^{2+} impurity. dM/dt of pure $NaNiAcac_3$benzene around H_c is shown in Fig.29. In Fig.30 and Fig.31, x=0.013 and 0.008 respectivly. The sweep rate of the pulsed magnetic field is 1.13×10^9 Oe/sec. When the concentration becomes large, the first peak of double peaks becomes small. The another effect of Co^{2+} impurity is shown in Fig.32 and Fig.33. dM/dt of x=0.013 is shown in Fig.32 and pure case is shown in Fig.33. There are peaks of dM/dt corresponding to $H=H_c$ and $H_c/3$ in pure crystal. However another peak apperes at lower than $H_c/3$ in x=0.013. We assume that the new peak is due to cross-relaxation among Co^{2+} and Ni^{2+}. In order to study the effect of cross-relaxation in detail, we measure a.c.susceptibility of the mixed crystals.

The field dependence of a.c.susceptibilities in x=0.013 are shown in Fig.34 and pure case is shown in Fig.35. The new peak appears at H=4.6kOe. If cross-relaxation among Ni^{2+}-Co^{2+} occurs at 4.6kOe, the energy difference between $|0\rangle$ and $|1\rangle$ of Ni is equal to that of $|\pm1/2\rangle$ of Co^{2+}. From it we calculate g value of doped Co^{2+} and obtain

$$g_{//} = 8.0$$

In order to obtain g value of $NaCoAcac_3$benzene, we measure the absolute value of susceptibility.

$$g_{//} = 7.4\sim8.0$$

This value is in good agreement with the calculated value. Therefore we concluded that the new peak at 4.6kOe is due to

cross-relaxation among Ni^{2+} and Co^{2+}. From E.S.R. measurement we obtain only $g_{\perp}$value of Co^{2+} in $NaCoAcac_3$benzene

$$g_{\perp} \cong 0.8$$

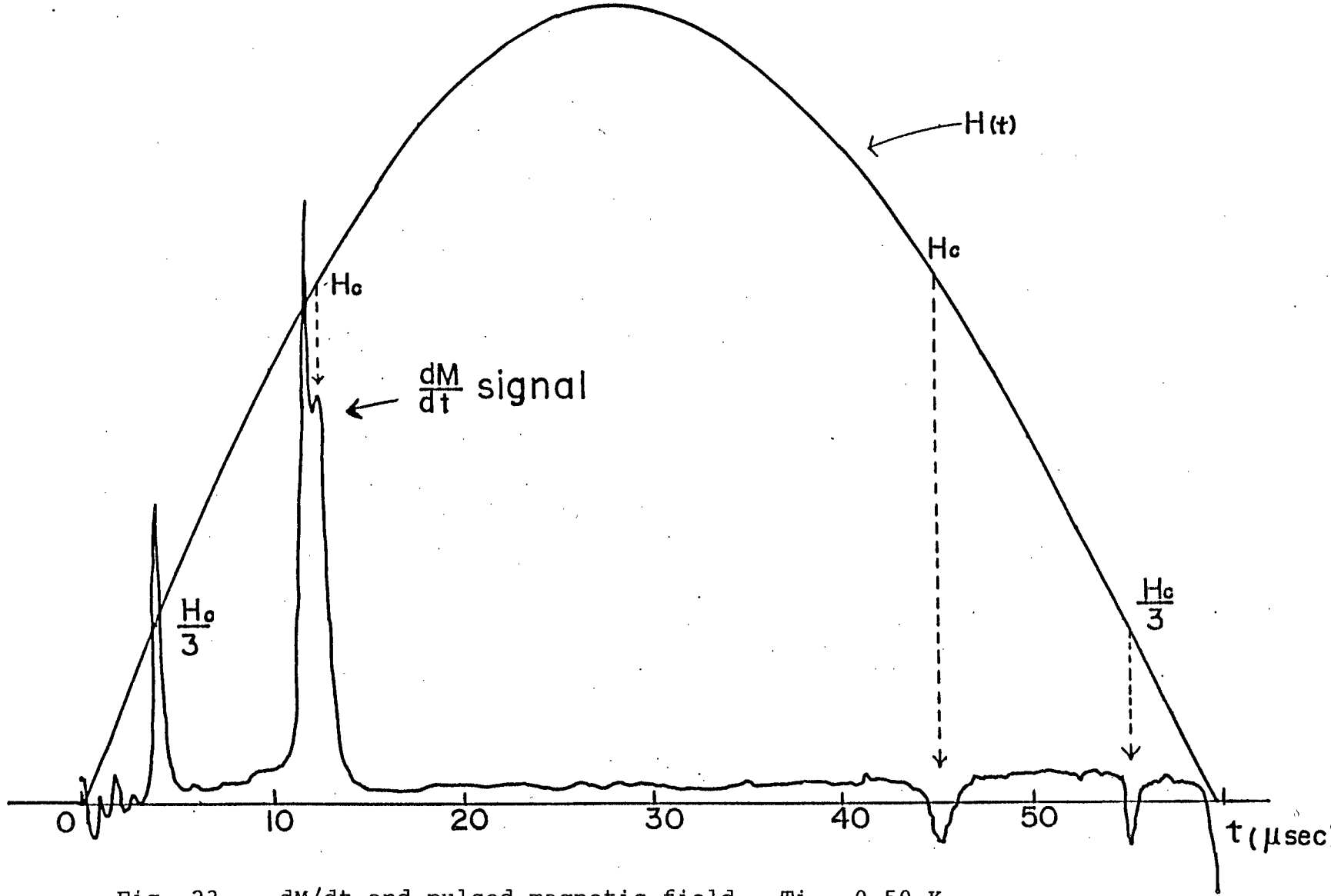

Fig. 23 dM/dt and pulsed magnetic field. Ti = 0.50 K .

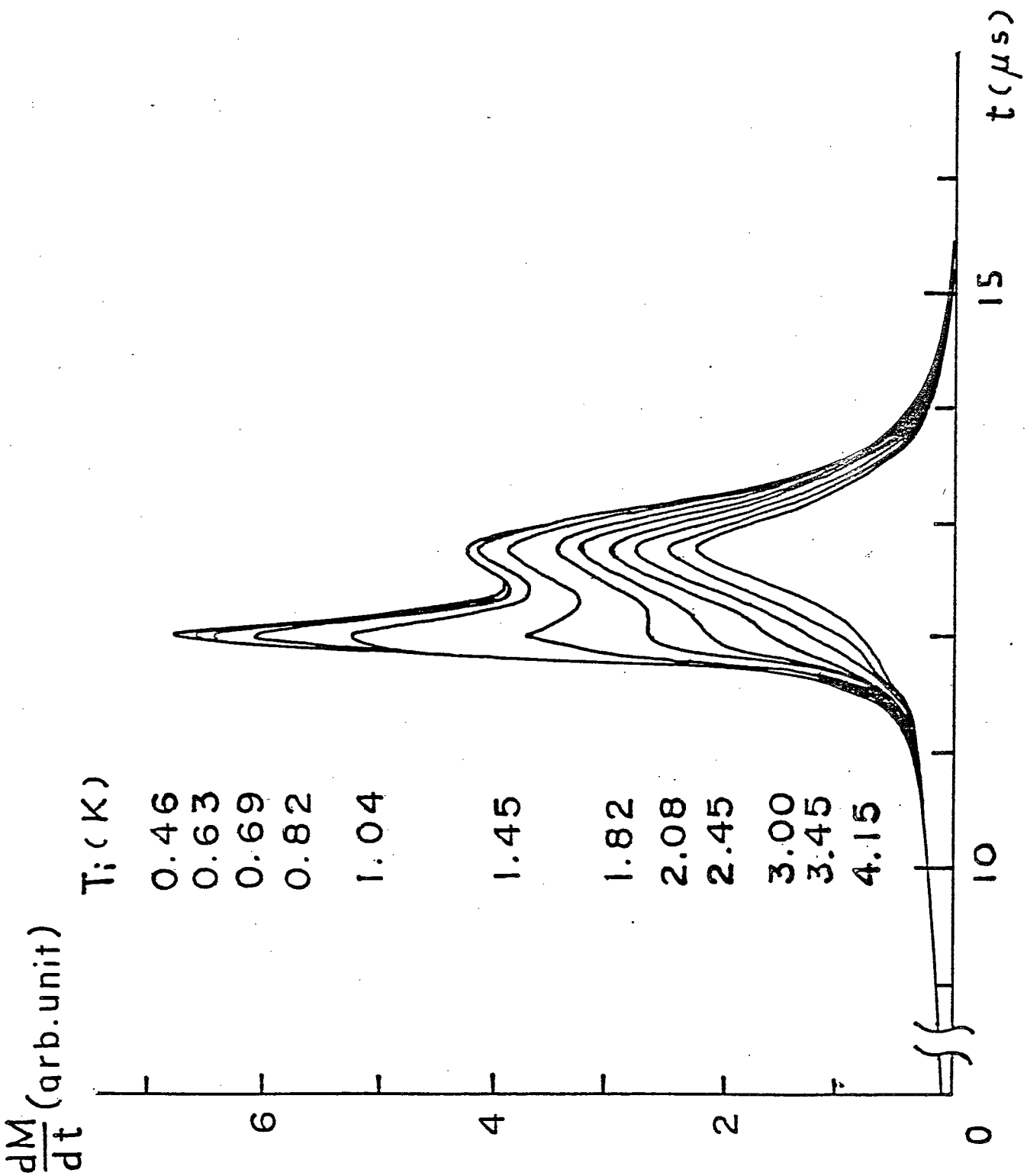

Fig. 24 dM/dt around Hc

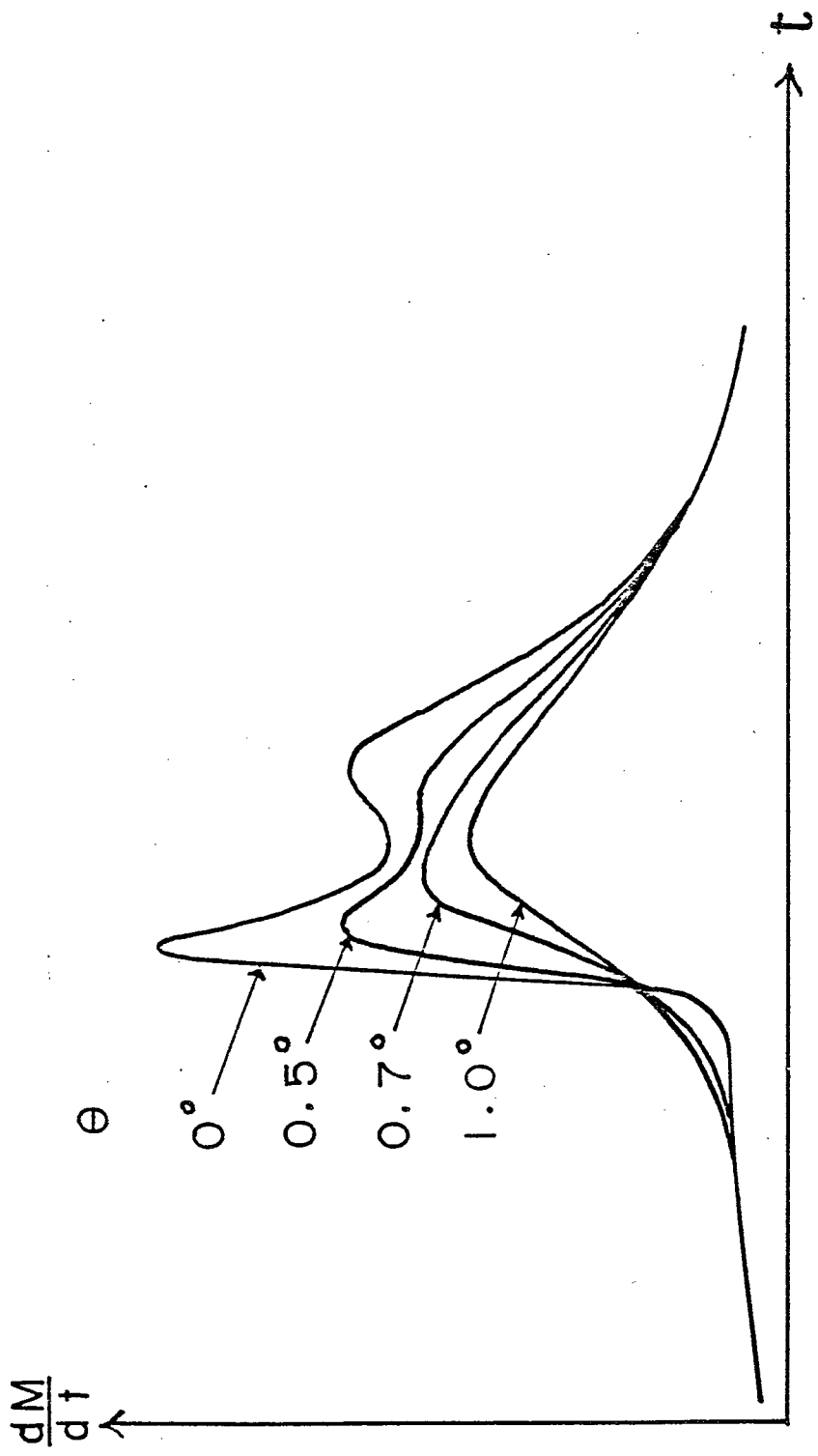

Fig. 25 Angular dependence of dM/dt around Hc

Fig. 26 dM/dt around Hc in miniature pulse coil

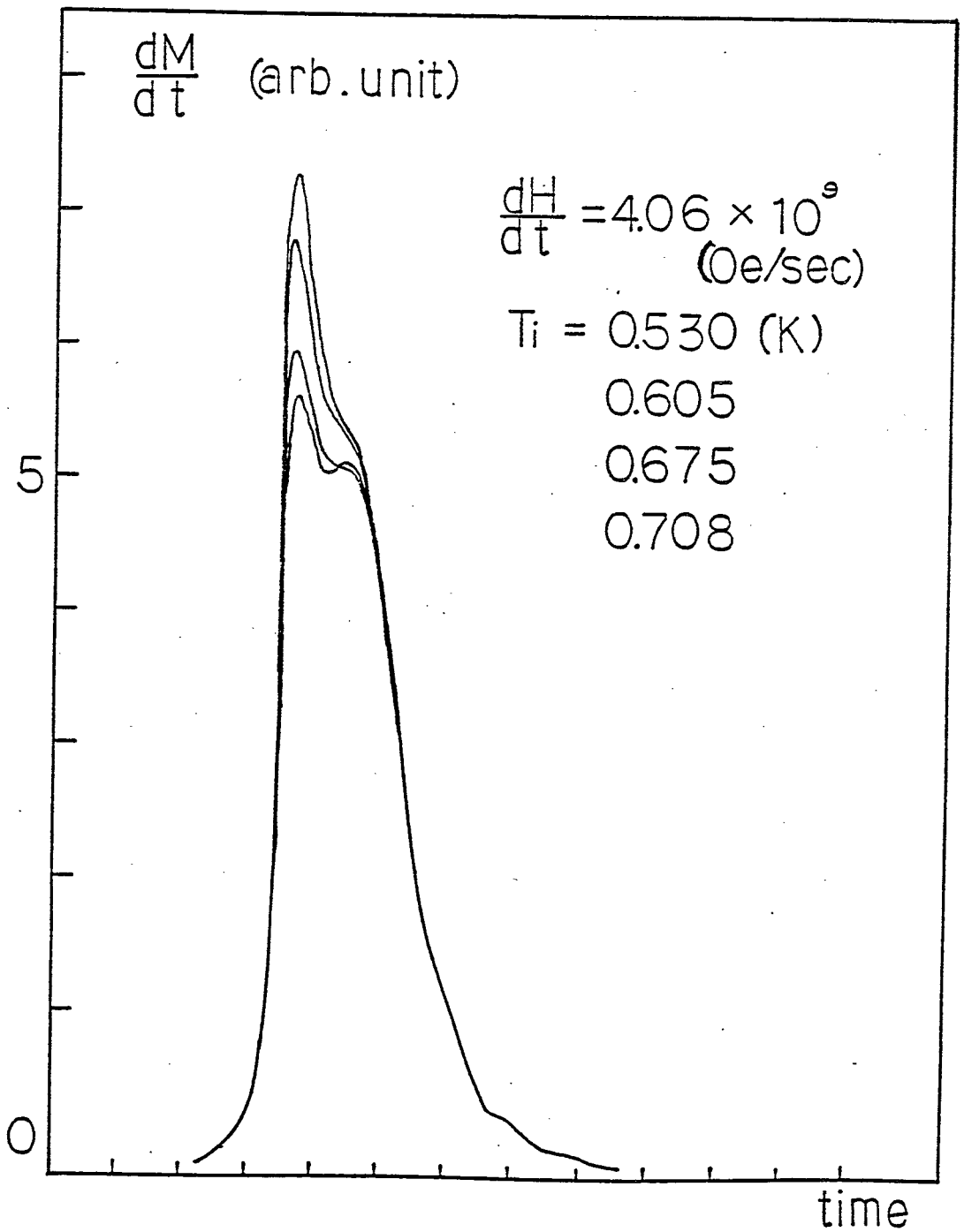

Fig. 27 dM/dt around Hc miniature pulse coil

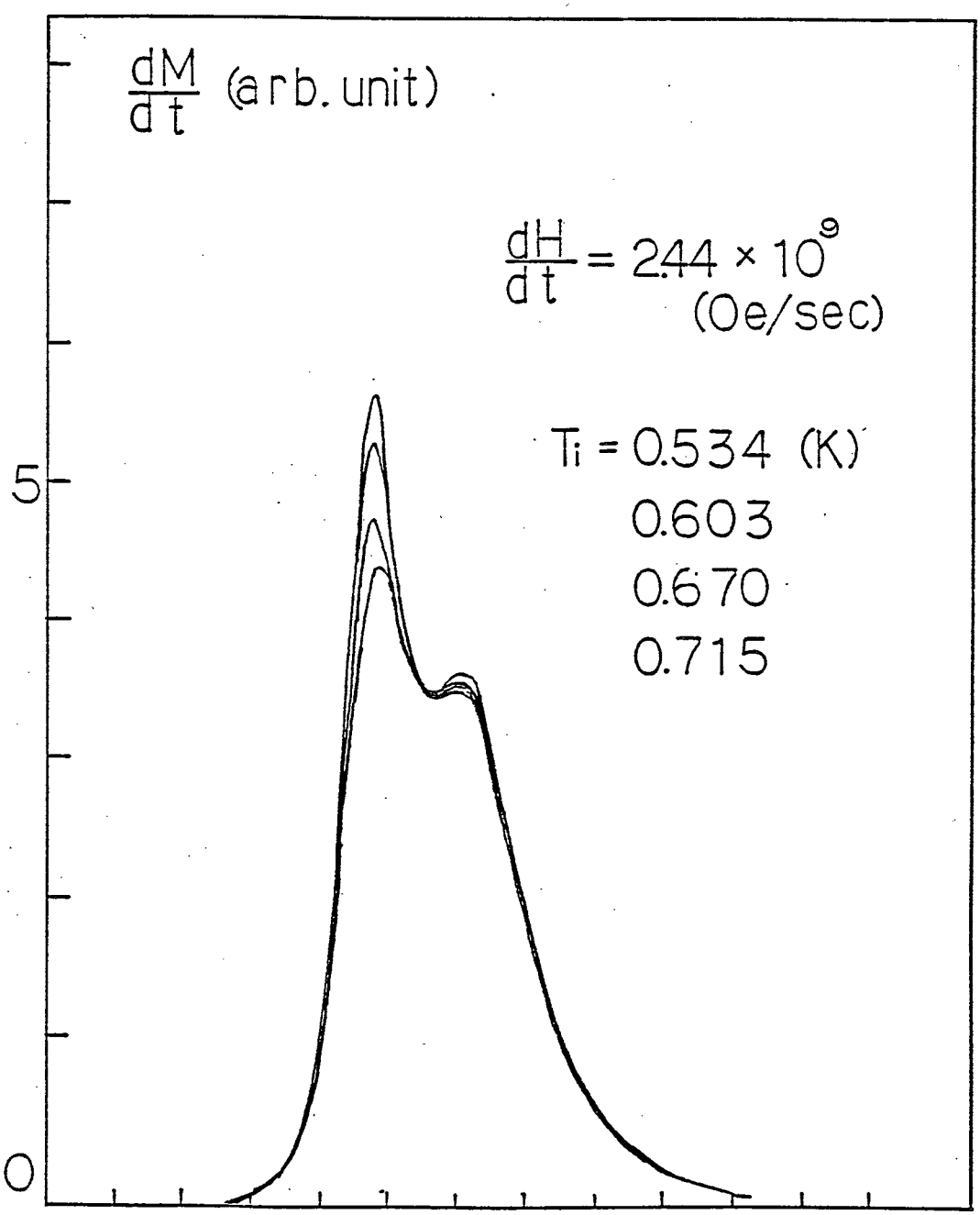

Fig. 28 dM/dt around Hc in miniature pulse coil

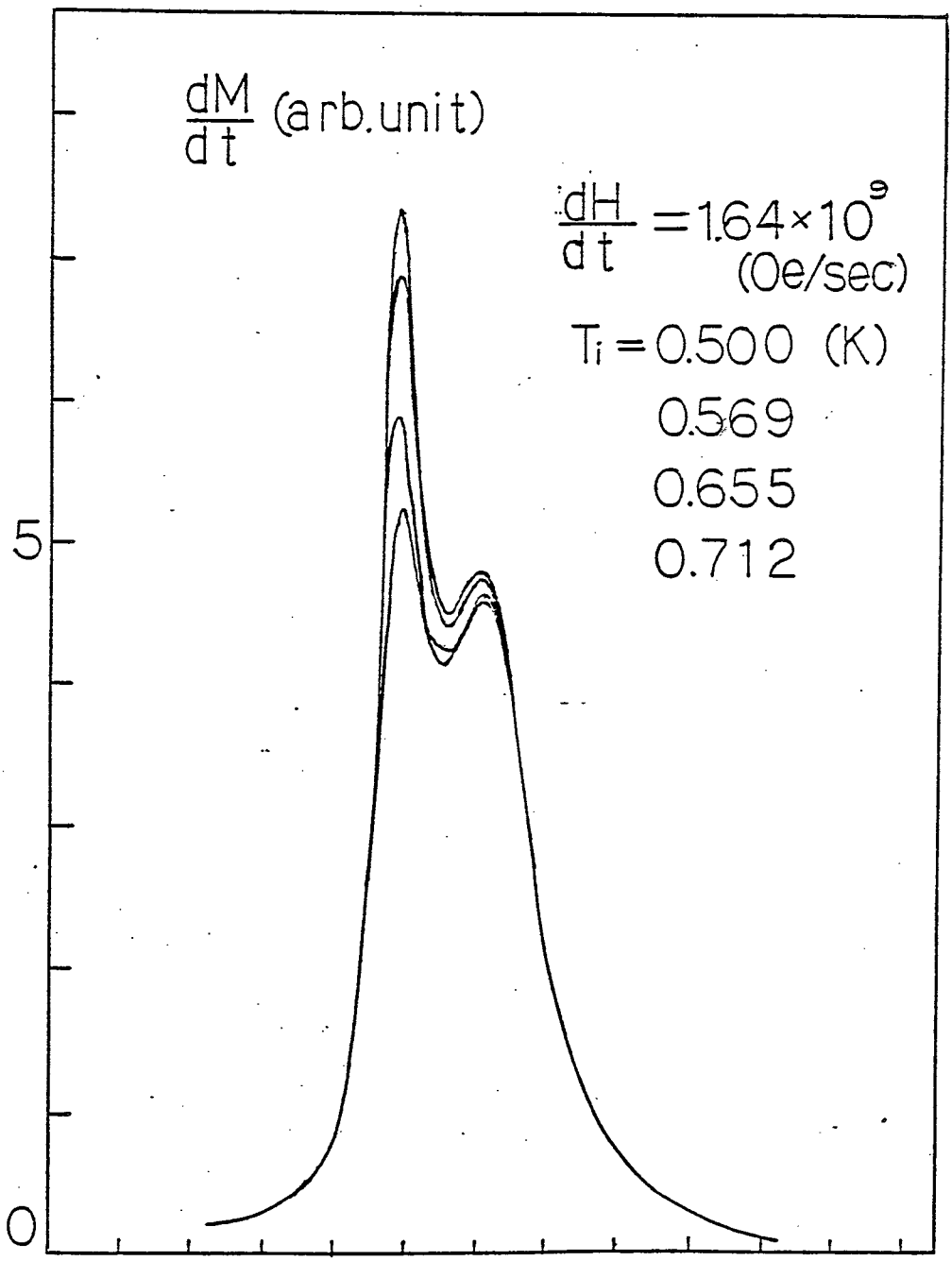

Fig. 29 dM/dt around Hc

$NaNiAcac_3$benzene

$(dH/dt)_{Hc} = 1.13 \times 10^9$ Oe/sec

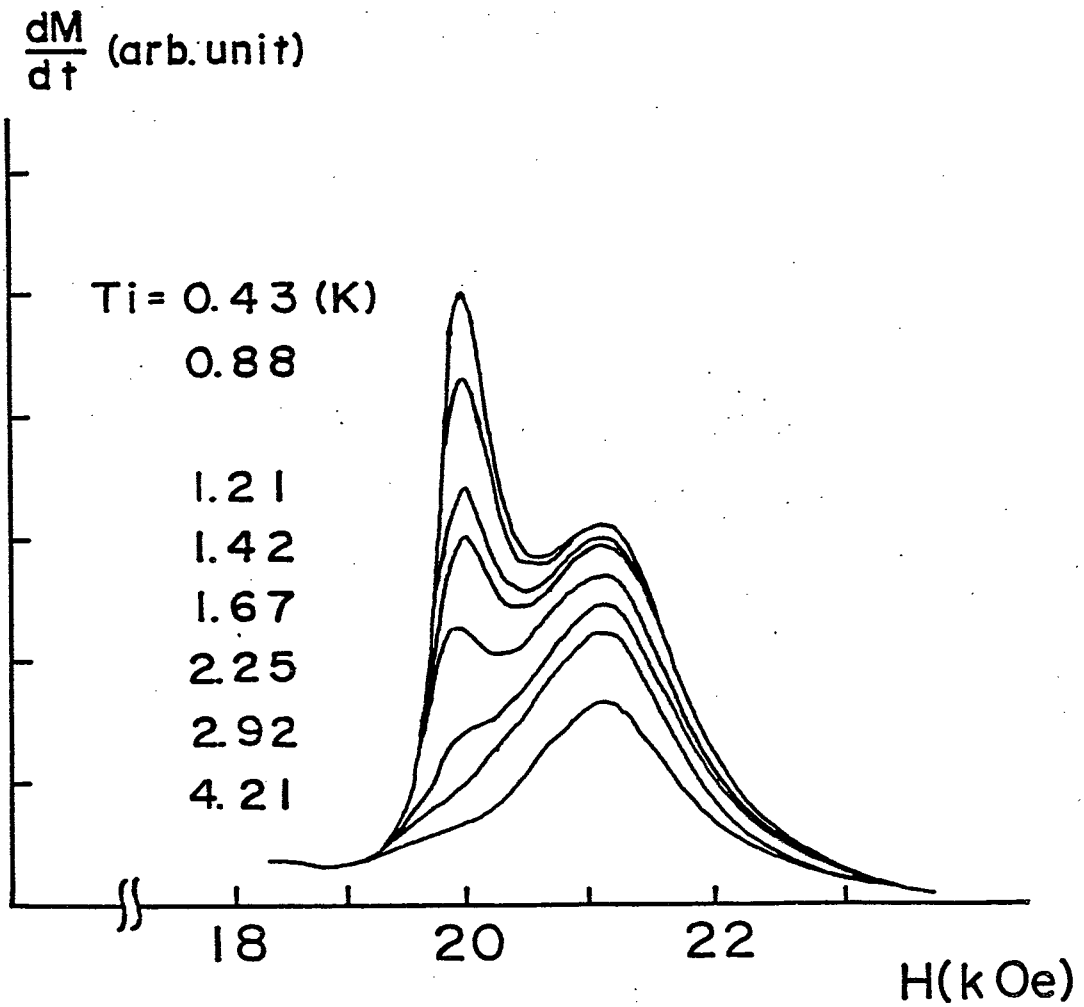

Fig. 30 dM/dt around Hc

$NaNi_xCo_{1-x}Acac_3benzene$ $x = 0.013$

$(dH/dt)_{Hc} = 1.13 \times 10^9$ Oe/sec

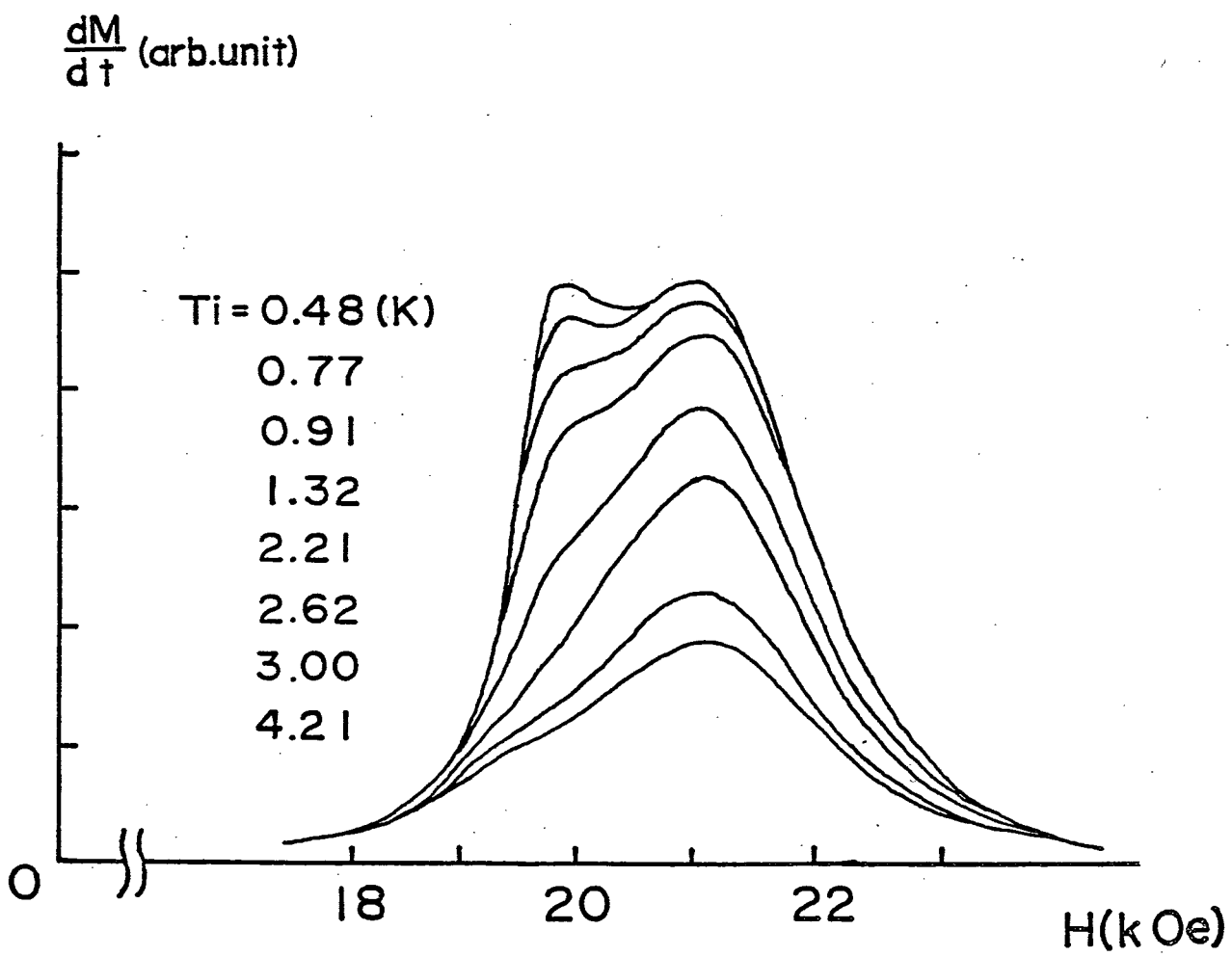

Fig. 31 dM/dt around Hc

$NaNi_{x-1}Co_xAcac_3benzene$ x = 0.009

$(dH/dt)_{Hc} = 1.13 \times 10^9$ Oe/sec

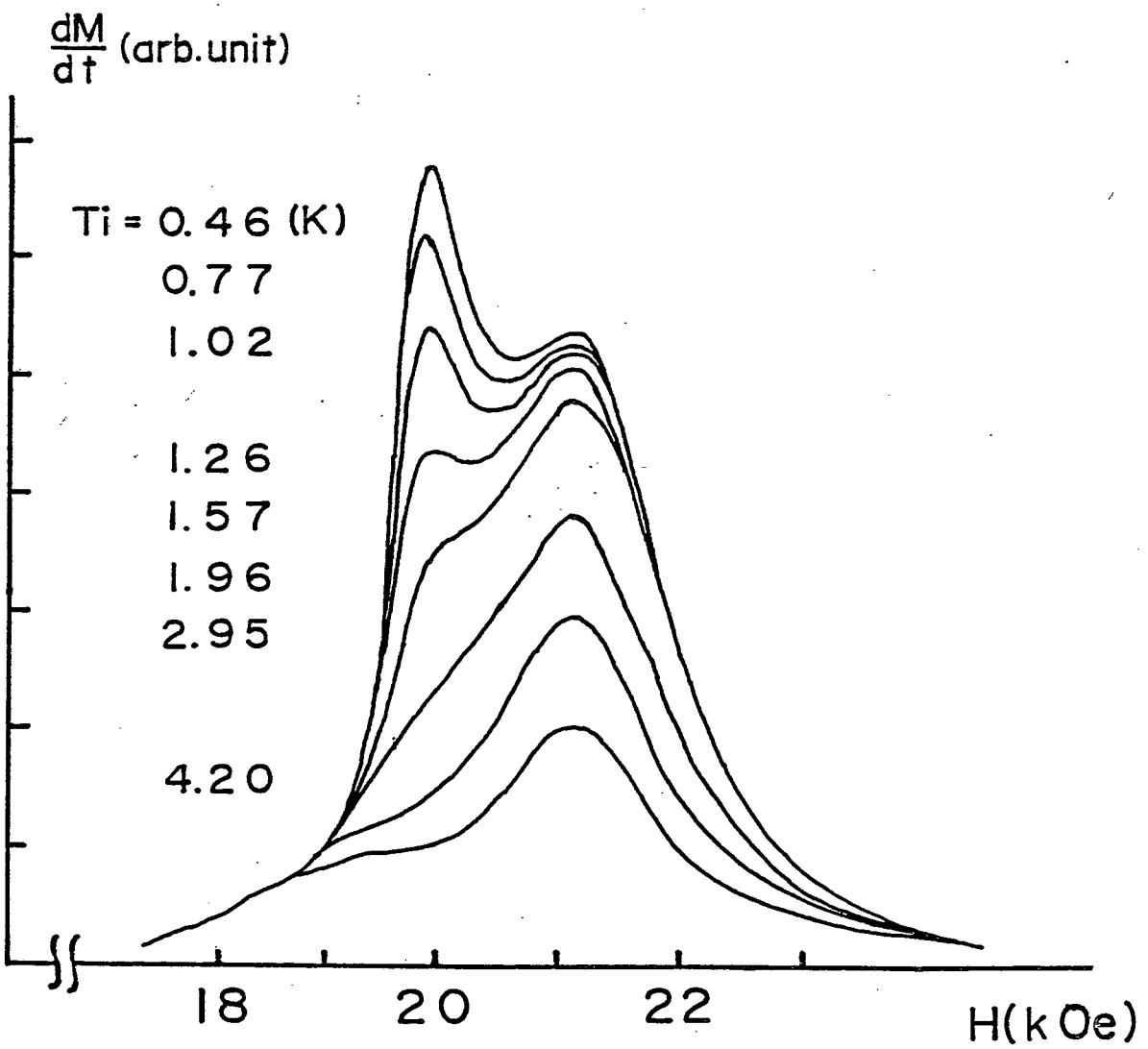

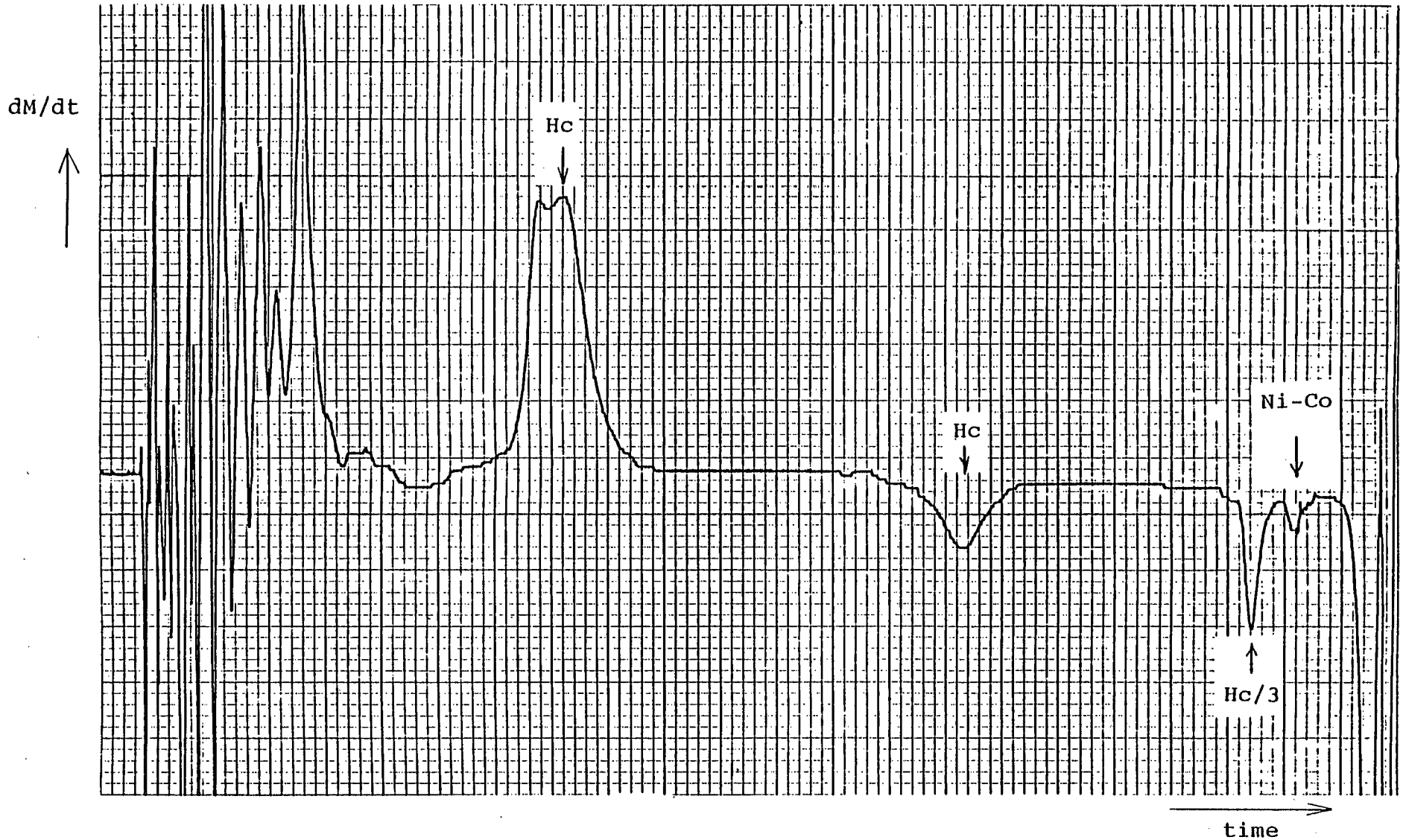

Fig. 32 dM/dt of mixed crystal x= 0.013

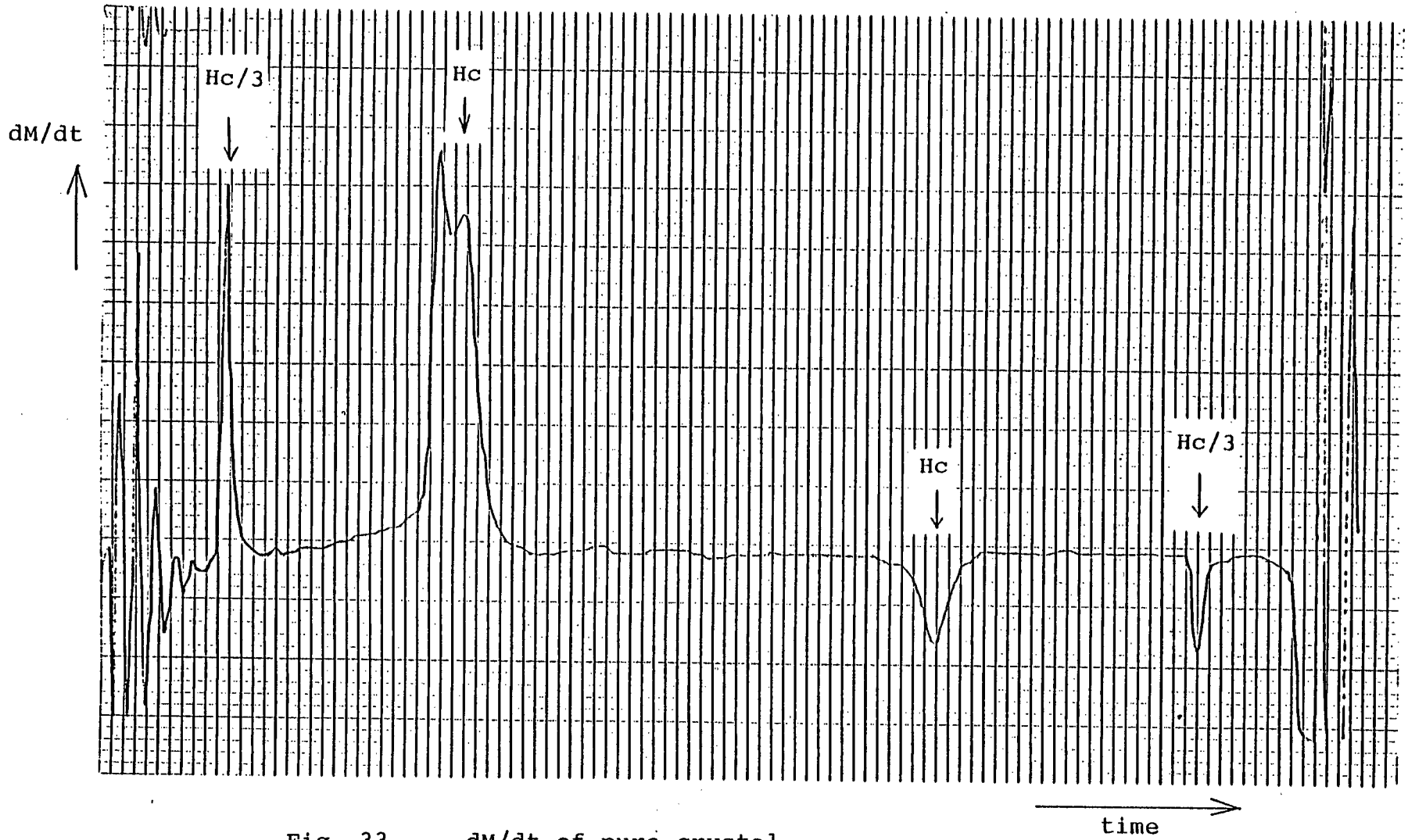

Fig. 33 dM/dt of pure crystal

Fig. 34 χ'' vs. H curve of $NaNi_{1-x}Co_xAcac_3$benzene at 1.30K

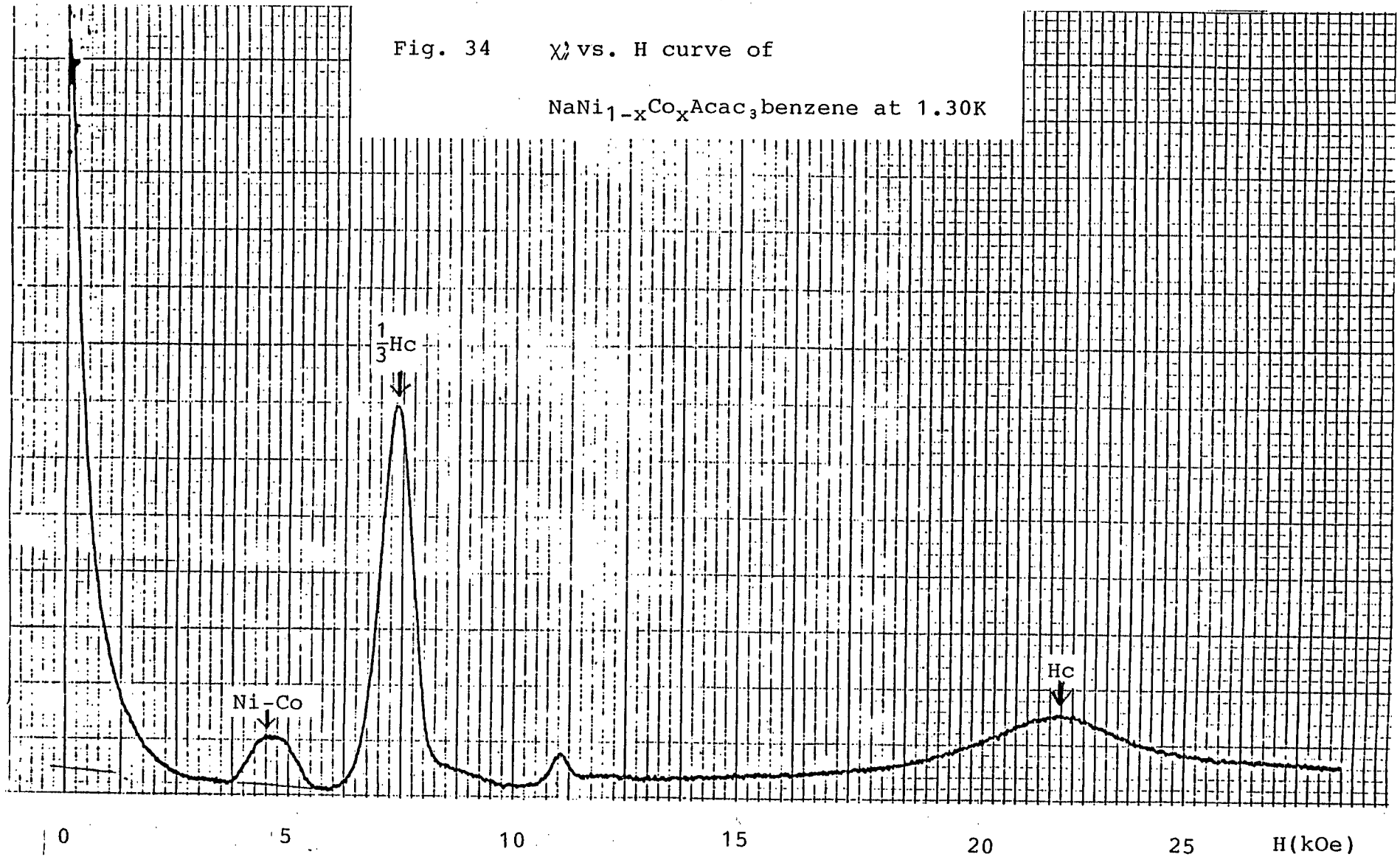

Fig. 35 $\chi'_{/\!/}$ vs. H curve of $NaNiAcac_3$benzene at 1.30K

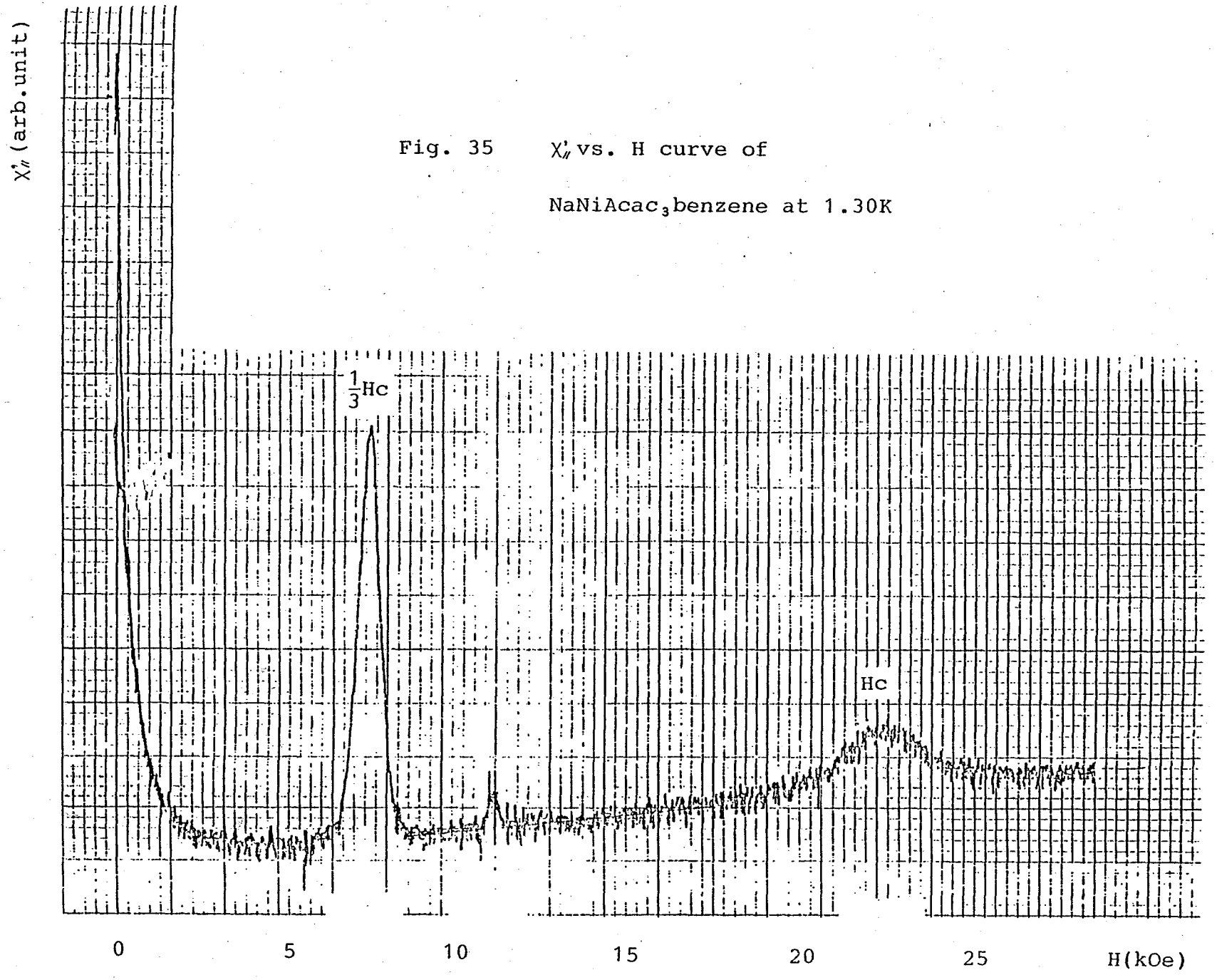

§ 4.5. Discussion

4.5.1. Excited state spin ordering

As is shown in Fig.24 , the temperature dependence of two peaks is completely different. The first pears appears at T_i 2K and becomes very sharp below 1K. The development of the second peak is not so drastic as the first one and a double peaks appears only in increasing field. In order to compare this result with spin ordering of ground state singlet system, we show dM/dt of $Cu(NO_3)_2 2.5H_2$ in Fig.36. A characteristic feature is the appearance of double peak with the initial temperature below 1.5K. However, there appears only small asymmetry, these two peaks show similar temperature dependence. These peaks correspond to the critical field H_{c1} and H_{c2}. Antiferromagnetic spin orderind occurs between H_{c1} and H_{c2}. In our case, the second peak does not correspond to H_{c2}. This peak is paramagnetic dM/dt at H_c where $|0\rangle$ and $|+1\rangle$ crosses each other. In order to explain the differance of two peaks, we assume two cross-relaxation time around H_c. The first relaxation time is defined within two levels $|0\rangle$ and $|+1\rangle$. The second relaxation time is defined among three levels $|0\rangle$ and $|\pm1\rangle$. These relaxation time mean the time attaining spin temperature among two or three levels respectively. We call cross-relaxation time of $|0\rangle$ and $|+1\rangle$ τ_2 , and all levels τ_3 . In general τ_2 , τ_3 have minimum at H_c. The high frequency susceptibility measurement shows that τ_3 at H_c is smaller than 0.1μsec and half-widths ΔH_{cr} is 1350 Oe[14].

A pulsed magnetic field is applied at $T_i \ll D/k$. The populations on $|\pm1\rangle$ are almost one half of total spins and mumber

is almost zero on $|0\rangle$ if the effect of cross-relaxation at $H_c/3$ is neglected. When the pulsed magnetic field approachs to H_{c1}, τ_2 gives rise to spin ordering around H_{c1} but at the same time causes a heating up of spin temperature. In our experiment, it takes about 1μsec to pass through the relaxation region of τ_3. Therefor, spin temperature of $|0\rangle$ and $|+1\rangle$ becomes higher than critical temperature of excited state ordering in a moment. After this relaxation, a pulsed magnetic field passes through H_c. Here at H_c the peak of dM/dt appears corresponding to paramagnetic state. In brief the first peak corresponds the spin ordering among excited spin levels at H_{c1} and the second peak shows paramagnetic susceptibility at H_c.

Results of experiment on miniture pulse coil shows that the dip between double peak becomes disappared and the peak at H_c is covered with the tail of H_{c1} when sweep rate is large, but the dM/dt at decreasing H_c has still single peak. Therefore, we conclude that spin temperature defined within excited states heats up around H_c at $dH/dt = 4\times10^9$Oe/sec (the fastest sweep rate in our experiment) and ordered state is destroyed by three levels cross-relaxation.

Most interesting feature of this spin ordering is that the system is diluted at random by the same ions $|-1\rangle$. This dilution is different from usual dilution with non magnetic ions such as Zn or Mg. Because, the probability for any spin being $|-1\rangle$ state, which does not contribute to excited spin ordering, is almost 50% when $T_i \ll D/k$.

Fig. 36 dM/dt and pulsed magnetic field around Hc

$Cu(NO_3)_2 \cdot 2.5H_2O$ Ref. 9.

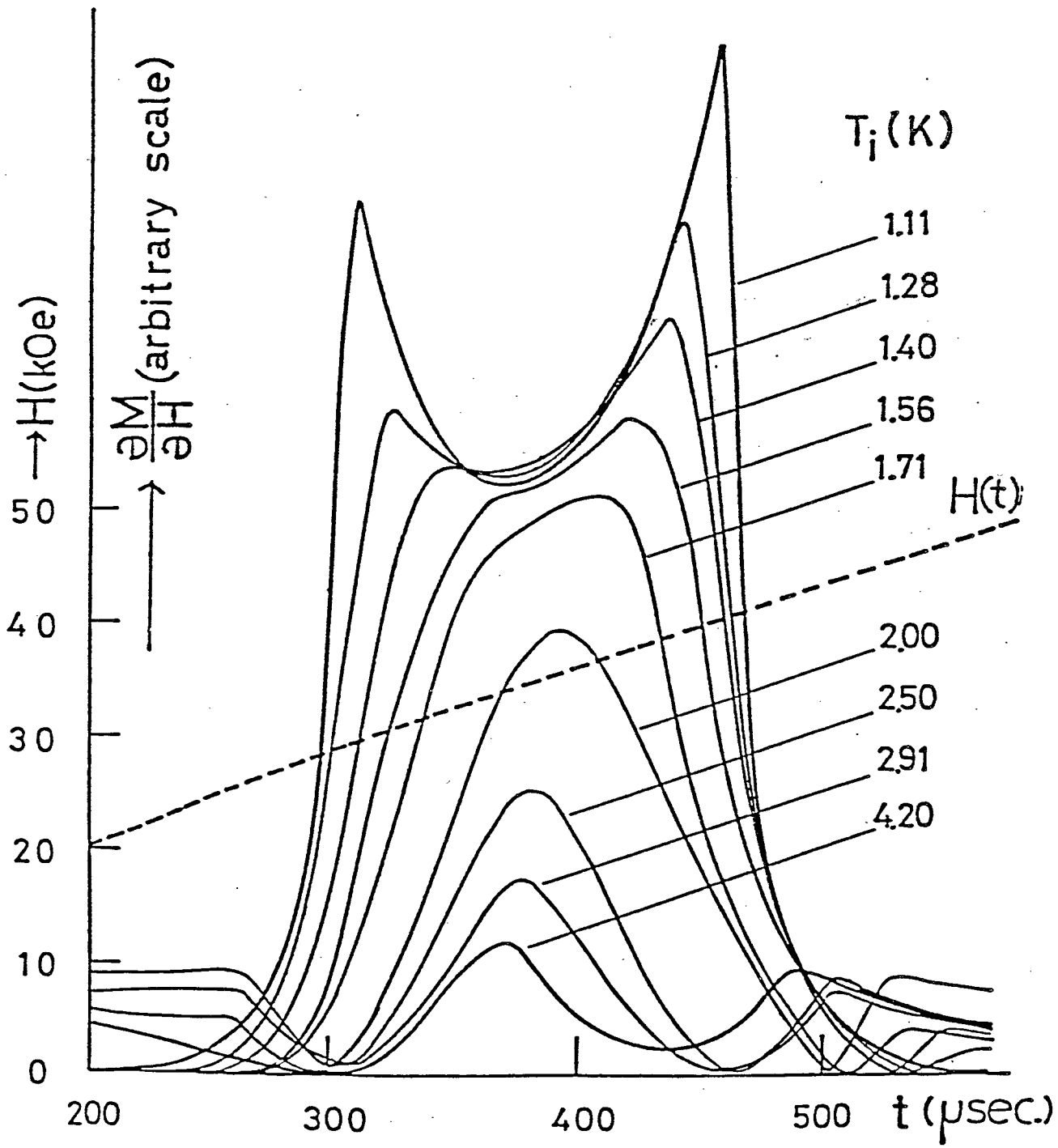

4.5.2. Cross-relaxation under pulsed magnetic field

When a pulsed magnetic field passes through at $H_c/3$,a peak of dM/dt appeares due to cross-relaxation as shown in Fig.23. The number of spins participated in the cross-relaxation is 2. At lower than $H_c/3$ there exist higher order cross-relaxations, so the population is almost constant before the pulsed magnetic field reaches at $H_c/3$. When $T_i << D/k$, the population of each state is

$$P(+1) \cong P(-1) \cong N/2$$
$$P(0) \cong 0 \qquad (22)$$

where P(i) is population of $|i\rangle$ state. When the pulsed magnetic field reaches around $H_c/3$, the change of population begins. dM/dt at $H_c/3$ vs. dH/dt is shown in Fig.37. dM/dt is saturated at $dH/dt > 2.0\times10^9$ Oe/sec. At $H_c/3$ the three spin states make a equal spacing as shown in Fig.1(b), so cross-relaxation proccess is simultaneous flips of two $|+1\rangle$ to $|0\rangle$ and $|-1\rangle$. The population is given as below.

When $T_i << D/k$,

$$P(0) = \Delta(t)$$
$$P(+1) = N/2-2\Delta(t) \qquad (23)$$
$$P(-1) = N/2+\Delta(t)$$

where $\Delta(t)$ is the change of population. We analyze the cross-relaxation with a simple rate equation.

$$d\Delta/dt = (\Delta(t)-\Delta_0)/\tau(H) \qquad (24)$$

where Δ_0 is equilibrium value of Δ, which is given by the condition :

$$P(0)/P(+1) = P(+1)/P(-1) \qquad (25)$$

We suppose that $\tau(H)$ is of gauss type as

$$\tau^{-1}(H) = \tau_o^{-1}\exp[-(H-Hc/3)/\delta] \qquad (26)$$

where δ is half-widths, in $NaNiAcac_3$benzene δ =330 Oe.

From the solution of eq. (24) we obtain dM/dt at $H_c/3$

$$dM/dt\Big]_{H_{c/3}} = 3g\beta\tau_o^{-1}\exp(-a/h)$$
$$a = \sqrt{\pi}\cdot\delta/2\tau_o \qquad (27)$$

The best fit with the experimental data shown in Fig.37 gives

$$a = 0.1\times10^{9} .$$

$$\tau_o = 2.7\,\mu\text{ sec.}$$

Kotzler obtained cross-relaxation time in $NaNiAcac_3$benzene by a.c.susceptibility. The temperature dependence of is shown in table 1.

Table 1 cross-relaxation at Hc/3
in $NaNiAcac_3$benzene

T(K)	4.22	3.30	2.35	1.65
τ (μ sec)	2.29±0.1	2.18±0.15	2.20±0.05	1.04±0.01

The relaxation time obtained by the pulse method is in good agreement with of a.c. method.

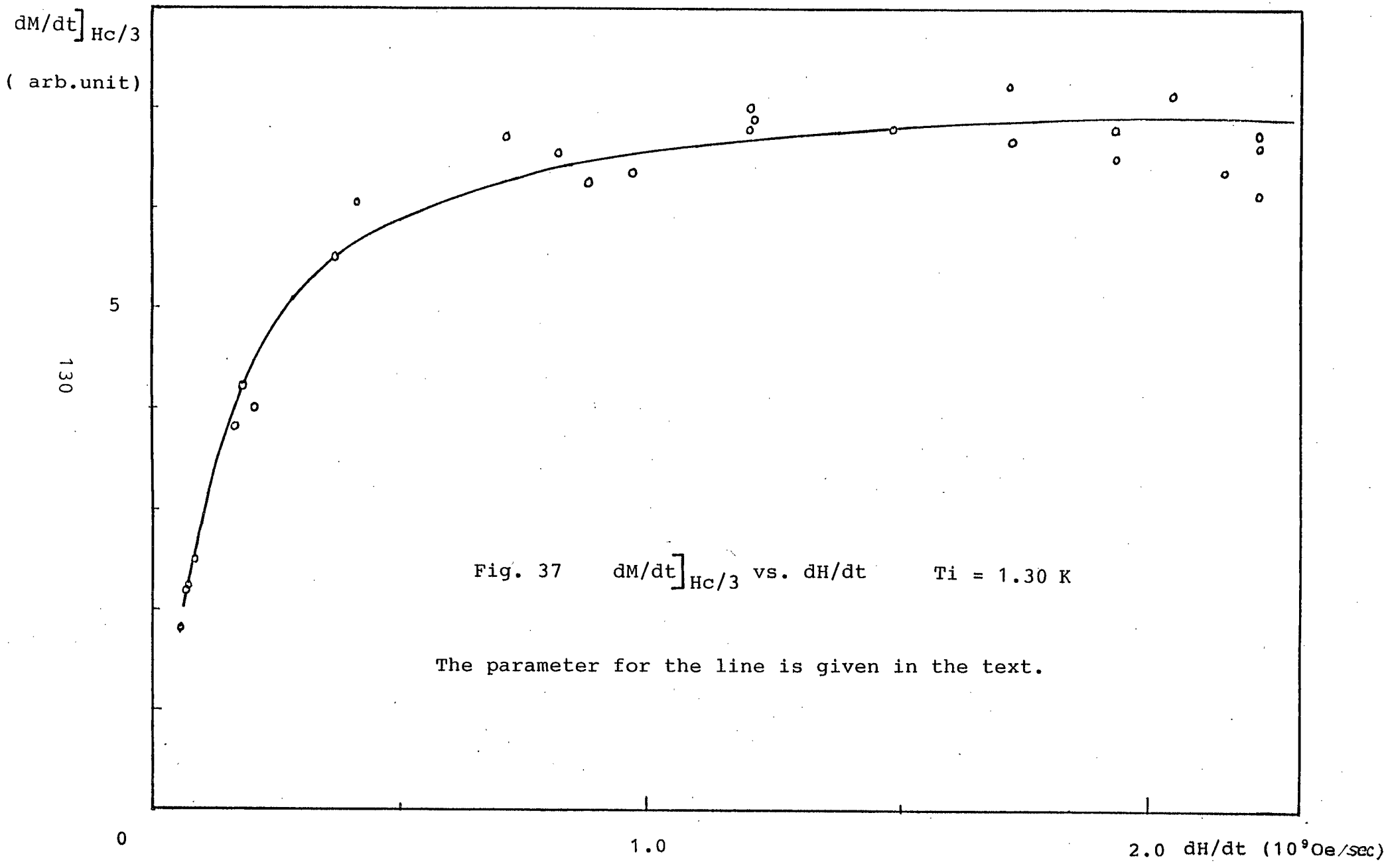

Fig. 37 $dM/dt]_{Hc/3}$ vs. dH/dt Ti = 1.30 K

The parameter for the line is given in the text.

4.5.3. The possibility of new type of excited state spin ordering

In the spin system possessing two doublets as shown in Fig.38, $|-3/2\rangle$ and $|1/2\rangle$ cross at $H=D/g\beta$. It is one example that may occur excited state spin ordering. The three conditions for spin ordering are slightly modified. Initial energy splitting is 2D, so the first condition is

$$Ti << 2D/k \qquad (28)$$

The second condition for sweep rate is the same. The third condition is about anticrosssing of excited levels around Hc. In this case energy gap ΔE is

$$\Delta E = D\theta^2 \qquad (29)$$

It is negligiblely small in comparison with energy gap of S=1 system. From effective spin model by Tachiki et al. the energy gap is regarded as Zeeman splitting for perpendecular magnetic field and g is very small in this case.

Spin Hamiltonian of Cr in $NaMgCr(C_2O_4)_3 9H_2O$ is given as below :

$$\mathcal{H} = D[S_z^2 - S(S+1)/3]+E(S_x^2-S_y^2)+g\beta\vec{S}\cdot\vec{H} \quad (S=3/2) \qquad (30)$$

$$2D/k = 1.94 \text{ K}, \quad E/k = 0.043 \text{ K}, \quad g_{//} = 1.977$$

Results of pulsed adiabatic magnetization is shown in Fig.39. Sweep rate is roughly proportional to charge voltage of the condenser. There are many peak owing to cross-relaxation. The sense of dM/dt at Hc changes from negative to positive when sweep rate becomes large. We also measure a.c.susceptibility of $NaMgCr(C_2O_4)_3 9H_2O$. Typical result is shown in Fig.40. The effects of rather high order cross-relaxation processes exist for 1kHz, so cross-relaxation time at simple process as H is very short. The second condition is not satisfied with our

experimental apparatus. The negative sense of dM/dt is explained by excess population of $|3/2\rangle$ due to cross-relaxation at C,D and so on as shown in Fig.38.

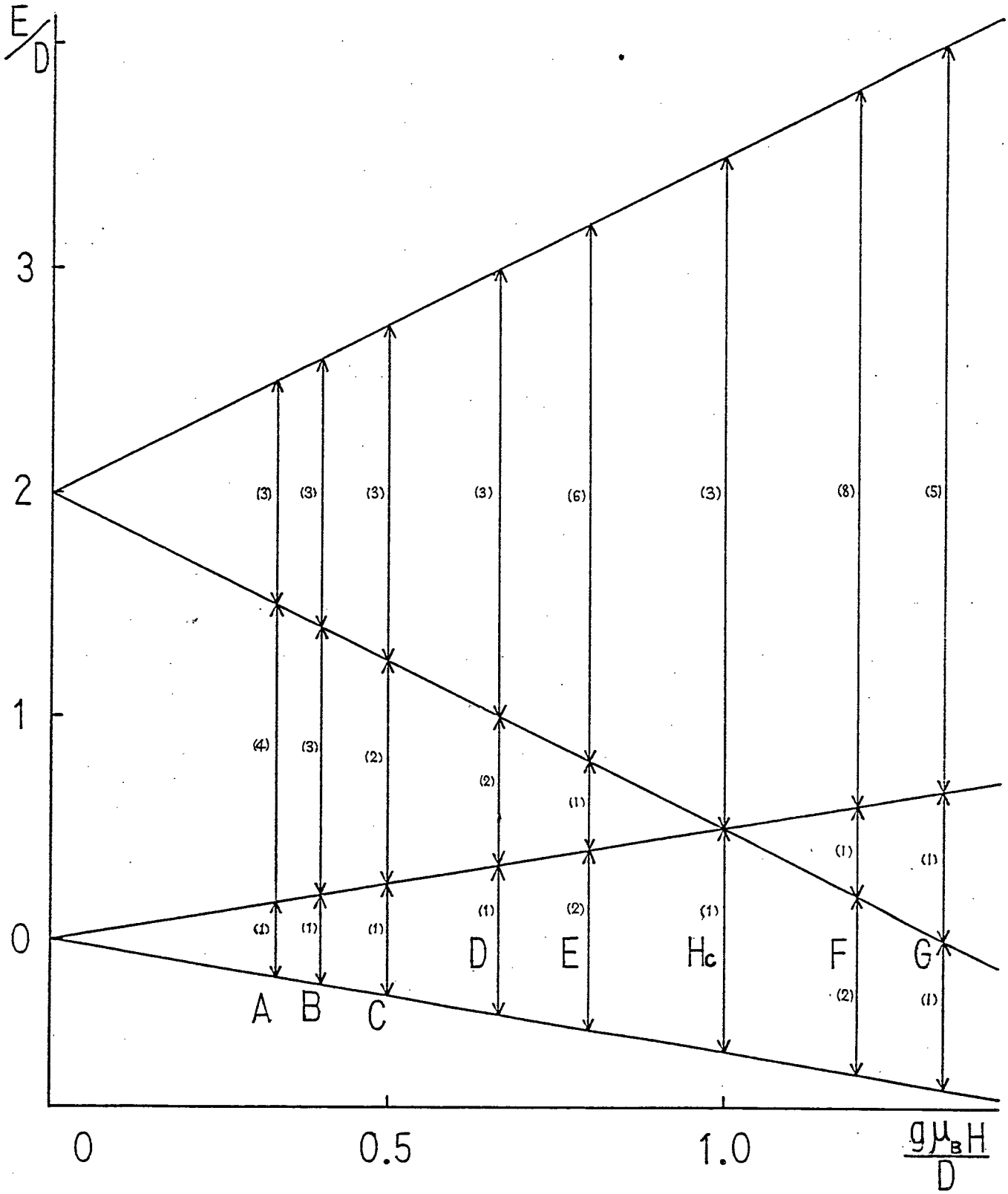

Fig. 38 Energy level given in spin Hamiltonian eq.30.

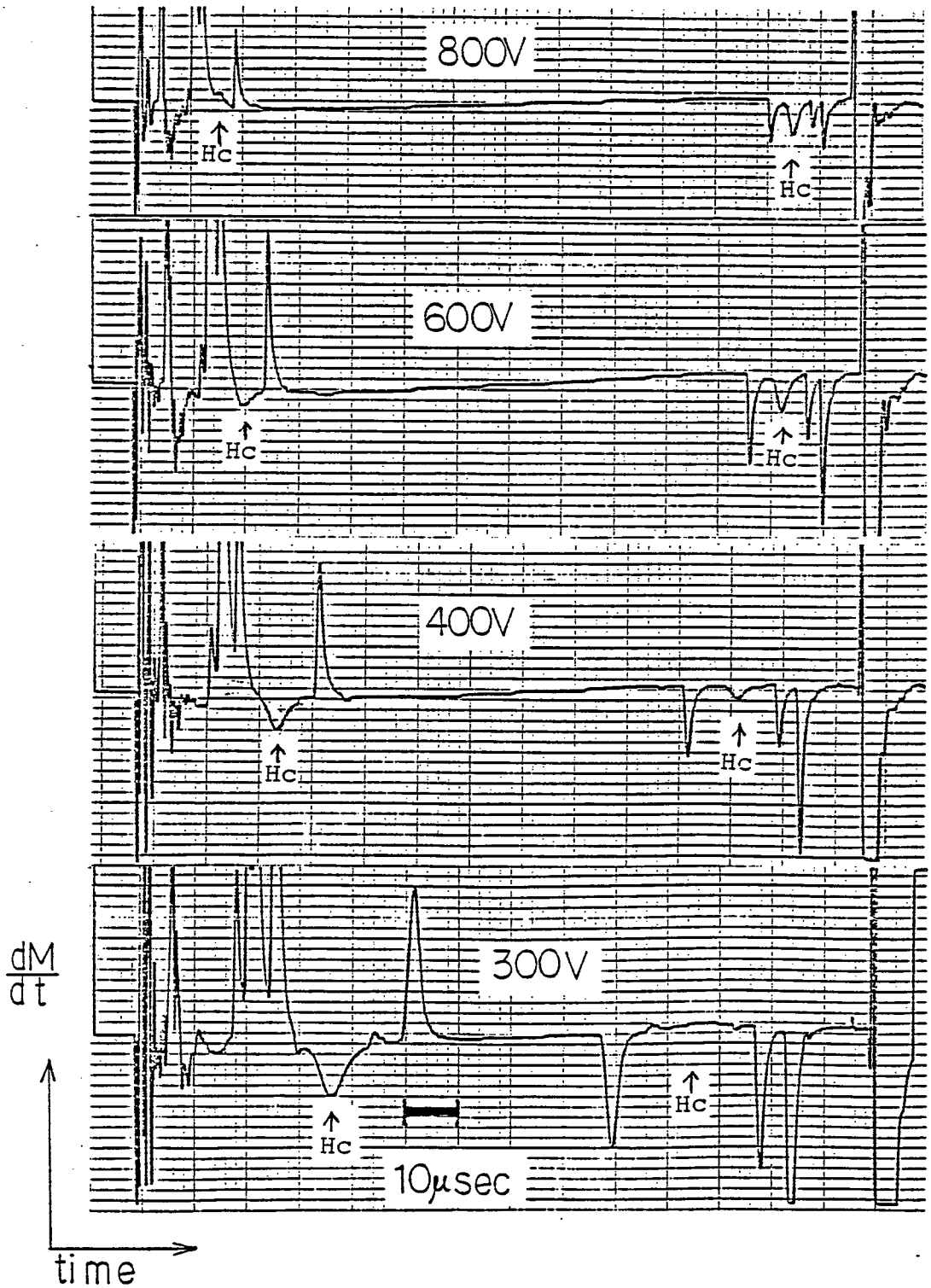

Fig. 39 dM/dt of $NaMgCr(C_2O_4)_3 9H_2O$ Ti=0.55 K

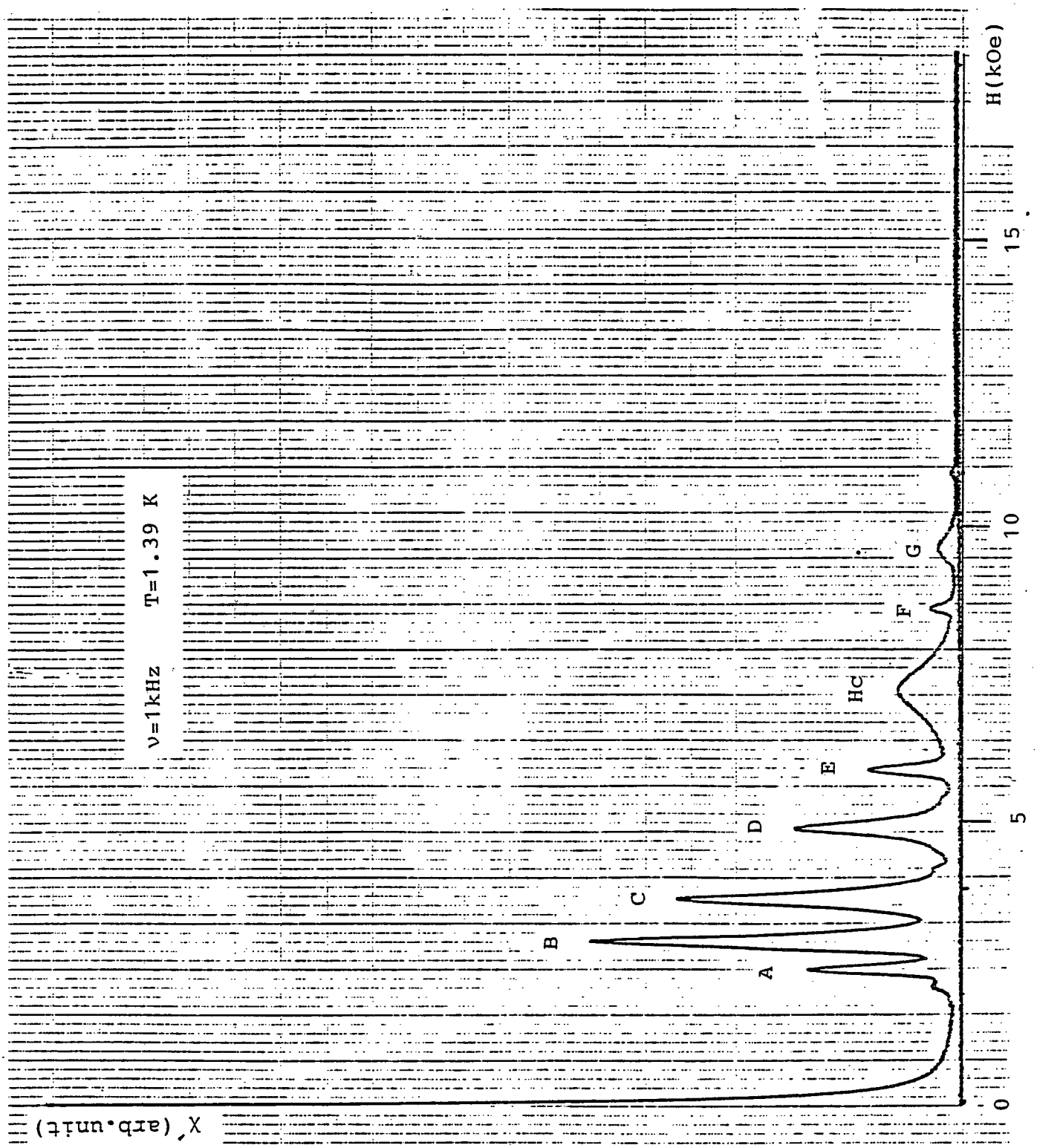

Fig. 40 AC susceptibility of $NaMgCr(C_2O_4)_3H_2O$ vs. magnetic field

§4.6. Summary

Excited state spin cooling and ordering is realized under the pulsed adiabatic magnetization process of $NaNiAcac_3$benzene.

Initial temperature and angular dependence of pulsed magnetic field to produce the spin ordering are consistent with the condition to occur a field induced spin ordering in a crystal field system.

The excited state spin ordering is, However, quasi-equilibrium state and breaks down in a moment by cross-relaxation around H_c, so we can not observe the whole phase boundary.

This spin ordering is ffective 50 % dilution state by ground state spins.

The experiment on excited state spin ordering is one of interesting experiments which need high sweep rate of pulsed magnetic field.

References (IV)

1. P.Debye: Ann. Physik 81(1926)1151.
2. W.F.Giaugue: J. Am. Chem. Soc. 49(1927)1864.
3. C.Kittel: Physica 24(1958)388.
4. W.P.Wolf: Phys. Rev. 1(1959)1196.
5. T.Haseda, Y.Tokunaga, R.Yamada, Y.Kuramitsu, S.Sakatsume and K.Amaya: Proc. 12th Int. Conf. on Low Temp. Phys. Kyoto, (1970)685.
6. M.Tachiki and T.Yamada: Suppl. Prog. Theor. Phys. 46(1970)291.
7. T.Tsuneto and T.Murao: Physica 51(1971)186.
8. N.Wada: Thesis (1980).
9. K.Amaya and N.Yamashita: J. Phys. Soc. Jpn. 42(1977)24.
10. K.Amaya, Y.Karaki, N.Yamada and T,Haseda: J. Phys. Soc. Jpn. 50(1981)3138.
11. L.G.Van Uitert and R.G.Treuiting: J. Chem. Phys. 32(1960)322.
12. M.Peter: Phys. Rev. 116(1959)1432.
13. G.H.Wannier: Phys. Rev. 79(1950)357.
14. M.Mekata: J. Phys. Soc. Jpn. 42(1977)76.
15. N.Yamada, Y.Karaki, N.Wada and K.Amaya: J. Phys. Soc. Jpn. 50(1981)3811.
16. J.Kotzler: Pysica 60(1972)375.

Acknowledgements

The author would like express his sincere thanks to professor T. Haseda for his promoting this study and stimulating discussions. He is indepted to Dr. K. Amaya for carrying out the experiment and his continuous discussions. He would express his sincere gratitude to Professor M. Matsuura for many discussions. He expresses his thanks to Dr.K.Takeda for helpful suggestions.

He is grateful to Professor T. Tsuneto and T. Hashi of Kyoto University for stimulative discussions about spin ordering among excited state of $NaNiAcac_3$benzene. The thanks are due to Dr.Y. Ajiro of Kyoto University for E.S.R. measurement of $NaCoAcac_3$-benzene.

He appreciates the kind assistance of Mr.A.Kawai for experimental apparatus. He also thanks to Mr.H. Deguchi for his cooperative work on the operation of the Dilution refrigerator and Mr. T. Tokuda for his help of the experiment on pulsed adiabatic magnetization.

Thanks are also due to members of Haseda Laboraty.